INCORPORATING CORRELATION IN THE ADEQUACY EVALUATION OF WIND INTEGRATED POWER SYSTEMS

A Thesis Submitted to the College of

Graduate Studies and Research

In Partial Fulfillment of the Requirements

For the Degree of Master of Science

In the Department of Electrical Engineering

University of Saskatchewan

Saskatoon

By

Dinesh Dhungana

PERMISSION TO USE

In presenting this thesis in partial fulfilment of the requirements for a Postgraduate degree from the University of Saskatchewan, I agree that the Libraries of this University may make it freely available for inspection. I further agree that permission for copying of this thesis in any manner, in whole or in part, for scholarly purposes may be granted by the professor or professors who supervised my thesis work or, in their absence, by the Head of the Department or the Dean of the College in which my thesis work was done. It is understood that any copying or publication or use of this thesis or parts thereof for financial gain shall not be allowed without my written permission. It is also understood that due recognition shall be given to me and to the University of Saskatchewan in any scholarly use which may be made of any material in my thesis.

Requests for permission to copy or to make other use of material in this thesis in whole or part should be addressed to:

Head of the Department of Electrical Engineering

57 Campus Drive

University of Saskatchewan

Saskatoon, Saskatchewan (S7N 5A9)

ABSTRACT

Environmental concerns caused by burning fossil fuel and the safety concerns associated with nuclear power plants have led to increased interest and investment in wind power. Wind penetration in power systems is rapidly increasing world-wide and creating significant impacts on the overall system performance. The impact of wind generation on the overall system performance increases substantially as wind penetration in power systems continues to increase to relatively high levels. It becomes increasingly important to accurately model the wind behavior, the interaction with other wind sources and conventional sources, and incorporate the characteristics of the energy demand in order to carry out a realistic evaluation of system reliability.

Analytical methods using annual wind models have generally been used for reliability evaluation of wind integrated power systems. These methods do not recognize the seasonal and diurnal load following capability of wind. In this thesis, the system adequacy indices are first evaluated on an annual and seasonal basis and then a technique is developed to incorporate the diurnal load following capability of wind.

Power systems with high wind penetrations are often connected to multiple wind farms at different geographic locations. Wind speed correlations between the different wind farms largely affect the total wind power generation characteristics of such systems, and therefore should be an important parameter in the wind modeling process. Another concern that arises is the lack of time-synchronized data, especially at the planning phase, which limits the capability of system planners to accurately model multiple correlated wind farms using simple analytical methods. A simple and appropriate probabilistic analytical wind model which can be used for adequacy evaluation of multiple wind-integrated power systems is proposed in the thesis. A simple analytical method to develop an approximate wind model of multiple correlated wind farms

when time-synchronized wind data is not available is also proposed in the thesis. The methods to incorporate correlations in the adequacy evaluations of wind integrated power systems presented in the thesis are expected to be highly useful for system planners and policy makers as wind penetration continues to increase.

ACKNOWLEDGMENTS

I would like to express my earnest gratitude to my supervisors, Dr. Rajesh Karki and Dr. Roy Billinton, for the invaluable guidance and encouragement I received throughout my research work as well as during the preparation of this thesis. Their tremendous knowledge and support was imperative for the completion of my research work. I would also like to thank the College of Graduate Studies and Research, the Department of Electrical and Computer Engineering, NSERC and SaskPower for providing the financial support for my graduate program.

I would like to sincerely thank my committee members for their valuable suggestions and inputs throughout the thesis writing process. I am very thankful to Mr. Suman Thapa for providing me with research related suggestions and guidance on numerous occasions.

I would like to express my deepest gratitude to my parents Lawanya Prasad Dhungana and Nirmala Dhungana for their lifelong love, support and encouragement. Finally, and most importantly, I would like to thank my loving wife Sonu Sainju for her constant patience and encouragement throughout the entire process.

.

TABLE OF CONTENTS

PERMISSION TO USE ……..i

ABSTRACT..... ii

ACKNOWLEDGMENTS iv

LIST OF TABLES..... vii

LIST OF FIGURES ix

LIST OF ABBREVIATIONS..... xii

1 INTRODUCTION.....1
1.1 Power System Reliability Evaluations..... 1
1.2 Incorporation of Wind in Power System Adequacy Evaluation..... 4
1.3 Problem Statement and Research Objective..... 6
1.4 Outline of the Thesis..... 10

2 BASIC CONCEPTS FOR ADEQUACY EVALUATION OF WIND INTEGRATED POWER SYSTEMS.....12
2.1 Introduction..... 12
2.2 Modeling Concepts..... 12
2.3 Load Model..... 13
2.4 Conventional Generation Models..... 15
2.5 Wind Model..... 18
2.6 Risk Indices..... 18
2.7 Peak Load Carrying Capability, Wind Capacity Credit and Wind Capacity Factor ……20
2.8 Period Analysis..... 22
2.9 Load Forecast Uncertainty..... 24
2.10 Conclusion..... 26

3 INCORPORATION OF CORRELATION BETWEEN WIND SPEED AND LOAD 27
3.1 Introduction..... 27
3.2 Basic Evaluations on an Annual Basis..... 27
3.2.1 Annual Wind Model 27
3.2.2 Analysis and Results.....33
3.3 Seasonal Evaluation..... 36
3.4 Diurnal Evaluation..... 39
3.5 Conclusion..... 45

4 INCORPORATING CORRELATION IN WIND SPEED BETWEEN WIND FARMS46
4.1 Introduction 46
4.2 Wind Data Modeling for Correlated Wind Farms 47
4.3 Wind Power Modeling 52
4.4 Impact of Wind Penetration and Wind Farm Correlation 53
4.5 Appropriate Wind Capacity Model Considering Wind Correlation and Penetration 56
4.6 Conclusion 59

5 A SIMPLIFIED WIND MODEL FOR GEOGRAPHICALY DISTRIBUTED WIND SITES LACKING TIME-SYNCHRONIZED WIND DATA 61
5.1 Introduction 61
5.2 Wind Capacity Model using Time-synchronized Data 63
5.3 The Proposed Algorithm 65
5.3.1 Estimation of the correlation coefficient 66
5.3.2 Development of individual capacity models for each wind site 69
5.3.3 Combination of the individual wind capacity models 70
5.3.4 Evaluation of the System LOLE and Comparison with the PPM 73
5.3.5 Discussions on the Proposed Algorithm 75
5.4 The Approximate Split Method 76
5.5 Extension of the split method 79
5.5.1 Combined model from individual models 81
5.5.2 Evaluation of the System LOLE and comparison with the PPM 84
5.5.3 Sensitivity studies 85
5.5.4 Evaluation of the system LOLE for more than three wind farms and comparison with the PPM 92
5.6 Conclusion 95

6 SUMMARY AND CONCLUSIONS 96

LIST OF REFERENCES 101

APPENDIX A – IEEE-RTS DATA 105

LIST OF TABLES

Table page

Table 2.1: Hourly load of the example power system 13

Table 2.2: Hourly loads arranged in descending order 14

Table 2.3: Conventional generating unit models for unit 1 and 2 16

Table 2.4: Multistate generating unit model for unit 3 16

Table 2.5: Equivalent conventional generation model 17

Table 2.6: Example of a wind farm capacity model 18

Table 2.7: System generation model for the example system 19

Table 2.8: Sub-division of the period for period analysis 23

Table 2.9: System generation model for sub-period ii 23

Table 2.10: Load data and load model for sub-period i 24

Table 2.11: Load data and load model for sub-period ii 24

Table 2.12: Seven-step normal distribution 25

Table 2.13: Incorporation of 4% LFU 26

Table 3.1: Seasonal sub-periods 37

Table 3.2: IEEE-RTS LOLE (hrs/yr) connected to the Swift Current wind farm using annual and seasonal period analysis 38

Table 3.3: Peak Load Duration 41

Table 3.4: LOLE for the IEEE-RTS connected to the Swift Current wind farm for 5% and 10% wind penetrations 42

Table 3.5: LOLE for the IEEE-RTS connected to the Swift Current wind farm for 15% and 20% wind penetrations 43

Table 3.6: PLCC (MW) at a LOLE criterion of 1 hr/yr for the IEEE-RTS connected to the Swift Current wind farm 44

Table 4.1: LOLE in h/yr for the RTS with varying wind correlation and penetration 54

Table 4.2: NoS for wind capacity model. 58

Table 5.1: Cross correlation between the wind speeds for Swift Current and Regina for one year of wind speed data 67

Table 5.2: Individual wind capacity models 69

Table 5.3: Split models for the Regina site 72

Table 5.4: Intermediate wind capacity model $p(WP_{ref+\rho 1})$ 72

Table 5.5: LOLE comparison for selected combinations of Saskatchewan sites. 75

Table 5.6: Combined wind capacity model for the three wind farms using the PPM 81

Table 5.7: Illustration example of three sites 82

Table 5.8: Combined capacity model of Swift Current and Regina, $p(WP_{R1R2})$ 83

Table 5.9: LOLE comparison for selected combinations of Saskatchewan sites 85

Table 5.10: Wind farm sites and their mean wind speeds 88

Table 5.11: Permutations for the order of reference site 89

Table 5.12: Combination of wind sites used for the study 90

Table 5.13: Wind farm combinations considered for the study 91

Table 5.14: Wind farm sites considered in the study with respective rated capacities 93

Table 5.15: Wind farm sites considered for the study 94

LIST OF FIGURES

Figure page

Figure 1.1: Hierarchical levels in power systems 2

Figure 1.2: Global cumulative installed wind capacity (Source: Global wind energy council, www.gwec.net) 5

Figure 2.1: System modeling steps 13

Figure 2.2: LDC for the example power system 14

Figure 2.3: Per unit LDC for the example power system 15

Figure 2.4: LOLE for a range of peak loads for the example power system 21

Figure 2.5: LOLE and PLCCs with and without wind 22

Figure 3.1: Wind speed probability distribution 29

Figure 3.2: Wind power curve 30

Figure 3.3: Annual CAPT for Swift Current 32

Figure 3.4: 11 state annual CAPT for Swift Current 33

Figure 3.5: Load duration curve for a typical Saskatchewan year 34

Figure 3.6: IEEE-RTS power system considered for the study 34

Figure 3.7: LOLE for IEEE-RTS connected to a wind farm with different penetration levels 34

Figure 3.8: Saskatchewan power system considered for the study 35

Figure 3.9: LOLE for Saskatchewan power system connected to centennial wind farm (149.4 MW) evaluated on an annual basis 36

Figure 3.10: Load and wind speed for a sample year 36

Figure 3.11: Annual and Seasonal load models used in the study 37

Figure 3.12: Annual and seasonal wind models for the Swift Current site 38

Figure 3.13: LOLE for the Saskatchewan power system which includes the Centennial wind farm using annual and seasonal period analysis 39

Figure 3.14: Load and wind speed of a typical day during (a) winter, and (b) summer seasons 39

Fig. 3.15 : Normalized daily load data for (a) winter, and (b) summer seasons.....41

Figure 3.16: Diurnal wind capacity models for each season 41

Figure 3.17: Diurnal load duration curves for each season 42

Figure 3.18: LOLE and PLCC (at a LOLE criterion of 1 hr/yr) for the IEEE-RTS connected to the Swift Current wind farm.....44

Figure 3.19: LOLE for the Saskatchewan power system connected to the Centennial wind farm using annual, seasonal and diurnal analysis 45

Figure 4.1: Generation of correlated random numbers using Cholesky decomposition. (a) Uncorrelated random numbers; (b) Correlated random numbers with $\zeta = 0.5$.49

Figure 4.2: Simulated wind speeds, (a) using uncorrelated random numbers (b) using correlated random numbers with $\zeta = 0.5$.....50

Figure 4.3: 2-day sample simulation of wind speeds for the two sites with a correlation of 0.11. 50

Figure 4.4: 2-day sample simulation of wind speeds for the two sites with a correlation of 0.56. 50

Figure 4.5: Probability distribution of wind speeds simulated at different correlations....51

Figure 4.6: 27 state capacity outage probability table for different wind speed correlations.....53

Figure 4.7: Variation in LOLE with peak load for different correlations.....55

Figure 4.8: Variation in LOLE results with the NoS in the wind model for different.....55

Figure 4.9: Variation in LOLE results with the NoS in the wind model at different wind penetrations. 56

Figure 4.10: Error produced by using reduced number of states in the Wind Capacity model.....57

Figure 4.11: LOLE errors at different peak loads obtained using the recommended wind capacity models.....59

Figure 5.1: Combined capacity model for the Swift Current (300 MW) and Regina (100 MW) sites obtained from the PPM 65

Figure 5.2: Saskatchewan map showing wind sites considered 68

Figure 5.3: Distance vs wind speed correlation for 12 Saskatchewan sites.....68

Figure 5.4: Combined wind capacity models obtained from the two methods 73

Figure 5.5: LOLE obtained from the two methods.....74

Figure 5.6: Error produced for a range of wind farm capacity ratios 76

Figure 5.7 Individual wind capacity models obtained assuming normal wind speed distribution 77

Figure 5.8: Combined wind capacity models from PPM, Split and approx. Split methods.....78

Figure 5.9: System LOLE obtained from the approximate method and the PPM.....78

Figure 5.10 : Three Saskatchewan wind sites considered in the study.....80

Figure 5.11: Capacity models obtained from two methods for three sites 83

Figure 5.12: LOLE obtained from the two methods.....84

Figure 5.13: Variation of the ratio of the rated capacity of R1 with respect to the rated capacity of R2 for 10.5% wind penetration 86

Figure 5.14: Variation of the ratio of the rated capacity of R2 and R3 for 10.5% wind penetration.....87

Figure 5.15: Variation in the order of reference sites used in Split method for different cases 90

Figure 5.16: Error in LOLE obtained due to the variation in $\rho_{12\text{-}3}$ 92

Figure 5.17: LOLE value for the IEEE-RTS connected to four wind farms at 5.5 % wind penetration.....93

Figure 5.18: System LOLE for the IEEE-RTS connected to multiple wind farms of equal capacity with the total wind capacity of 400 MW. 94

LIST OF ABBREVIATIONS

A	Availability
ARMA	Auto Regressive and Moving Average
CAPT	Capacity Available Probability Table
CC	Capacity Credit
CF	Capacity Factor
COPT	Capacity Outage Probability Table
DPLVC	Daily Peak Load Variation Curve
FOR	Forced Outage Rate
HL-I	Hierarchical Level I
HL-II	Hierarchical Level II
HL-III	Hierarchical Level III
HPOS	Hourly Power Output Series
hrs	Hours
IEEE	Institute of Electrical and Electronics Engineers
IEEE-RTS	IEEE- Reliability Test System
Km	Kilometre
LDC	Load Duration curve
LFU	Load Forecast Uncertainty
LOEE	Loss of Energy Expectation
LOLE	Loss of Load Expectation
MCS	Monte Carlo Simulation
MW	Megawatt
NERC	North American Electric Reliability Corporation
NIC	Normally and Independently Distributed
NoS	Number of States
pd	Period
PJM	Pennsylvania-New Jersey Maryland
PLCC	Peak Load Carrying Capability
PPM	Point to Point Method
SM	System Minutes
U	Unavailability
UPM	Units Per Million
WECS	Wind Energy Conversion System
WIPS	Wind Integrated Power System
WPTS	Wind Power Time Series
WTG	Wind Turbine Generator

1 INTRODUCTION

1.1 Power System Reliability Evaluations

Power systems are expected to provide electric power supply to their customers with satisfactory quality and continuity. The ability to do so is generally perceived as the reliability of the power system. Failure to provide a reliable electric supply can have remarkable impacts on the customers. The adverse impacts generally branch out to affect many other sectors directly or indirectly. Power outages can have broad socio-economic impacts. Reliable electric supply is therefore considered by many as an important prerequisite of a modern economy. A high level of reliability generally requires a high amount of investment. Reliability can be improved by incorporating redundancies during planning and operations which results in an increase in the associated costs. The additional investment made however, at some point, yields minimal improvement in the reliability. Very high investment therefore results in a very high cost of electricity which cannot be justified by the minimal improvement in reliability. Power system reliability evaluation is, therefore, a process to provide a reliable power supply to the system customers as economically as possible.

Power system reliability evaluation is generally divided into two parts, system adequacy and system security [1, 2]. System adequacy deals with whether or not sufficient infrastructure is present in the power system to satisfy the customer electricity requirements. An adequate amount of generating capacity along with adequate transmission and distribution facilities to actually

transport the generated electricity to the demand point should be present in the system in order to deem the system to have sufficient adequacy [1]. Adequacy studies are generally performed during the planning phases to ensure that the system is sufficiently equipped to achieve and maintain the expected reliability. System security studies however, deal with the dynamic disturbances that the power system can face during operation [1]. A system is deemed to be secure based on its ability to respond to the disturbances to which it is subjected during its operation. Disturbances are events such as the loss of generating units, transmission lines, distribution links, etc. The scope of the work presented in this thesis is restricted to the area of adequacy studies of power systems.

A power system can be divided into the three functional zones of generation, transmission and distribution. Reliability assessment can be performed within the functional zones or at the three hierarchical levels shown in Figure 1.1.

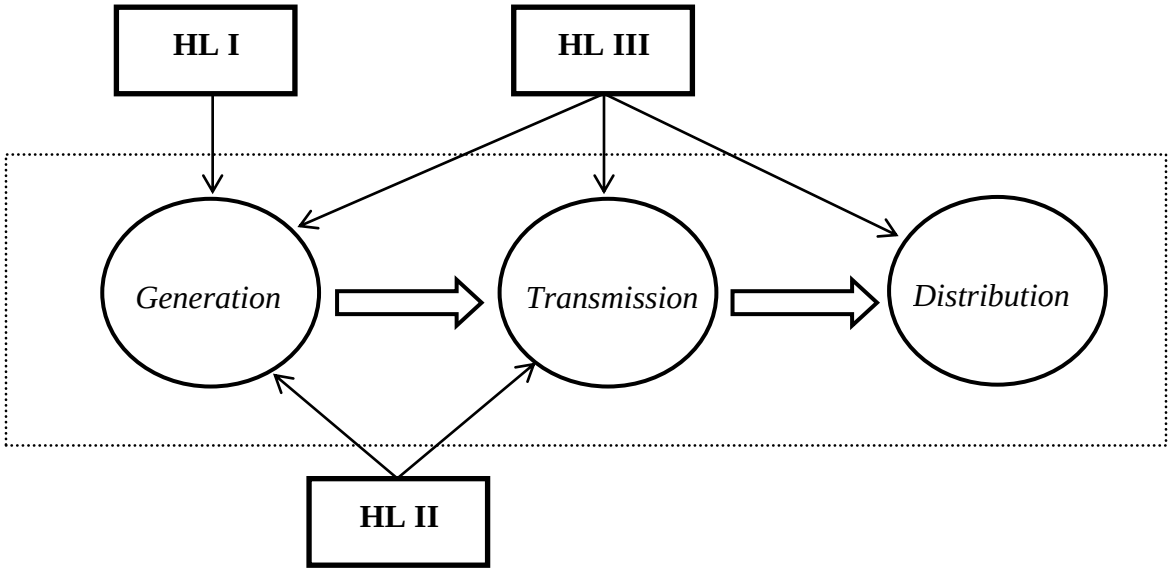

Figure 1.1: Hierarchical levels in power systems

Reliability assessment done considering only the generation is designated as reliability assessment at hierarchical level I (HL I). Assessment done taking both generation and transmission into consideration is said to be at hierarchical level II (HL II). Similarly, the assessment done including all the three functional zones, i.e. generation, transmission and distribution, is said to be at hierarchical level III. The complexity of the analysis increases remarkably as the hierarchical level increases from I to III. An HL I analysis is the most basic type of study and therefore a large amount of research has been done in this area [2–5]. These studies are usually done to determine the future generation capacity requirements of a system. An HL II study generally follows the HL I study to determine transmission requirements considering the location of the new generation and load in the system. Probabilistic HL II evaluation is relatively complex compared to an HL I study and a considerable amount of research has been done in this area as well [2–7]. HL III studies, on the other hand, are mainly limited to past performance analysis. The scope of the work presented in this thesis is restricted to HL I studies.

Power system reliability analysis can be performed using either deterministic or the probabilistic techniques. Deterministic techniques are generally techniques based on a rule of thumb. They are extremely simple and have been widely used in the past. Deterministic techniques are still in significant use for planning and operational analysis[1] owing to their simplicity. Power system behavior however is stochastic in nature, and the deterministic techniques cannot represent this aspect in a realistic way. Probabilistic techniques, on the other hand, use probability concepts to evaluate the system reliability using data based on past performance of the system components. Probabilistic techniques are therefore able to realistically

represent the future behaviors of the power system. The studies presented in this thesis use probability techniques.

Power system reliability is evaluated using a range of quantitative reliability indices. There are two basic approaches for the evaluation of power system reliability indices and are designated as Analytical techniques and Simulation techniques [1]. An analytical technique [1] is an approach to evaluate the risk indices using mathematical models of the system components with direct numerical solutions. References [8–10] use analytical techniques for reliability evaluation. A simulation technique on the other hand, uses computer generated random numbers to represent system states. Risk indices are then calculated using the simulated system states over a long period of simulation time. Simulation techniques are used in [11–13] for the reliability evaluation of wind integrated power systems(WIPS). The work presented in this thesis mainly uses analytical techniques. Simulation techniques are only used in the studies to generate synthetic wind data when adequate historical data is not available.

1.2 Incorporation of Wind in Power System Adequacy Evaluation

Fossil fuel is presently the major source for electricity production, and is considered to be a major contributor to greenhouse gas emissions. Burning fossil fuel therefore has significant adverse environmental impacts. The general public and governments around the world are well aware of this. Enormous effort has therefore been placed on the development and application of green energy sources. Wind is a promising alternative, which has the potential to be a major power source in future power systems. Huge investments are being made in this sector, which have led to considerable advancement in wind power technology. It is expected that wind power installations will grow substantially to produce clean energy in electric power systems. Another

concern arises from the fact that the dwindling reserves of conventional fuel and increasing energy demands will eventually lead to rising costs for fossil fuel and other conventional energy generation. The installed capacity of wind farms in Canada is currently 7051 MW [14]. Wind penetration, which is defined as the ratio of the installed wind capacity to the total installed capacity of a power system is currently about 3% in Canada. More than 6000 MW of additional wind capacity is expected to come into operation before 2015 [14], increasing the penetration level to about 5%. This is a trend not only in Canada but all around the world. Figure 1.2 shows the global cumulative installed wind capacity from the year 1996 to 2012. The wind capacity has increased rapidly from 6,100 MW in 1996 to 282,430 MW in 2012.

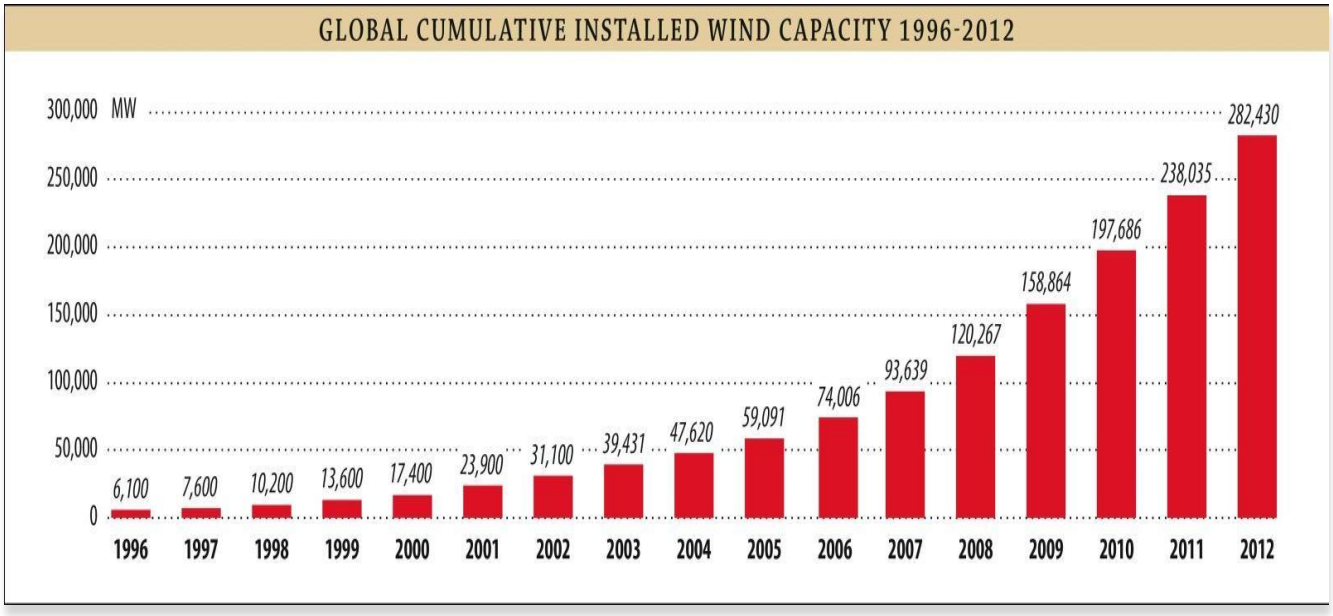

Figure 1.2: Global cumulative installed wind capacity (Source: Global wind energy council, www.gwec.net)

The graph clearly shows the sharp increase in installed wind capacity in the last two decades. This trend is expected to continue for the next few decades. These statistics indicate that high levels of wind power penetration can be anticipated in the near future.

A wind turbine generator (WTG) converts wind energy into electric energy. Its operating characteristic is remarkably different than that of conventional electric energy sources. The output power of a WTG can vary over a range between zero and the rated capacity value, in a random fashion. The variation in power generation, and the uncertainty associated with the power output levels cause significant challenges in planning and operating a power system to meet the projected demand with an acceptable level of reliability. The overall system reliability indices are not very sensitive to the available wind capacity at lower penetration levels. The system indices, however, become heavily dependent on the wind capacity as the wind penetration increases. The utilization of detailed wind power models and the incorporation of various system factors in the reliability evaluation of WIPS becomes increasingly important as the wind penetration increases.

1.3 Problem Statement and Research Objective

Wind power generation can be highly variable and uncertain depending on the wind characteristics at the geographic site. The power output profile of a wind power plant is remarkably different from that of conventional power plants, and requires appropriate modeling for valid system performance evaluation. The basic methods [5–7,15–17] for the evaluation of conventional generating units have been extended to incorporate wind resources in power system reliability evaluation with the addition of techniques which can appropriately respond to the uncertainty, variability and the intermittency of wind. A considerable number of publications have been made recently related to the incorporation of wind resource in reliability studies [11, 18–26] which utilize both analytical and the simulation techniques. As discussed in the previous

section, the importance of proper wind resource modeling has increased due to increased wind penetration, and will continue to do so as wind penetration further increases.

There are basically two kinds of correlation that have to be incorporated in wind modeling during the reliability evaluations of a WIPS; (1) the cross correlation between the load and wind characteristics, and (2) the cross correlation between the wind characteristics of different wind farms connected to the power system. There exists a certain variation pattern in the wind speed of any wind farm site on a seasonal basis as well as on an hourly basis within a 24 hour period of a day. The load in a power system also generally has an inherent seasonal and hourly variation pattern. A specific level of cross correlation between the wind speed and the load therefore exists in a WIPS. Failure to incorporate this correlation in the evaluation of reliability indices may lead to inaccurate results. Similarly, the cross correlation between wind speeds at multiple wind farms considerably affects the variability of the total available wind power. The variability generally decreases as the correlation between multiple wind farms decreases, and this characteristic should be reflected in a wind generation model developed for reliability studies. Geographically distant wind sites tend to have lower correlations [27, 28] than geographically close sites. This suggests that the adequacy benefits of geographically diversifying wind sites should be considered in wind energy policy and planning. A quantitative assessment of the adequacy benefits requires a suitable reliability evaluation technique that incorporates a wind model which is appropriately responsive to wind site correlations.

Monte Carlo Simulation [1] can be used to incorporate the cross correlation between the wind speed and load as well as the cross correlation between the wind speeds at different wind farms. Monte Carlo Simulation when applied as a time sequential process is capable of capturing these types of correlations [11–13]. Customized simulation programs and expertise in the field

however, are generally required to implement simulation techniques in practice. System planners usually evaluate the impacts of different system development options before making a decision. Customized software needs to be purchased and/or an expert in simulation techniques needs to be hired if Monte Carlo Simulation is to be used. This is less appealing from a practical implementation point of view rather than having a simple and straight forward technique which can be readily applied. An analytical technique [1], on the other hand, is usually a relatively simple method, and should therefore be more attractive to system operators and planners. A considerable amount of literature is available on the incorporation of wind resources in power system reliability evaluation [9, 10, 19, 29–31]. An inherent problem with the analytical method, however, is the difficulty in incorporating correlations described earlier. The development of a mathematical model that provides reasonably accurate results is the main challenge in this approach. Techniques which are responsive to the different types of correlation related to wind power are not readily available in the analytical domain.

Adequacy evaluation of a WIPS using an analytical technique is basically done on an annual basis[1]. Analysis done using a single annual period cannot incorporate the seasonal and diurnal correlation between the wind speed and the load. A simple technique which can incorporate seasonal and diurnal correlations between wind speed and load is therefore desirable.

A wind energy conversion system (WECS) can generally be represented by a multi-state generation model [32]. The selection of a suitable number of states in the multi-state wind model plays an important role in the simplicity and accuracy of the wind model. Studies have been done to simplify wind models in order to facilitate real world applications. References [32] and [19] suggested a simple five state and seven state analytical wind models respectively. The correlation between multiple wind farms was, however, not considered in the study. Simplified

wind models which incorporate the correlations between the wind speeds of different wind farm sites is therefore desirable as the amount of wind power connected to the power system increases.

A simple and intuitive approach to incorporate multiple correlated wind sites in reliability analysis using an analytical technique is to aggregate the power data obtained from each wind farm in the system for each time interval, and create a probability distribution of the available wind capacities to derive an overall wind generation model. This simple technique however requires sufficient time-synchronized wind data from each wind farm site connected to the power system. Other analytical techniques to incorporate multiple correlated wind sites have been proposed [9, 10] but all of these techniques require sufficient time-synchronized wind data for each wind farm site. Sufficient time-synchronized wind data however is generally not available when system planners and wind policy makers are considering different wind locations as potential sites. Correlated random numbers can be used to generate synthetic wind speed data using time series methods like Auto Regressive and Moving Average (ARMA) models [31, 33] which do not require time-synchronized data. Reliable time series models used in this approach however can only be developed if sufficient historical wind speed data of the wind farms are present [19, 22, 34]. Many wind power planning and policy formulation situations can, however, arise where no wind data or extremely limited data is available for prospective wind sites. The development of a simple wind model for correlated wind farm sites without having sufficient time-synchronized wind data could therefore be very useful for system planners and policy makers.

The objective of this research work is to address some of the problems noted above as listed below:

- To develop a simple analytical technique to incorporate seasonal as well as diurnal correlations between wind speed and load.
- To develop a simple analytical wind model considering correlations between the wind speeds of different wind farms.
- To develop an approximate analytical technique for a suitable wind model of multiple correlated wind farm sites in the absence of adequate time-synchronized wind data.
- To compare the performance of the developed techniques with existing techniques.

1.4 Outline of the Thesis

This thesis is divided into six chapters:

Chapter 1 introduces the basic concepts regarding generating systems reliability and the incorporation of wind in HL I reliability assessment. It also describes the problem and outlines the research objective of the thesis and the outline of the thesis.

Chapter 2 illustrates the basic concepts applicable in an adequacy evaluation at HL I of a power system containing wind farms. A very simple hypothetical power system is used to illustrate the concepts applied in the studies presented in this thesis.

Chapter 3 presents a simple analytical technique to incorporate the cross correlation between the system load and the wind speed of a wind farm on a seasonal and a diurnal basis. It first explains the process of developing annual generation (conventional and wind) and load models in order to perform a basic annual adequacy evaluation, which is later extended to seasonal and diurnal period analysis. The correlation between the wind speed and load is incorporated in the studies by splitting the annual period into seasonal and diurnal sub-periods.

Chapter 4 presents a simple analytical model for multiple correlated wind farms. It introduces a method of using the ARMA models of two wind farms to generate synthetic wind speeds which have a cross correlation close to a desired value. The method for evaluating wind power from wind speed data is described. Sensitivity analysis is performed to see the effect of various factors on the wind model and finally a suitable wind model incorporating the cross correlation is proposed.

Chapter 5 proposes a simple analytical method to develop a combined wind model for multiple correlated wind farms when adequate time-synchronized wind data is not available. It first introduces the basic method to develop the combined wind model of multiple correlated wind farms when time-synchronized wind data is available. It then proposes a novel technique to develop the combined wind model of two correlated wind farms using actual data from two Saskatchewan wind sites. Sensitivity studies on the proposed method are performed in order to propose some guidelines for minimization of the error produced when using the proposed method. An approximate method is also proposed in Chapter 5 for situations in which only the mean and the standard deviation in wind speeds are available for the wind sites. Chapter 5 finally extends the proposed method to incorporate more than two sites.

Chapter 6 summarizes the work done in this research project and concludes the thesis.

2 BASIC CONCEPTS FOR ADEQUACY EVALUATION OF WIND INTEGRATED POWER SYSTEMS

2.1 Introduction

Adequacy evaluation of a wind integrated power system involves modeling the conventional generating units, modeling the wind farms, modeling the load and finally conducting an evaluation of the required indices using the developed models. This chapter illustrates the basic modeling concepts that have been used in the work reported in the thesis. A simple hypothetical power system with three conventional generating units, one wind farm and a ten hour evaluation period is utilized in this chapter to illustrate the concepts used in the thesis. It should be noted that the hypothetical power system presented in this chapter is only for illustration purposes and has not been used for any other studies in the following chapters. The development of conventional generation and load models are presented in this chapter. The development of wind models is discussed in the following chapters. The concepts involved in the evaluation of the risk indices, the peak load carrying capability of a power system, capacity factor and capacity credit of a wind farm, period analysis and load forecast uncertainty are discussed in this chapter.

2.2 Modeling Concepts

The system modeling steps for the evaluation of the HL I adequacy indices of a wind integrated power system is shown in Figure 2.1. The conventional generation model, the wind model and the load model are first developed independently. The conventional generation model and the wind model are then combined to develop the overall system generation model. The

overall generation model is then combined with the load model to obtain the required risk indices.

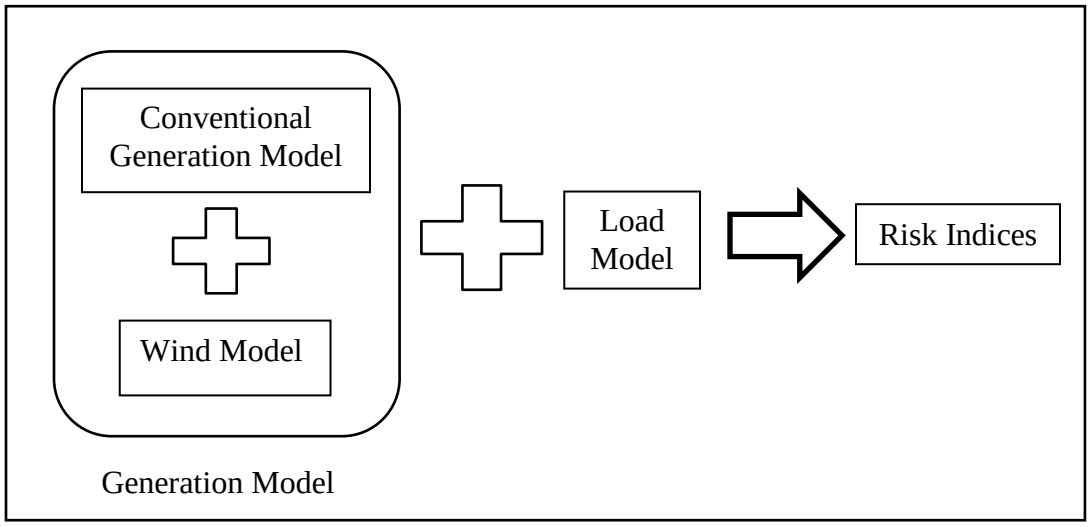

Figure 2.1: System modeling steps

2.3 Load Model

A load model is generally a tabular or a graphical representation of the system load characteristics. The load model used in this thesis is the load duration curve (LDC). The hourly system load for a specified period of time is first arranged in a descending order to form a cumulative load model. The resulting model indicates the total duration that a particular load level occurs in a specified time period. Table 2.1 shows the hourly peak load for a ten hour period of the example power system utilized in this chapter.

Table 2.1: Hourly load of the example power system

Hour	Load (MW)	Hour	Load (MW)
0	58	5	28
1	85	6	64
2	24	7	52
3	65	8	49
4	78	9	83

The hourly peak loads for the specified period are then arranged in a descending order as shown in Table 2.2. The third column can then be created to show the total duration in hours that the corresponding load is exceeded. The load arranged in the descending order is plotted against the duration in Figure 2.2 to create the load duration curve (LDC). The LDC can also be represented in per unit by normalizing the values with the maximum load and the maximum duration which are shown in the fourth and the fifth columns of Table 2.2. The LDC in per unit values is shown in Figure 2.3.

Table 2.2: Hourly loads arranged in descending order

Hour	Load (MW)	Duration(hrs)	Load (pu)	Duration (pu)
1	85	0	1.0000	0.000
9	83	1	0.9765	0.111
4	78	2	0.9176	0.222
3	65	3	0.7647	0.333
6	64	4	0.7529	0.444
0	58	5	0.6824	0.556
7	52	6	0.6118	0.667
8	49	7	0.5765	0.778
5	28	8	0.3294	0.889
2	24	9	0.2824	1.000

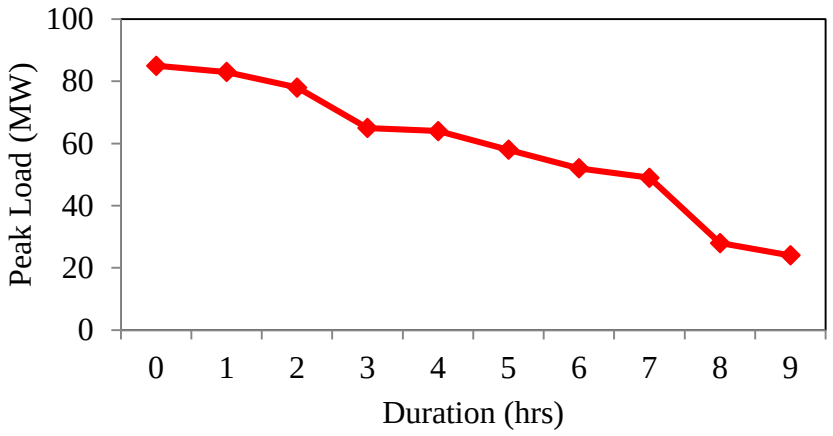

Figure 2.2: LDC for the example power system

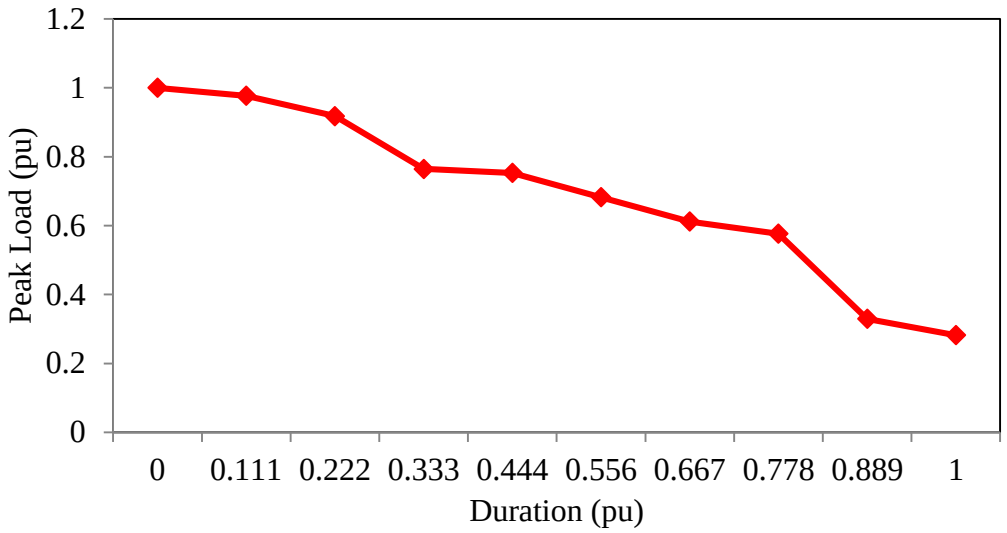

Figure 2.3: Per unit LDC for the example power system

A load model can be similarly created using the daily peak loads instead of hourly peak loads if the period of time considered is longer than a day. The load model thus obtained is designated as the daily peak load variation curve (DPLVC).

2.4 Conventional Generation Models

Conventional generating units like hydro units and thermal units are generally modeled in terms of the probability of finding the unit in an outage state. The probability of a generating unit being in a forced outage state is called the forced outage rate (FOR) or the unavailability (U) of the generating unit. The complementary long term probability of a generating unit not being in an outage state is called the availability (A) of the generating unit [1]. The availability and unavailability of the generating unit can be calculated using (2.1) and (2.2). Two generating units with rated capacities of 25 MW and 30 MW, and FOR of 1% and 0.5% respectively are shown in Table 2.3.

$$Unavailability\ (FOR) = U = \frac{\sum down\ time}{Total\ operating\ time} \qquad (2.1)$$

$$Availability = A = 1 - U = \frac{\sum up\ time}{Total\ operating\ time} \quad (2.2)$$

Table 2.3: Conventional generating unit models for unit 1 and 2

Unit ID	Unit Type	Rated Capacity (MW)	FOR/U	A
1	Thermal	30	0.010	0.990
2	Hydro	25	0.005	0.995

The generating unit model shown in Table 2.3 is a two state representation of the generating unit since it only shows the probability of the unit being in the fully available and unavailable states. A two-state model however is sometimes insufficient to properly represent a generating unit which can reside in one or more derated state(s) due to various events. In such a case, a generating unit can be represented as a multistate unit in terms of its capacity states and their corresponding probabilities. An example of a multi-state generating unit model is shown in Table 2.4.

Table 2.4: Multistate generating unit model for unit 3

Unit ID	Capacity Available(MW)	Capacity Out (MW)	Probability
3	0	45	0.01
	25	20	0.37
	45	0	0.62

The example power system used in this chapter consists of the three conventional generating units shown in Table 2.3 and Table 2.4 with a total system generating capacity of 100 MW.

The individual generating unit models are combined to form an equivalent conventional generation model of the entire power system. A recursive algorithm[16] shown in (2.3) can be used to sequentially combine the generating unit models to create the system model.

$$P(X) = \sum_{i=1}^{n} p_i \times P'(X - C_i) \quad (2.3)$$

where,

$P'(X)$ = the cumulative probability of the capacity outage state of X MW before the addition of the unit.

$P(X)$ = the cumulative probability of the capacity outage state of X MW after the addition of the unit.

n = number of unit states

C_i = capacity outage of state i for the unit being added

p_i = probability of existence of the unit in state i.

Equation (2.3) is initialized by setting $P'(X) = 1$ for X≤0 and $P'(X) = 0$ for other cases. The detailed illustration of the application of the recursive algorithm shown in (2.3) has been given in [16]. The conventional generation model obtained by combining the three generating unit models using the recursive algorithm is shown in Table 2.5. The generating unit model shown in Table 2.5 is represented in terms of the possible capacity outage states with their corresponding probabilities of occurrence and called the Capacity Outage Probability Table (COPT).

Table 2.5: Equivalent conventional generation model

Capacity Out (MW)	**Probability**
0	0.6107310
20	0.3644685
25	0.0030690
30	0.0061690
45	0.0116820
50	0.0036815
55	0.0000310
70	0.0000495
75	0.0001180
100	0.0000005

2.5 Wind Model

Wind power generation is highly variable and uncertain and depends on the wind characteristics at the geographic site. The power output profile of a wind power plant is, therefore, remarkably different from that of conventional power plants. The generation capacity profile of a wind power plant is usually represented by a multistate capacity model. The capacity output of a wind farm can vary in a range from zero to the rated capacity. The number of capacity states in a wind generation model, therefore, is significantly higher than in conventional generation models to accommodate the wide variation in output capacity. Details regarding wind farm modeling are presented in the following chapters. An example of a 20 MW wind farm represented by a five state capacity model is shown in Table 2.6.

Table 2.6: Example of a wind farm capacity model

Capacity Out (MW)	Probability
0	0.004
5	0.250
10	0.340
15	0.276
20	0.130

2.6 Risk Indices

The wind farm capacity model and the equivalent conventional generation model are combined to create the overall generation model of the wind integrated power system. The recursive algorithm (2.3) can be used to convolve the generation models. The system generation model obtained by combining the conventional generation model in Table 2.5 and the wind farm model in Table 2.6 is shown in Table 2.7

Table 2.7: System generation model for the example system

Capacity Out (MW)	Probability	Capacity Out (MW)	Probability
0	0.0024429	65	0.0025453
5	0.1526828	70	0.0004873
10	0.2076485	75	0.0000169
15	0.1685618	80	0.0000463
20	0.0808529	85	0.0000538
25	0.0911294	90	0.0000390
30	0.1247112	95	0.0000153
35	0.1031790	100	0.0000000
40	0.0503254	105	0.0000001
45	0.0021483	110	0.0000002
50	0.0037372	115	0.0000001
55	0.0048924	120	0.0000001
60	0.0044837		

The developed system generation model is combined with the load model to obtain the risk indices. Loss of load is an undesired situation where the available generating capacity is insufficient to meet the load demand. Loss of load indices are widely used as a measure of the system reliability. The loss of load expectation (LOLE)[16] is the expected amount of time that loss of load occurs in a power system. The LOLE is expressed in hours/period if the LDC is used as the load model, and in days/period if the DPLVC is used as the load model. The term 'period' refers to the total duration covered by in the load model. This is 10 hours in the example LDC shown in Table 2.2. The period is usually a year in a practical system study. The LOLE in hours/period is calculated using (2.4).

$$LOLE = \sum_{i=1}^{n} P_i(C_i - L_i) \text{ hours/period} \qquad (2.4)$$

where,

C_i = available capacity on hour i.

L_i= peak load on hour i.

$P_i(C_i - L_i)$ = probability of loss of load on hour i, directly obtained from the generation capacity outage probability model.

Further explanation and illustrations regarding the evaluation of the LOLE are given in [16]. Other risk indices in general use are the Loss of Energy Expectation (LOEE), Units per Million (UPM), System Minutes (SM), etc. LOEE is the total expected amount of energy curtailed due to any system outage during the evaluation period. The UPM and SM are defined by (2.5) and (2.6) respectively [1], [35].

$$UPM = \frac{LOEE}{E} \times 10^6 \qquad (2.5)$$

$$SM = \frac{LOEE}{PL} \times 60 \qquad (2.6)$$

where,

E= Total energy demand for the evaluation period.

PL= System peak load.

The LOLE for the example system with 100 MW of conventional capacity, a 20 MW wind farm and a peak load of 85 MW was evaluated by combining the generation model in Table 2.7 with the load model in Figure 2.2 using (2.4). The resulting LOLE is 0.1657 hrs/period.

2.7 Peak Load Carrying Capability, Wind Capacity Credit and Wind Capacity Factor

The per-unit load model in Figure 2.3 can be used to evaluate the LOLE values for a range of peak loads for the example power system. The LOLE values for a range of peak loads are shown in Figure 2.4. Generally, power system planning is done using a pre-specified risk criterion. The generation facilities are planned in order to maintain the risk criterion for the forecast peak load. The peak load that an existing or a planned generation can carry while maintaining the risk criterion, is therefore, an important parameter in the planning process. The peak load carrying

capability (PLCC) of a power system is defined as the maximum peak load the power system can serve without exceeding the pre-specified risk criterion. Assuming the risk criterion to be 0.1 hr/(10 hr period), the PLCC for the example power system is shown to be 81.1 MW in Figure 2.4.

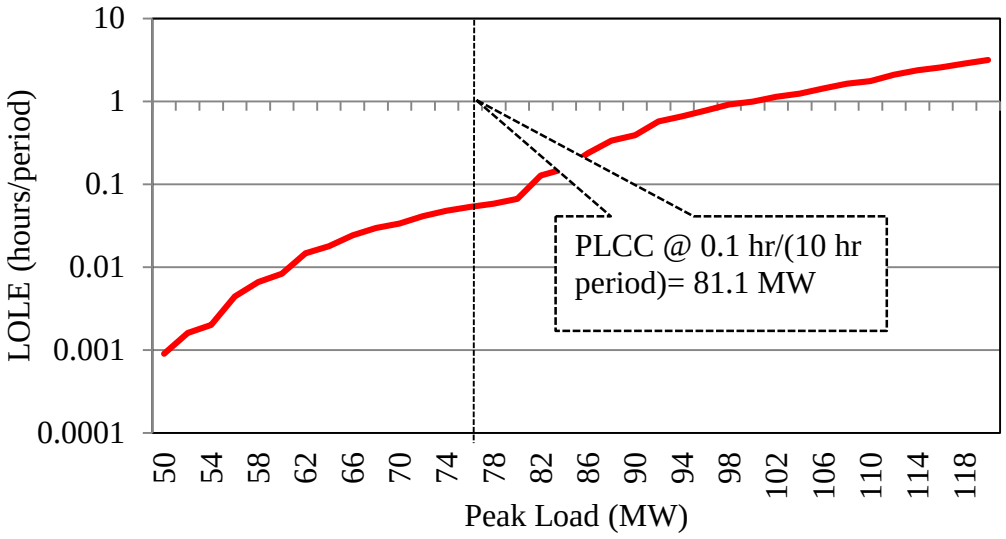

Figure 2.4: LOLE for a range of peak loads for the example power system

When wind farms are considered in the generation planning process, system planners are generally interested in knowing the capacity value of a wind farm addition. Indices that are widely used to evaluate the capacity worth of a wind farm are the capacity credit and the capacity factor.

The capacity credit (CC) of a wind farm is defined as the increase in the PLCC of a power system by adding the wind farm to the power system. Figure 2.5 shows the LOLE values for the example power system with and without the wind farm. Figure 2.5 also shows the PLCCs for the example power system with and without the wind farm. The increase in PLCC due to the addition of the wind farm in the example power system is 4.3 MW as shown in Figure 2.5. The wind capacity credit (CC) expressed as a percentage of the rated capacity of the wind farm is 21.5% in this case.

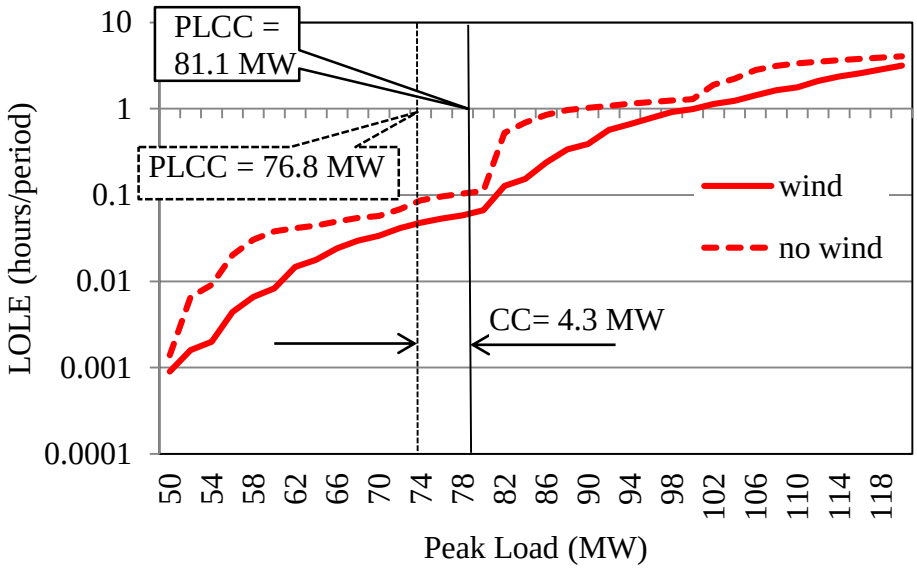

Figure 2.5: LOLE and PLCCs with and without wind

The Capacity Factor (CF) of a wind farm is the average or expected output capacity of the wind farm. The capacity factor of the example wind farm can be determined from the capacity model of the wind farm shown in Table 2.6 and is 8.61 MW or 43.05%.

2.8 Period Analysis

The LOLE evaluations done up to this point are based on the assumption that the conventional generation model, the wind model and the load model are applicable for the evaluation period, which is 10 hours in this case. Many situations can occur in which the models vary within the period of analysis. Seasonal deratings of the generating units, scheduled maintenance, variability of the basic wind and load characteristics are some examples in which the models vary within the period of analysis. A sub-period analysis should be performed in such cases. Sub-period analysis is the process of splitting the analysis period into smaller sub-periods, developing separate component models for each sub-period, evaluating the required risk index for each sub-period

and finally combining the risk indices of each sub-period to obtain the risk index of the entire period.

A case is considered for illustration assuming that the 30 MW generating unit is scheduled to be on maintenance from hour 3 to hour 5. The period of 10 hours should therefore be split to two sub-periods as shown in Table 2.8.

Table 2.8: Sub-division of the period for period analysis

Sub-period	Hours considered
i	(hour 0 to hour 2) and (hour 6 to hour 9)
ii	(Hour 3 to hour 5)

Separate generation models should therefore be developed for each sub period. The generation model for sub-period i is identical to the generation model shown in Table 2.7, whereas the generation model for sub-period ii only contains the 25 MW generating unit, the 45 MW multistate generating unit and the 20 MW wind farm. The system generation model for sub-period ii is shown in Table 2.9.

Table 2.9: System generation model for sub-period ii

Capacity Out (MW)	Probability	Capacity Out (MW)	Probability
0	0.0024676	50	0.0029500
5	0.1542250	55	0.0040120
10	0.2097460	60	0.0032568
15	0.1702644	65	0.0015340
20	0.0816696	70	0.0000002
25	0.0920000	75	0.0000125
30	0.1259460	80	0.0000170
35	0.1026634	85	0.0000138
40	0.0487151	90	0.0000065
45	0.0004502		

The hourly loads shown in Table 2.1 for 10 hours should also be separated into two groups based on the period chosen as shown in Table 2.10 and Table 2.11. It should be noted that the

peak load for sub-period i is 85 MW, which is the same as in the previous study, whereas the peak load of the sub-period ii is only 78 MW.

Table 2.10: Load data and load model for sub-period i

Original load data		**load arranged in a descending order**	
hour	**load (MW)**	**duration**	**load (MW)**
0	58	0	85
1	85	1	83
2	24	2	64
6	64	3	58
7	52	4	52
8	49	5	49
9	83	6	24

Table 2.11: Load data and load model for sub-period ii

Original load data		**load arranged in a descending order**	
hour	**load (MW)**	**duration**	**load (MW)**
3	65	0	78
4	78	1	65
5	28	2	28

The LOLE values for each sub-period evaluated using the corresponding generation and load models which are 0.1181 hrs/(7 hours) and 0.8188 hrs/(3 hours) for sub-period i and ii respectively. The risk indices of each sub-period can be added to obtain the index of the entire period. The system LOLE is 0.9369 hrs/(10 hours) in this case, which is much larger than in the previous study due to a generator being taken out of service for sub-period ii.

2.9 Load Forecast Uncertainty

The load model presented in Section 2.3 and subsequently used in this chapter is the forecast hourly load for a ten hour period. Load forecasts are required in the planning phase in order to

incorporate future load demands on the generation facilities and are generally based on existing load data and future system conditions which are unknown. This kind of uncertainty is termed as the load forecast uncertainty (LFU) and can be incorporated in the risk index evaluation process.

The LFU is generally incorporated by assuming the forecast peak load to be normally distributed [16] rather than as a single value used in the previous sections. The forecast peak load is considered as the mean, and the uncertainty as the standard deviation of the normal distribution. A seven-step normal distribution[16] that can be used to model the LFU is shown in Table 2.12.

Table 2.12: Seven-step normal distribution

No. of Standard Deviations from the mean	**Probability**
-3	0.006
-2	0.061
-1	0.242
0	0.382
1	0.242
2	0.061
3	0.006

The LFU value utilized in a practical risk evaluation is usually based on past experience, statistical analysis, and some subjective evaluation. A 4% LFU is used for illustration purposes in this section. The peak load of 85 MW is modeled as seven peak loads with corresponding probabilities as shown in Table 2.13. LOLE values are then evaluated for each peak load case as shown in Table 2.13. Each LOLE value are then weighted with the corresponding probability of occurrence and finally added to obtain the system LOLE value which is also shown in Table 2.13.

Table 2.13: Incorporation of 4% LFU

No. of standard deviation from mean	Forecast peak load (MW)	Probability	LOLE (hrs/pd)	Weighted LOLE(hrs/pd)
-3	85-(3*4)% of 85=74.8	0.006	0.0495	0.0002970
-2	85-(2*4)% of 85=78.2	0.061	0.0586	0.0035746
-1	85-(1*4)% of 85=81.6	0.242	0.1167	0.0282414
0	85+(0*4)% of 85=85	0.382	0.1657	0.0632974
1	85+(1*4)% of 85=88.4	0.242	0.3477	0.0841434
2	85+(2*4)% of 85=91.8	0.061	0.5520	0.0336720
3	85+(3*4)% of 85=95.2	0.006	0.7135	0.0042810
	∑weighted LOLE(hrs/pd) =			0.2175068

Table 2.13 shows that the LOLE value obtained considering 4% LFU is 0.2175 hrs/(10 hour) which is considerably larger than the LOLE of 0.1657 hrs/(10 hour) obtained without LFU.

2.10 Conclusion

The basic concepts regarding an adequacy evaluation of a wind integrated power system is briefly introduced in this chapter. The process of load and conventional generation modeling are presented. A simple power system with three conventional generating units and one wind farm is used to illustrate the concepts and the adequacy evaluation methodology. The period of analysis, which is generally a year, was considered to be only 10 hours in order to simplify the application. An example five-state wind model is used to illustrate the basic concepts without involving detailed wind modeling which is discussed in the following chapters. The example power system and models are extremely simple but hopefully serve to explain the basic concepts used in the more detailed analysis in the following chapters.

3 INCORPORATION OF CORRELATION BETWEEN WIND SPEED AND LOAD

3.1 Introduction

A basic reliability evaluation of a power system using an analytical method is generally done on an annual basis [1]. The combined annual wind capacity model and the conventional generation model is convolved with the annual load model [1] to obtain the annual risk indices of the WIPS [22]. This approach does not incorporate the load following capability of the wind power. The method also cannot incorporate factors such as unit seasonal derating, unit maintenance, seasonal power import/export etc. Seasonal period analysis is required to overcome these challenges[1]. Seasonal analysis however, cannot incorporate the diurnal load following capability of the wind power. This chapter performs annual and seasonal period analysis of a WIPS and presents a technique to incorporate the correlation between load and wind during peak and off-peak periods of a day. The developed technique is applied to the IEEE- Reliability Test System (IEEE-RTS) [36] connected to a wind farm characterized by wind data from Swift Current, Saskatchewan. The IEEE-RTS has 3405 MW of conventional generating capacity and a forecast peak load of 2850 MW.

3.2 Basic Evaluations on an Annual Basis

3.2.1 Annual Wind Model

The development of a suitable wind model for reliability evaluation of a WIPS requires historical wind speed data collected over a large number of years. It has been shown [34]

however that the long term wind characteristics of a particular site can be represented by an ARMA model that can be written in the form of (3.1):

$$y_t = \Phi_1.y_{t-1} + \Phi_2.y_{t-2} + \cdots + \Phi_s.y_{t-s} + \alpha_t - \theta_1.\alpha_{t-1} - \theta_2.\alpha_{t-2} - \cdots \theta_m.\alpha_{t-m} \quad (3.1)$$

where Φ_i (i = 1, 2, 3,…, s) and θ_j (j = 1, 2, 3,…, m) are autoregressive and moving average coefficients of the wind model respectively. These coefficients can be calculated using the historical data of a site [34]. α_t is a Normally and Independently Distributed (NID) white noise process with zero mean and σ^2 variance generally expressed in the form $\alpha_t \in \text{NID}(0, \sigma^2)$. Equation (3.1) represents a time series for y, which can be generated using the value of α_t randomly generated for each time interval and the previous values of y and α. An hourly time interval is used in this study. The time series of y obtained using (3.1) can then be used to calculate the simulated hourly wind speeds using (3.2).

$$SW_t = \mu_t + \sigma_t.y_t \quad (3.2)$$

where,

SW_t = Simulated wind speed for hour t.

μ_t = Hourly mean wind speed for hour t.

σ_t= Hourly standard deviation of wind speed for hour t.

It should be noted that there are 8760 hourly mean and standard deviation values for a wind site obtained from its historical data. An ARMA model for the Swift Current site, which is located in Saskatchewan, Canada is presented in [37] and expressed in (3.3).

$$y_t = 1.1772y_{t-1} + 0.1001y_{t-2} - 0.3572y_{t-3} + 0.0379y_{t-4} + \alpha_t - 0.5030\alpha_{t-1} - 0.2924\alpha_{t-2} + 0.1317\alpha_{t-3} \quad (3.3)$$

$$\alpha_t \in NID(0, 0.524760^2)$$

α_t can be generated using a suitable normally distributed random number generator. For the initial four calculations, i.e., y_1 to y_4, the initial preceding values of y and α at the right hand side of (3.3) were assumed to be zero.

The hourly mean and standard deviation of the wind speed site at Swift Current was obtained from Environment Canada. A probability distribution of wind speed was developed using 2000 years of simulated data, and is shown in Figure 3.1.

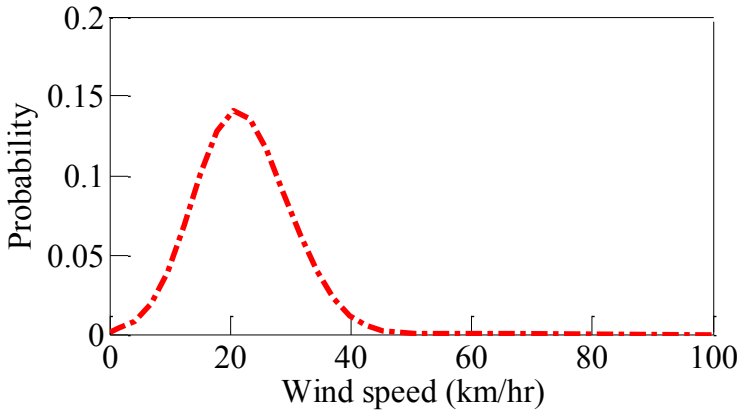

Figure 3.1: Wind speed probability distribution

The output power of a WTG at any time depends on the wind speed of the site at the time, the forced outage rate (FOR) and the characteristics of the WTG influenced by the cut in, rated and cut out speed. Cut-in speed (V_{ci}) is the minimum wind speed required for a WTG to generate power. Rated speed (V_r) is the wind speed required for a WTG to generate maximum or rated power. Cut-out speed (V_{co}) is the maximum wind speed that the WTG can safely handle, *i.e.*, the WTG is shut down for safety reasons at the cut-out speed. The relationship between wind speed (v) and the corresponding output power of a WTG is presented in [8] and can be expressed as (3.4).

$$p(v) = \begin{cases} 0\,, & 0 \le v \le V_{ci} \\ (A + Bv + Cv^2)P_r, & V_{ci} \le v \le V_r \\ P_{r,} & V_r \le v \le V_{co} \\ 0, & v \ge V_{co} \end{cases} \quad (3.4)$$

where, P_r is the rated capacity of the WTG, and the constants A, B and C depend on V_{ci}, V_r and V_{co} [8]. The V_{ci}, V_r and V_{co} of 15 km/h, 50 km/h, and 90 km/h respectively were used in this study. The relationship between wind speed (v) and the corresponding output power of a WTG as shown in (3.4) is represented graphically in Figure 3.2 and is called the WTG power curve.

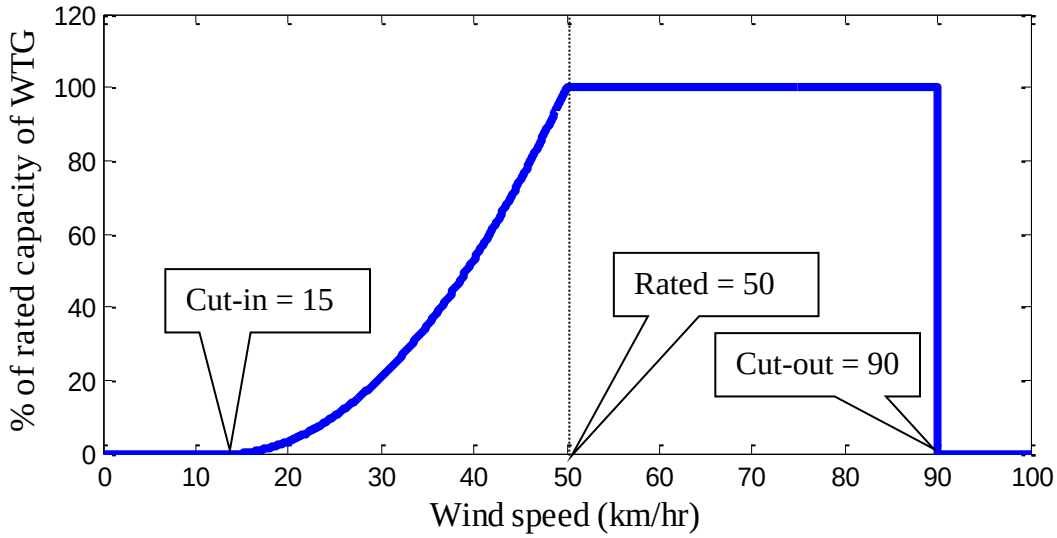

Figure 3.2: Wind power curve

The simulated hourly wind speeds were converted to hourly power output values using (3.4). The effect of the FOR of the WTGs in a wind farm can be considered in the evaluation of the power output model of the wind farm. It has, however, been shown in [32] that the FOR of a WTG can be omitted during a WECS reliability evaluation without losing unacceptable accuracy. The effect of FOR has therefore been omitted in this study to simplify the wind model. Another assumption made in this study is that all the WTGs in a wind farm experience the same wind speed in any particular hour.

Hourly power generation obtained using (3.4) can be grouped into a suitable number of class intervals in ascending or descending order to obtain the wind capacity model. This model is a probability distribution of different capacity output states which can either be expressed as a capacity outage probability table (COPT) [1] or a capacity available probability table (CAPT). Sturges' Rule [38] was used to determine the appropriate number of class intervals (NoCI) using (3.5) while grouping the data .

$$NoCI = 1 + 3.3\, log_{10}(8760 \times N) \qquad (3.5)$$

where, (8760 × *N*) is the number of data points considered.

The number of class intervals for 2000 sample years calculated from (3.5) is therefore 25. The class size (CS) is calculated using (3.6):

$$CS = TIC/NoCI \qquad (3.6)$$

where,

$TIC = \sum_{k=1}^{NWTG} P_{rk}$ is the total installed capacity of the wind farm under consideration.

P_{rk} = rated capacity of *WTG k*.

$NWTG$ = number of *WTG* in the wind farm.

If the wind capacity model is represented by a COPT with $NoCI$ capacity states then the capacity outage, CO_i for a state i is given by (3.7). The probability of CO_i outage state $P(CO_i)$ is given by (3.8):

$$CO_i = TIC - [(i-1)CS + CS/2] \qquad (3.7)$$

$$P(CO_i) = DP_i/(8760 \times N) \qquad (3.8)$$

where, DP_i is the number of wind power data points in the interval i.

Similarly, if the wind capacity model is represented by a CAPT with $NoCI$ available capacity states then the capacity available, CA_j for a state j is given by (3.9). The probability of CA_j available state $P(CA_j)$ is given by (3.10):

$$CA_j = (j-1)CS + CS/2 \qquad (3.9)$$

$$P(CA_j) = DP_j/(8760 \times N) \qquad (3.10)$$

The CAPT for the Swift Current wind farm site obtained using the above method and 2000 years of synthetic hourly data is shown in Figure 3.3.

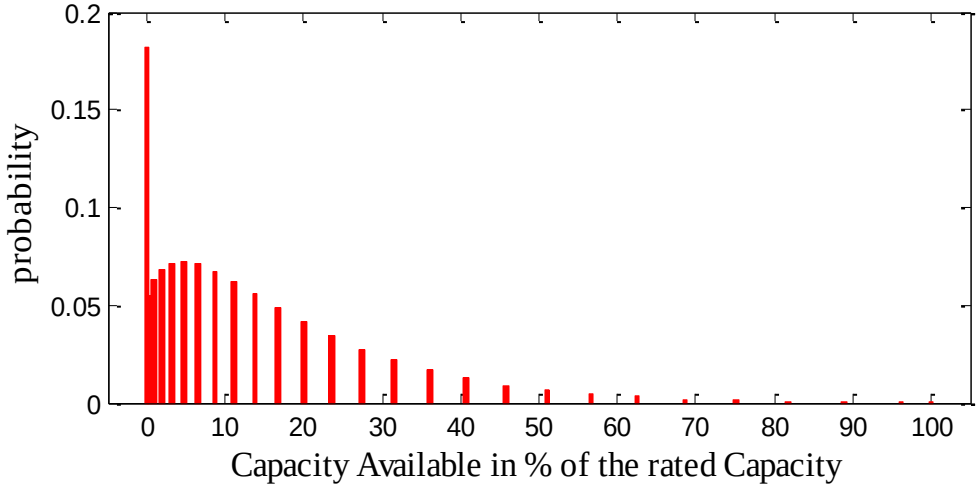

Figure 3.3: Annual CAPT for Swift Current

The capacity model shown in Figure 3.3 can be simplified by reducing the number of capacity states using the apportioning method presented in [17]. The step size of the reduced capacity model, y is given by (3.11).

$$y = TIC/(n-1) \qquad (3.11)$$

where, n is the number of states (NoS) of the reduced CAPT or COPT. The denominator in (3.11) has been taken as (n−1) so as to include 0% and 100% of TIC in the reduced capacity

model. The annual wind capacity model in Figure 3.3 was reduced to 11 states using the method described above and is shown in Figure 3.4.

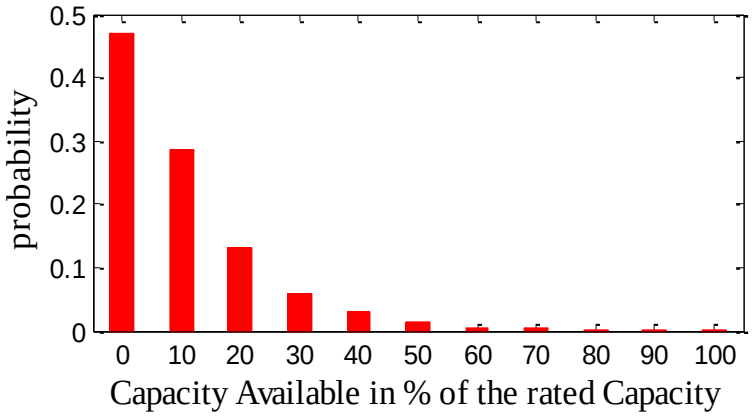

Figure 3.4: 11 state annual CAPT for Swift Current

3.2.2 Analysis and Results

The IEEE Reliability Test System (IEEE-RTS) [36] has been extensively used in the research work presented in this thesis to test the effectiveness of the proposed techniques. The IEEE-RTS is a system proposed by an IEEE task force for testing and comparison purposes. It has 32 generating units ranging from 12 MW to 400 MW capacities with a total installed capacity of 3405 MW. The system peak load is 2850 MW. The list of generating units and hourly load model of the IEEE-RTS is given in Appendix A.

The annual wind capacity model obtained in Section 3.2.1 was convolved with the generation model of the IEEE-RTS. Evaluations were done for wind penetrations of 5%, 10%, 15% and 20% corresponding to installed wind capacities of 179 MW, 378 MW, 601 MW, and 851 MW, respectively. The hourly load model for Saskatchewan in a typical year shown in Figure 3.5 was used in this study. Saskatchewan load is a winter peaking load. The loss of load expectation (LOLE) [39] of the system shown in Figure 3.6 was evaluated for a range of peak loads and is shown in Figure 3.7. The load forecast uncertainty (LFU) was considered to be 4% in the study.

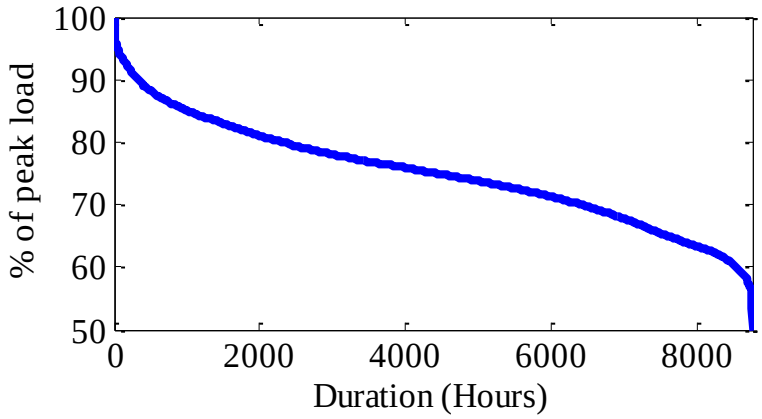

Figure 3.5: Load duration curve for a typical Saskatchewan year

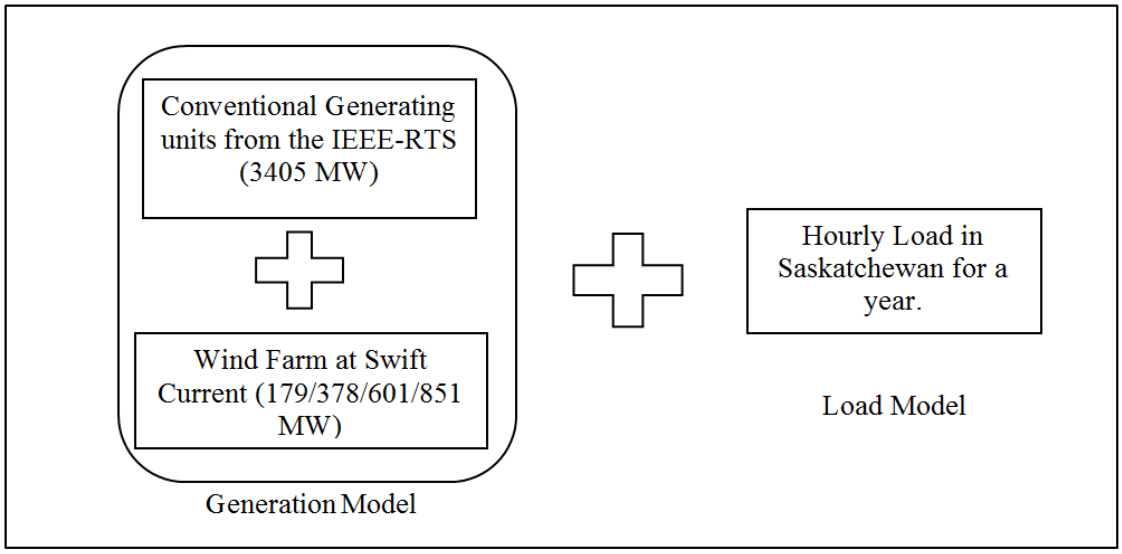

Figure 3.6: IEEE-RTS power system considered for the study

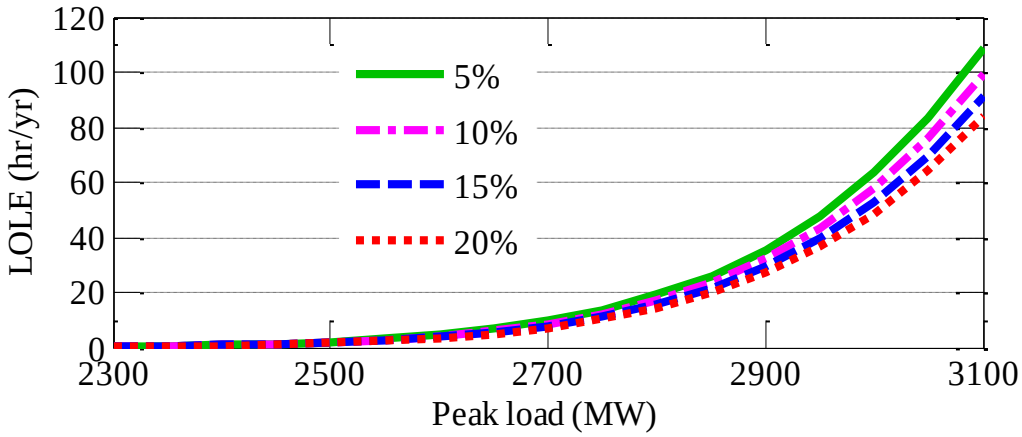

Figure 3.7: LOLE for IEEE-RTS connected to a wind farm with different penetration levels

An analysis was also performed for the electric power system in Saskatchewan, Canada operated by SaskPower. The conventional generating units connected to the Saskatchewan power system at the end of 2010 were used for the study. The conventional generating units considered consist of hydroelectric power plants, coal power plants, natural gas power plants, etc. with a total installed capacity of 3815 MW. The load model of a typical Saskatchewan year shown in Figure 3.5 was used in the study. The hourly power output of a Saskatchewan wind farm located at Centennial was used to create a wind model in the form of a CAPT. The rated capacity of the Centennial wind farm is 149.4 MW. The power system considered in this study is shown in Figure 3.8. System LOLE values of the Saskatchewan power system connected to the Centennial wind farm were obtained for the range of peak loads shown in Figure 3.9. The load forecast uncertainty was considered to be 4% in this study.

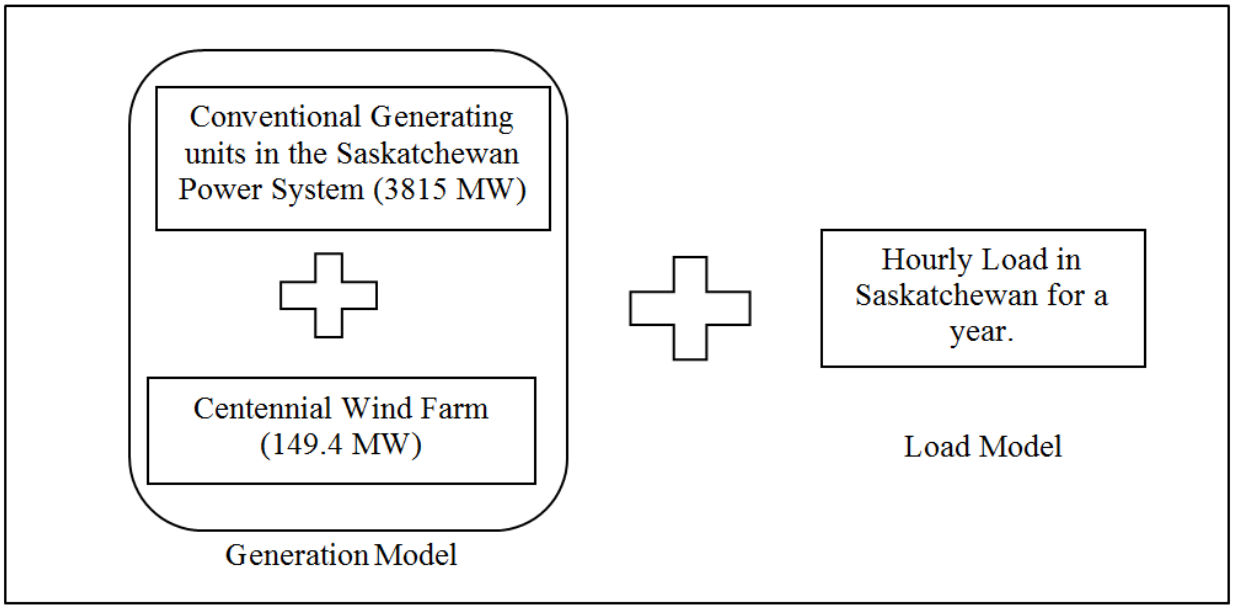

Figure 3.8: Saskatchewan power system considered for the study

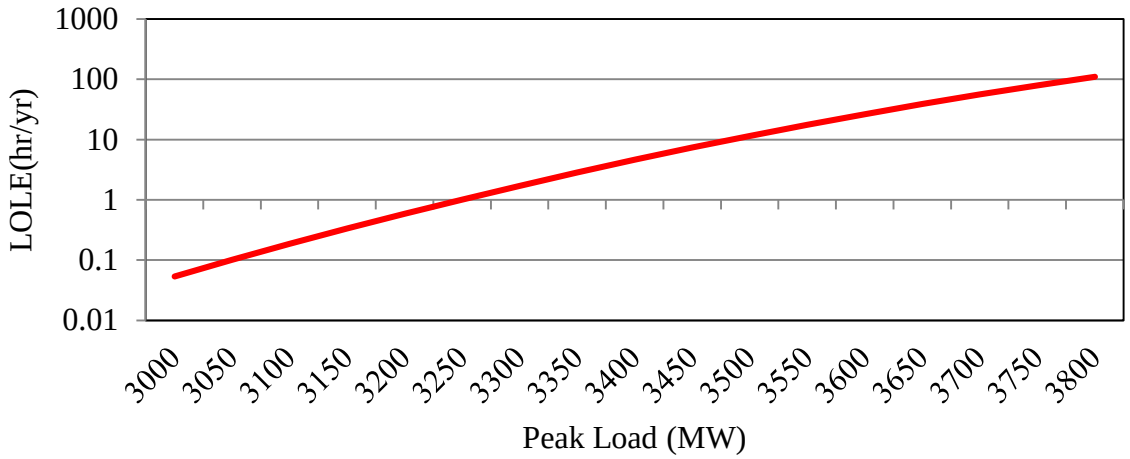

Figure 3.9: LOLE for Saskatchewan power system connected to centennial wind farm (149.4 MW) evaluated on an annual basis

3.3 Seasonal Evaluation

The chronological variation of the wind speed at the Swift Current site and the system load in a sample year is shown in Figure 3.10. It can be seen that there is a load following pattern in the wind profile. The seasonal load following capability of a wind resource can be incorporated in the adequacy assessment of a power system using period evaluation. The annual period was divided into four seasonal sub-periods as shown in Table 3.1 in an adequacy evaluation of the Saskatchewan system.

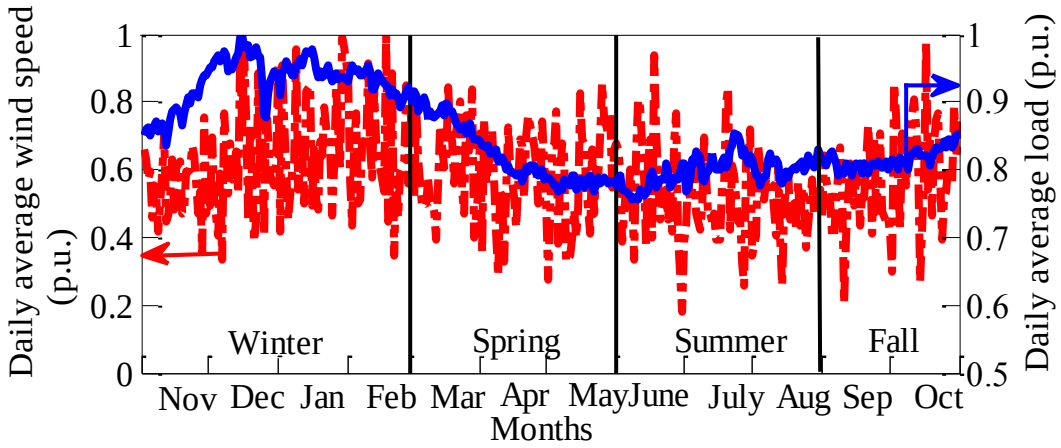

Figure 3.10: Load and wind speed for a sample year

Table 3.1: Seasonal sub-periods

Season	Months
Winter	November-February
Shoulder 1	March-May
Summer	June-August
Shoulder 2	September-October

Period analysis is the process of dividing the annual period into smaller sub-periods and evaluating the reliability indices for each sub-period. The indices from each sub-period are then summed to obtain the annual indices. A period analysis was carried out for the IEEE-RTS by creating a load model and a wind model for each sub-period. The annual load and wind capacity models for each sub-period are shown in Figure 3.11 and Figure 3.12, respectively. It should be noted that the load in Figure 3.11 is expressed in per unit of the peak for the respective season. The LOLE for a range of annual peak loads were evaluated using the period analysis. The results are shown in Table 3.2. All the evaluations were done considering a load forecast uncertainty of 4%.

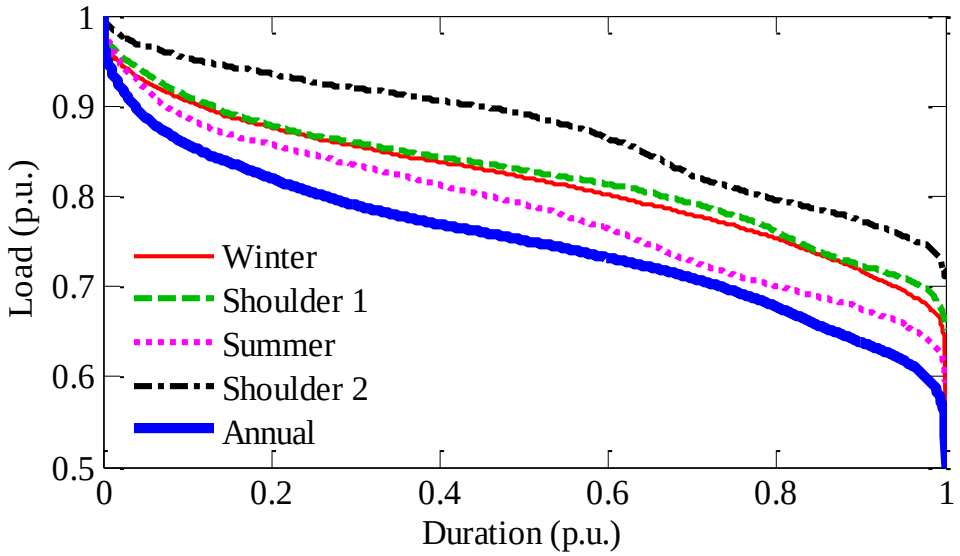

Figure 3.11: Annual and Seasonal load models used in the study

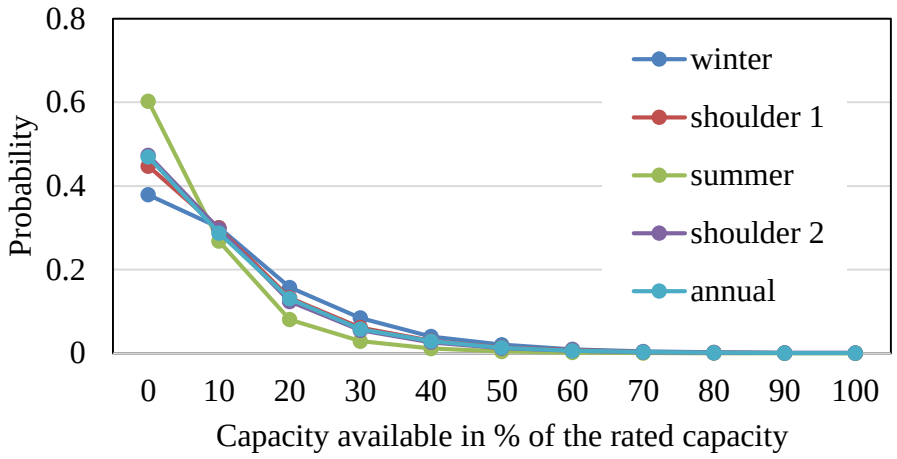

Figure 3.12: Annual and seasonal wind models for the Swift Current site

Table 3.2: IEEE-RTS LOLE (hrs/yr) connected to the Swift Current wind farm using annual and seasonal period analysis

Peak Load (MW)	5% penetration		10% penetration		15% penetration		20% penetration	
	annual	seasonal	annual	seasonal	annual	seasonal	annual	seasonal
2300	0.372	0.359	0.325556	0.304553	0.291676	0.265830	0.266	0.237
2400	0.925	0.896	0.519933	0.487835	0.466612	0.426802	0.669	0.601
2500	2.144	2.082	0.815206	0.766979	0.732587	0.672325	1.566	1.417
2600	4.692	4.565	1.253418	1.182247	1.128097	1.038603	3.458	3.147
2700	9.724	9.482	1.900185	1.796479	1.712631	1.581427	7.237	6.622
2800	19.063	18.629	2.836731	2.687065	2.560565	2.370625	14.323	13.180
2900	35.510	34.775	4.177875	3.965267	3.777173	3.505916	26.963	24.959
3000	63.370	62.170	6.068694	5.770281	5.495222	5.112726	48.595	45.230
3100	108.601	106.732	8.704241	8.291154	7.894801	7.362487	84.104	78.692

The difference in the calculated indices suggests that an annual analysis is not adequate, and that seasonal correlations between the load and wind speed are important consideration especially at high penetration levels.

Seasonal evaluation was also conducted for the Saskatchewan power system shown in Figure 3.8 which includes the Centennial wind farm (149.4 MW). Seasonal load and wind models were developed considering the four seasonal sub-periods shown in Table 3.1. The results obtained considering a 4% LFU are shown in Figure 3.13.

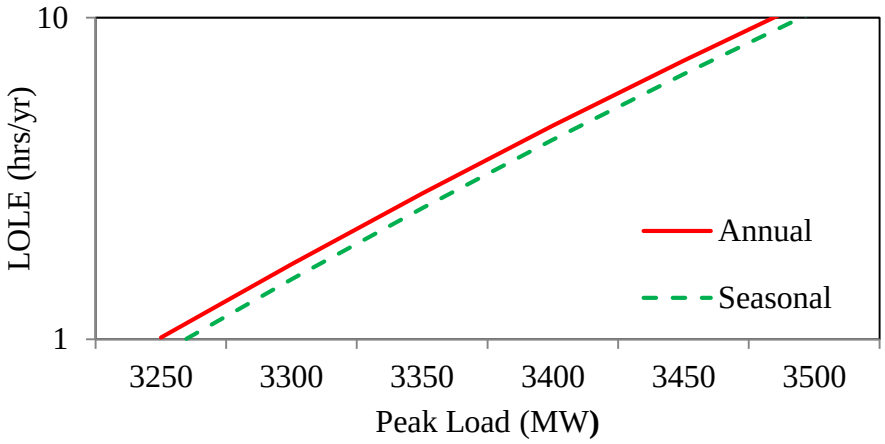

Figure 3.13: LOLE for the Saskatchewan power system which includes the Centennial wind farm using annual and seasonal period analysis

3.4 Diurnal Evaluation

Both the system load and the wind at a particular site have a specific diurnal variation pattern. Figure 3.14 shows the load and wind patterns for a typical day in winter and in summer. It can be seen that the wind on a typical summer day has a strong load following capability, whereas this capability is greatly reduced on a typical winter day.

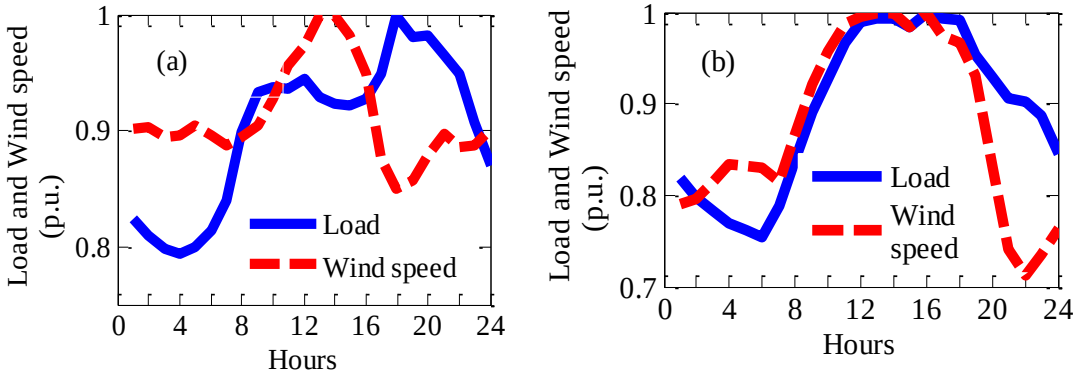

Figure 3.14: Load and wind speed of a typical day during (a) winter, and (b) summer seasons

A realistic reliability evaluation of this load following capability can be incorporated using hourly sub-periods. This approach however, is very cumbersome. The method can be greatly

simplified by considering only two diurnal sub-periods for the entire season. The peak load period generally makes the highest contribution to the overall annual reliability indices and therefore the correlation between load and wind during this period should be carefully incorporated in the evaluation to obtain accurate results. Two sub-periods constituting the peak and off-peak hours of a day are considered in this study.

The contribution of wind power to avoiding load curtailments during the peak hours of the year is important in assessing the capacity value of wind sources. The capacity credit of wind in the Pennsylvania-New Jersey-Maryland (PJM) interconnected system is calculated based on the wind generation during the peak 5 hours from 3 PM to 7 PM of the peak season from June 1 through August 31 [25, 30]. The New York Independent System Operator determines wind capacity credit using the wind generation between 2-6 PM from June through August and 4-8 PM from December through February [25, 30]. The peak 5 hours of the day in the winter season was, therefore, considered in this study to determine the peak load period for the diurnal evaluation. The system load was above 98% of the peak load as shown in Fig. 3.15 (a). The duration for which the system load exceeds 98% of the daily peak was therefore considered as the diurnal peak load period for each season. Fig. 3.15 shows average load data for a day normalized by the daily peak load for each season. Fig. 3.15 (b) shows the peak and the off-peak load periods of an average summer day. The peak periods for each season are presented in Table 3.3. The remaining hours of day are off-peak hours.

The wind capacity models and the load models were developed for each diurnal sub-period. The diurnal wind models and load models are shown in Figure 3.16 and Figure 3.17 respectively. The LOLE obtained for a range of peak loads using the diurnal analysis considering 4% LFU are shown in Table 3.4 and Table 3.5.

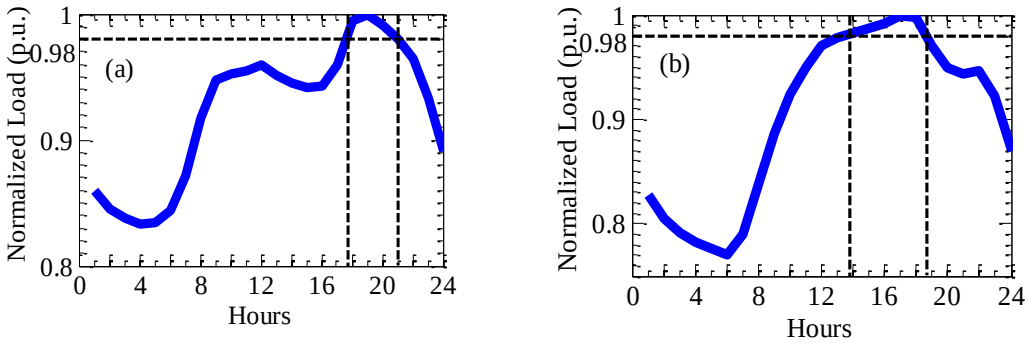

Fig. 3.15 : Normalized daily load data for (a) winter, and (b) summer seasons

Table 3.3: Peak Load Duration

Season	**Peak hours**
Winter	17th-21st hour
Shoulder 1	9th-22nd hour
Summer	12th-19th hour
Shoulder 2	15th-22nd hour

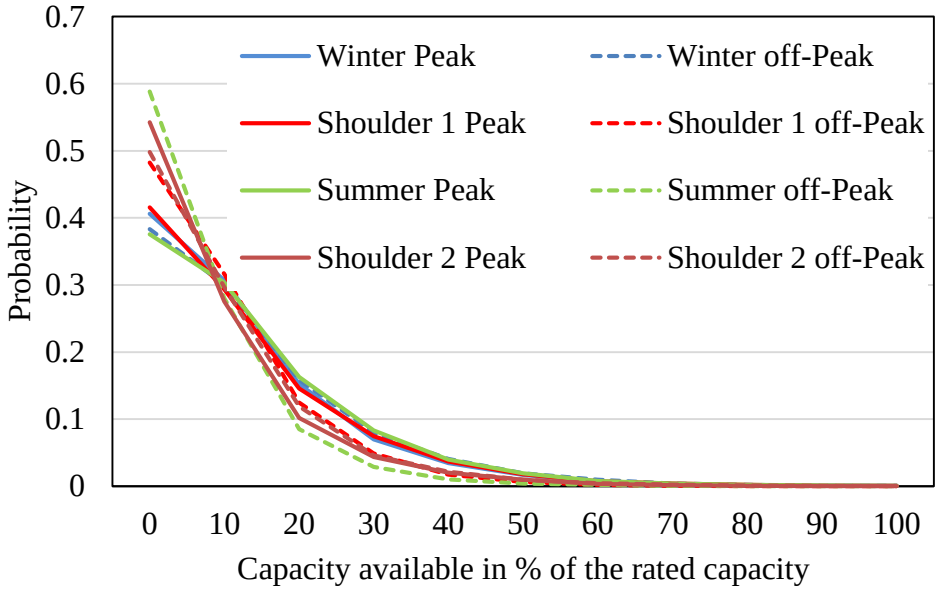

Figure 3.16: Diurnal wind capacity models for each season

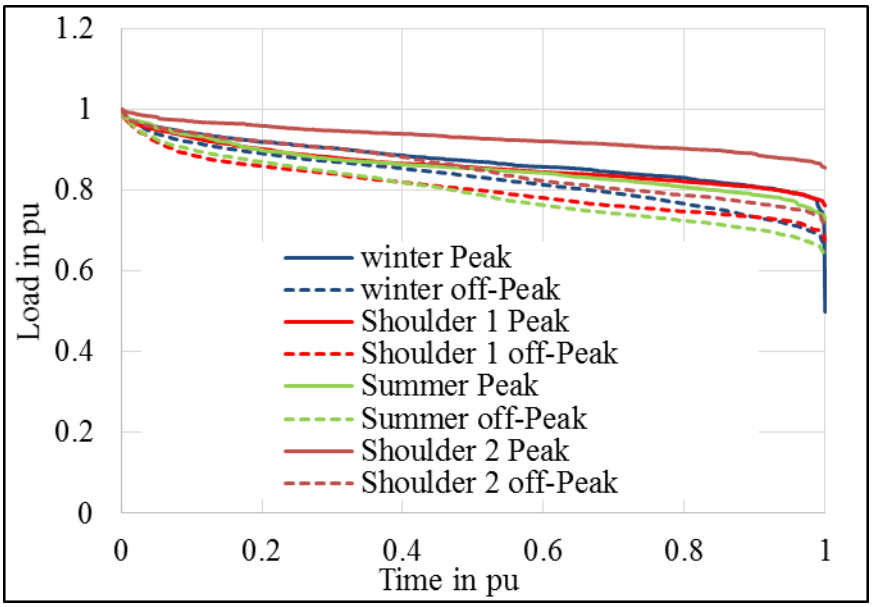

Figure 3.17: Diurnal load duration curves for each season

Table 3.4: LOLE for the IEEE-RTS connected to the Swift Current wind farm for 5% and 10% wind penetrations

Peak Load (MW)	5% penetration			10% penetration		
	Annual	Seasonal	Diurnal	Annual	Seasonal	Diurnal
2300	0.372	0.359	0.360	0.326	0.305	0.307
2350	0.592	0.572	0.574	0.520	0.488	0.491
2400	0.925	0.896	0.899	0.815	0.767	0.772
2450	1.418	1.375	1.379	1.253	1.182	1.189
2500	2.144	2.082	2.087	1.900	1.796	1.806
2550	3.193	3.103	3.111	2.837	2.687	2.701
2600	4.692	4.565	4.575	4.178	3.965	3.983
2650	6.798	6.621	6.635	6.069	5.770	5.796
2700	9.724	9.482	9.500	8.704	8.291	8.324
2750	13.711	13.381	13.405	12.308	11.745	11.788
2800	19.063	18.629	18.655	17.156	16.406	16.458
2850	26.164	25.598	25.626	23.600	22.614	22.673
2900	35.510	34.775	34.804	32.120	30.834	30.900
2950	47.670	46.725	46.758	43.224	41.565	41.639
3000	63.370	62.170	62.200	57.595	55.474	55.554
3050	83.358	81.847	81.880	75.946	73.267	73.353
3100	108.601	106.732	106.771	99.155	95.810	95.913

Table 3.5: LOLE for the IEEE-RTS connected to the Swift Current wind farm for 15% and 20% wind penetrations

Peak Load	15% penetration			20% penetration		
(MW)	Annual	Seasonal	Diurnal	Annual	Seasonal	Diurnal
2300	0.292	0.266	0.269	0.266	0.237	0.240
2350	0.467	0.427	0.431	0.426	0.381	0.385
2400	0.733	0.672	0.678	0.669	0.601	0.607
2450	1.128	1.039	1.047	1.031	0.929	0.938
2500	1.713	1.581	1.593	1.566	1.417	1.429
2550	2.561	2.371	2.387	2.342	2.126	2.143
2600	3.777	3.506	3.528	3.458	3.147	3.172
2650	5.495	5.113	5.144	5.034	4.594	4.627
2700	7.895	7.362	7.404	7.237	6.622	6.667
2750	11.177	10.448	10.503	10.254	9.408	9.466
2800	15.606	14.626	14.693	14.323	13.180	13.252
2850	21.510	20.214	20.292	19.759	18.238	18.323
2900	29.328	27.628	27.717	26.963	24.959	25.057
2950	39.533	37.330	37.430	36.389	33.781	33.893
3000	52.748	49.918	50.028	48.595	45.230	45.353
3050	69.648	66.053	66.174	64.265	59.973	60.107
3100	91.083	86.572	86.706	84.104	78.692	78.841

The system LOLE values for 5% and 20% wind penetration are shown in Figure 3.18 for graphical comparison. The peak load carrying capability (PLCC) of the system for different penetration levels at a LOLE criterion of 1 hr/yr were also calculated for all the methods and are shown in Table 3.6.

It can be seen from Table 3.4-3.6 and Figure 3.18 that there is a noticeable difference in the evaluated indices between the annual and the seasonal analysis but only very small difference in the evaluated indices between the seasonal and the diurnal analysis. The results however, should not be interpreted as diurnal analysis being unnecessary. The results largely depend on the wind regime and the load characteristics. The results from a diurnal analysis could be significantly different in other systems. Diurnal analysis should therefore be considered to obtain accurate adequacy indices.

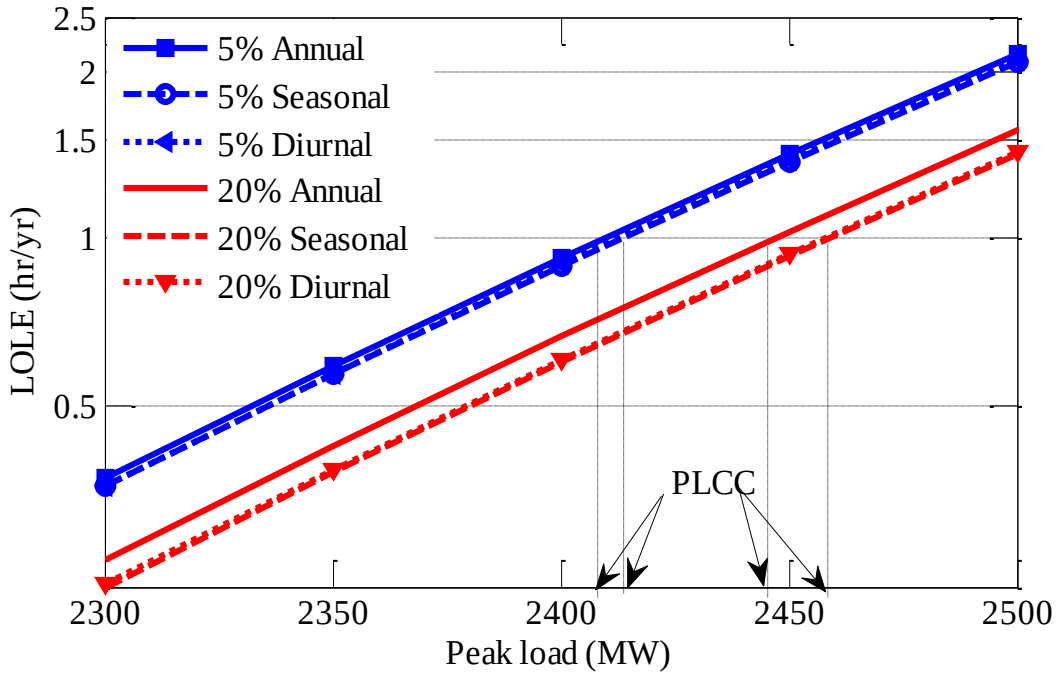

Figure 3.18: LOLE and PLCC (at a LOLE criterion of 1 hr/yr) for the IEEE-RTS connected to the Swift Current wind farm

Table 3.6: PLCC (MW) at a LOLE criterion of 1 hr/yr for the IEEE-RTS connected to the Swift Current wind farm

Penetration	**0%**	**5%**	**10%**	**15%**	**20%**
Annual	2392	2410	2424	2436	2447
Seasonal	2392	2413	2431	2446	2459
Diurnal	2392	2413	2430	2445	2458

Diurnal evaluations were also done for the Saskatchewan power system connected to Centennial wind farm. Diurnal wind capacity models of the Centennial wind farm were developed for the diurnal sub-periods shown in Table 3.3. The results obtained are shown in Figure 3.19.

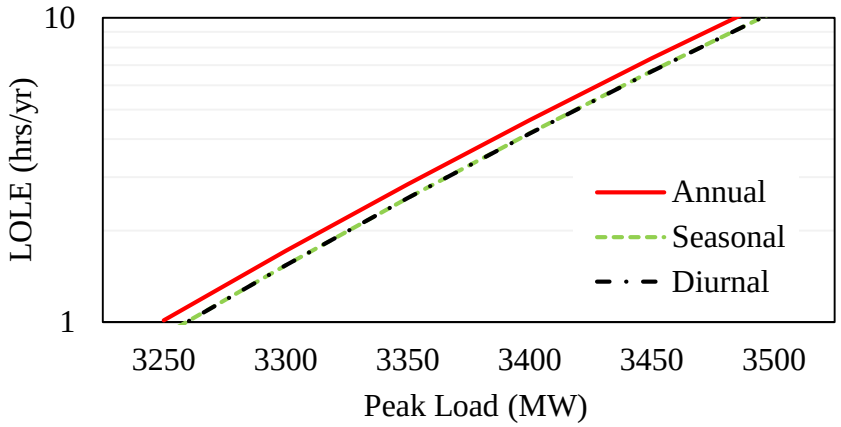

Figure 3.19: LOLE for the Saskatchewan power system connected to the Centennial wind farm using annual, seasonal and diurnal analysis

3.5 Conclusion

This chapter introduces the concept of correlation in the wind and load variations and describes methods to incorporate them in adequacy evaluation. The basic evaluation method on an annual basis is first presented with appropriate wind and load models. The period analysis method is then utilized to incorporate the seasonal load following capability of wind. This chapter also describes an analytical technique to recognize the diurnal load following capability of wind using a sub-period analysis for peak load and off-peak hours of a day. The results obtained from the test system show the differences in the system indices when the seasonal load following capability of wind is incorporated. The results obtained using diurnal analysis are close to those from the seasonal analysis. The results could, however, be quite different for wind regimes that have strong diurnal load following capability during the peak load season. The method presented can be used to investigate the impact of diurnal load following capability of wind in adequacy evaluation of wind integrated power systems, and applied if the impacts are significant.

4 INCORPORATING CORRELATION IN WIND SPEED BETWEEN WIND FARMS

4.1 Introduction

The impact of the accuracy of the wind models on the accuracy of the system reliability indices increases as the wind penetration in a power system increases. The cross correlations between the wind speeds of multiple wind farms play an important role in the combined power output characteristics of the wind farms. Poorly correlated wind farms tend to have lower intermittency in the overall power output characteristics compared to highly correlated wind farms that tend to have higher intermittency in the overall power output characteristics. The impact of such variation in intermittency due to the inherent correlation in wind speeds between the wind farms is significant, specially at substantial penetration levels. It is therefore important to incorporate these correlations in the wind models.

Studies have been done to incorporate the effect of correlation in wind speeds between multiple wind farms in reliability studies [9–13, 23]. An auto-regressive time series based mathematical model for wind speeds of correlated wind farms was introduced in [23]. Reference [11] used auto regressive and moving average (ARMA) model to generate wind speeds of correlated wind farms using correlated random number seeds, and studied the impact of correlations on the adequacy indices of a WIPS using sequential Monte Carlo Simulation (MCS). The results showed that correlation has considerable impact in adequacy indices of a WIPS. Reference [12] used a genetic algorithm to obtain the optimum random number seeds to generate wind speeds of correlated wind farms and used Monte Carlo simulation to study the

effect of wind penetration and correlation on system risk. Reference [9] introduced an analytical model of a WECS using conditional probabilities to obtain a joint model of correlated WECSs. References [12] and [13] used this conditional method to build an analytical wind model. It is important to develop simple models that are readily acceptable in real world reliability evaluation applications. Studies have been done to reduce the number of states in multi-state models to simplify the evaluation. Reference [19] suggests a simple seven-state analytical wind model. The correlation between multiple wind farms was, however, not considered in the study. The methods used in [11]–[13], [23] to generate correlated random number seeds are quite complex. The research work described in this chapter uses a simple algorithm using Cholesky decomposition [40] to generate correlated random numbers to recognize the correlation between two wind farms. The chapter focuses on simplifying the wind models incorporating wind correlations and wind penetration levels.

4.2 Wind Data Modeling for Correlated Wind Farms

Two sites each having the wind characteristics of Swift Current represented by (3.3) are considered in this work. Independently simulating the two sets of wind speed data using (3.3) resulted in correlations close to zero. The two sets of wind speed data are therefore simulated with random numbers in order to obtain a specified correlation between the two sites. The impact of wind correlation on the system reliability was then investigated. Correlation between two sets of simulated wind speed data can be established using correlated random numbers during the hourly simulation [11]. The correlation between the two sets of simulated wind speed data obtained is close to the correlation between the random numbers used. Various methods are available that can be used for the generation of correlated random numbers. The Cholesky

Decomposition [40] method is used in this paper. Cholesky Decomposition is the process of decomposing any symmetric and positive definite matrix into the product of two triangular matrices as represented by (4.1).

$$A = G^T . G \tag{4.1}$$

where, A = A symmetric positive definite matrix,

G = An upper triangular matrix with positive diagonal entries.

G^T = Transpose of matrix *G*.

A set of *r* uncorrelated random number series may be represented by matrix *X* shown in (4.2).

$$X = \begin{bmatrix} x_1^1 & \cdots & x_1^r \\ \vdots & \ddots & \vdots \\ x_q^1 & \cdots & x_q^r \end{bmatrix} \tag{4.2}$$

where, each column of matrix *X* is an uncorrelated random number series with q members. The desired correlation between any two sets of series may then be represented by (4.3).

$$A = \begin{bmatrix} a_{11} & \cdots & a_{1r} \\ \vdots & \ddots & \vdots \\ a_{r1} & \cdots & a_{rr} \end{bmatrix} \tag{4.3}$$

where, a_{ij} is the desired correlation between i^{th} and j^{th} column of matrix *X*. Upper triangular matrix *G* can then be calculated using Cholesky Decomposition. Matrix X_c which contains r correlated random number series as defined in matrix A can be deduced using (4.4).

$$X_c = X . G \tag{4.4}$$

This method can be simplified when only two random number series are present as shown in (4.5).

$$X_c = X_1 . \zeta + X_2 . \sqrt{1 - \zeta^2} \tag{4.5}$$

where, X_1 and X_2 are a series of uncorrelated random numbers. ζ is the desired correlation coefficient. Series X_c calculated using (4.5) has a correlation of ζ with series X_1. A particular case

was considered taking $\zeta = 0.5$. The scatter plots of 1000 pairs of correlated random numbers are shown in Figure 4.1 (b). Figure 4.1 (a) shows the scatter plots when the 1000 pairs of random numbers are uncorrelated.

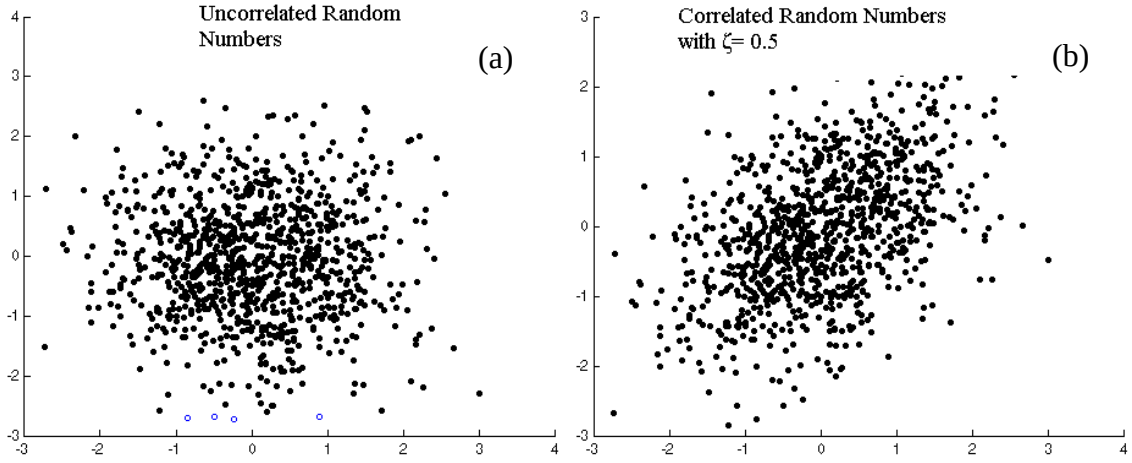

Figure 4.1: Generation of correlated random numbers using Cholesky decomposition. (a) Uncorrelated random numbers; (b) Correlated random numbers with $\zeta = 0.5$.

Two separate wind speed series can be synthesized using correlated random numbers X_1 and X_c in (3.2) and (3.3). The hourly mean and hourly standard deviation values used for the Swift Current site were obtained from Environment Canada. Two pairs of wind speed data series were simulated using $\zeta = 0$ and $\zeta = 0.5$. The scatter plots for 1000 data pairs for two cases are shown in Figure 4.2.

It can be seen from Figure 4.1 and Figure 4.2 that the pairs of wind speed series simulated using (3.2) and (3.3) have a correlation close to the correlation of the random numbers used. The actual correlation between the two pairs of simulated wind speed series using random numbers with $\zeta = 0$ and $\zeta = 0.5$ were 0.11 and 0.56 respectively. The wind speed profile for the 21st and 22nd day are shown in Figure 4.3 and Figure 4.4 respectively for the two cases to illustrate how the wind speeds follow each other at the two correlation levels.

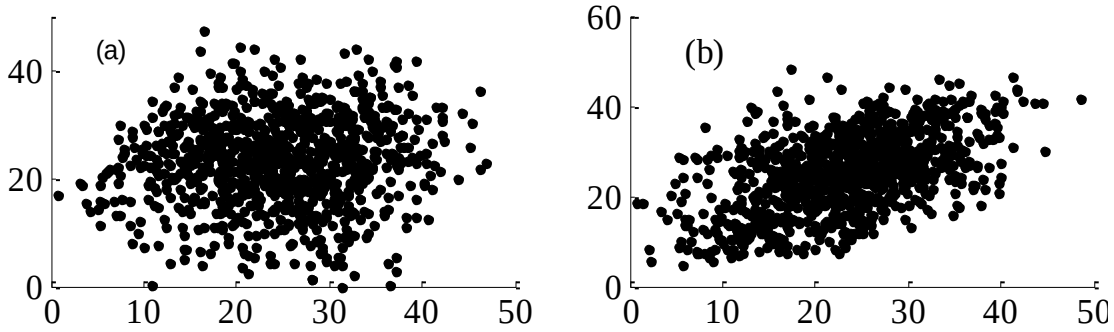

Figure 4.2: Simulated wind speeds, (a) using uncorrelated random numbers (b) using correlated random numbers with ζ =0.5

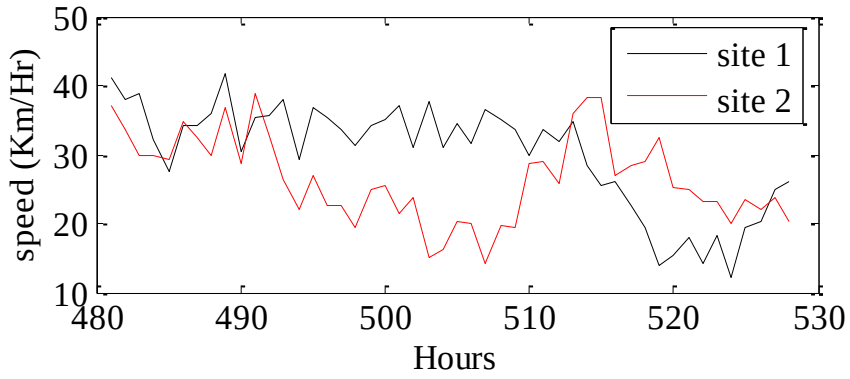

Figure 4.3: 2-day sample simulation of wind speeds for the two sites with a correlation of 0.11.

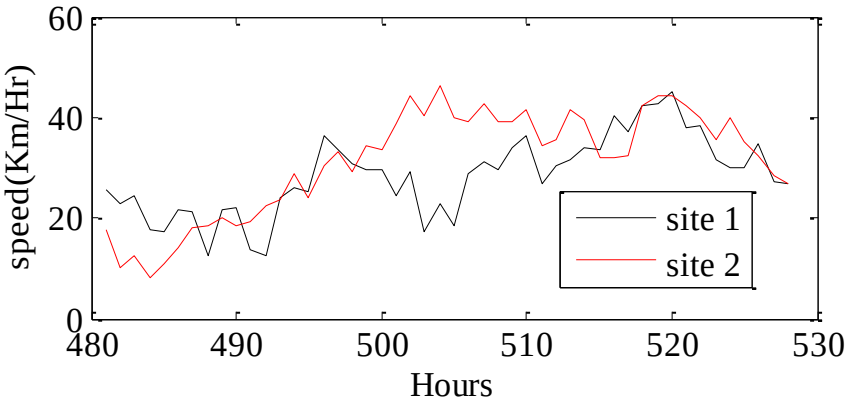

Figure 4.4: 2-day sample simulation of wind speeds for the two sites with a correlation of 0.56.

Wind speeds in Figure 4.4 follow each other more closely than the ones in Figure 4.3 due to the induced correlation. The actual correlation obtained in the simulated wind speeds of the

two sites were very close to the correlations of random numbers used. Pairs of correlated wind speed data were simulated with correlations 0, 0.25, 0.5, 0.75 and 1 using the same ARMA model for Swift Current for 8000 sample years. The probability distribution of the wind speed for all of the generated series with varying correlations is given in Figure 4.5.

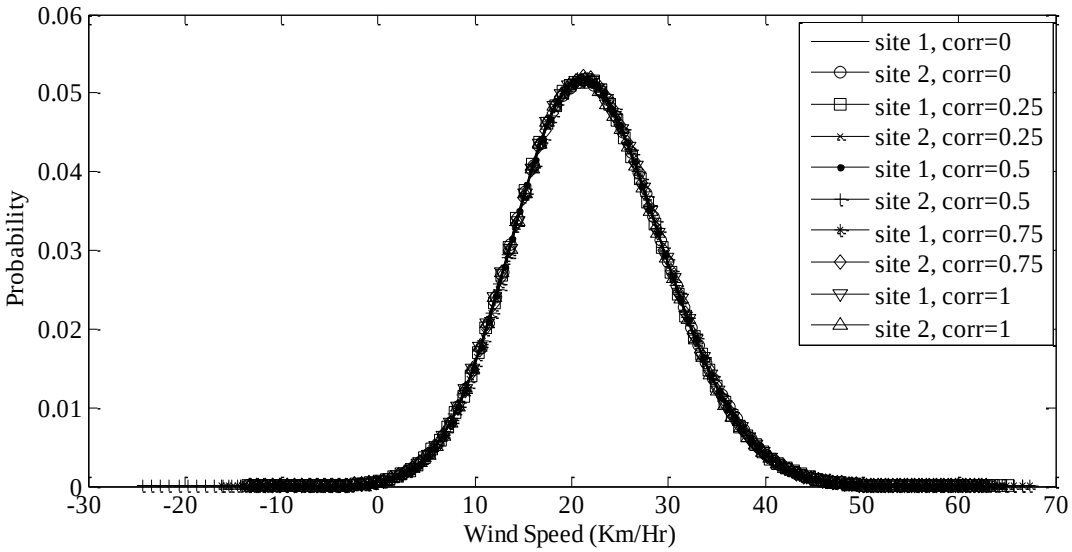

Figure 4.5: Probability distribution of wind speeds simulated at different correlations.

It can be seen in Figure 4.5 that the simulated wind speeds for the two sites have almost identical probability distributions even if they have different correlations because they use the same wind characteristic for both sites. Some of the simulated speeds obtained from the above method have negative values, which cannot be defined. Different methods to deal with negative values produced during simulation are presented in [19]. A straight forward method proposed by [19] is to set all the negative values to zero after the completion of simulation process used in this study.

4.3 Wind Power Modeling

Five pairs of hourly power output series (HPOS) were developed by applying the power curve shown in Figure 3.2 to the respective pairs of hourly wind speed series for correlations of 0, 0.25, 0.5, 0.75 and 1. The V_{ci}, V_r and V_{co} of 14.4 km/h, 46.8 km/h, and 90 km/h respectively were used in the study in this chapter. Both wind farms in each pair were assumed to have equal installed capacities for all the cases in this study. The total hourly power generated by two correlated wind farms denoted by $P_{\rho i}$ can be calculated by aggregating the output power of each wind farm for each time interval using (4.6).

$$P_{\rho i} = \sum_{j=1}^{NWF} p_{\rho ji} \tag{4.6}$$

where, $p_{\rho ji}$= power output of wind farm *j* at hour i,

i = 1 to 8760 × *N*

N = number of years considered.

NWF = number of wind farms considered.

ρ = correlation between wind farms which can be in the form of a correlation matrix if more than two wind farms are considered.

The combined hourly power output series of two wind farms, $P_{\rho i}$, can be grouped into a suitable number of class intervals to develop a probability distribution of the combined power output of the two wind farms. This can be generalized for any number of wind farms. This method of developing the combined output power probability distribution has been designated as the point to point method (PPM) in this thesis.

A 27-state [38] wind capacity model for a WIPS containing two wind farms each rated at 425 MW was obtained from the combined hourly power output series with the process described in section 3.2.1 using (3.7) and (3.8). Both sites were assumed to have wind profiles represented by

the Swift Current, Saskatchewan wind data. Figure 4.6 shows the wind capacity models considering five different correlations of 0, 0.25, 0.5, 0.75 and 1 between the two wind farms. The different correlations between the two sites were created using the method in (4.5)

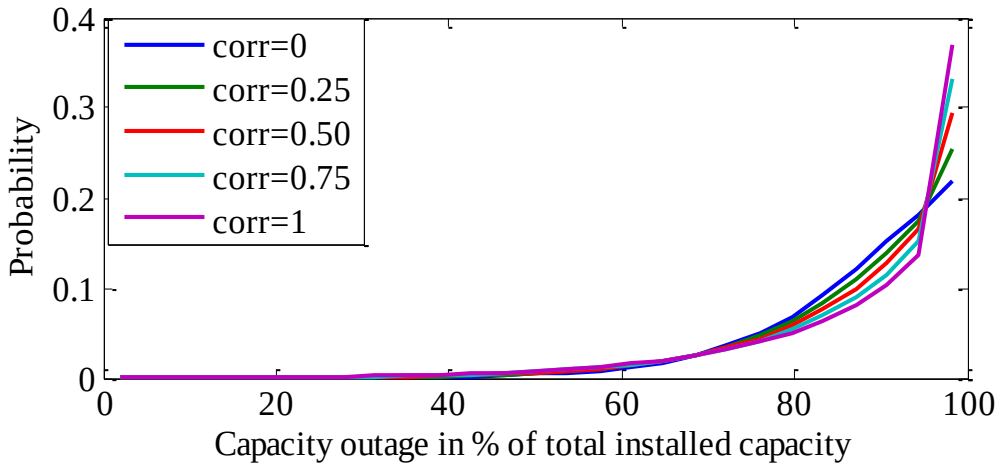

Figure 4.6: 27 state capacity outage probability table for different wind speed correlations

The 27 state capacity models were then simplified by reducing the number of capacity states using the apportioning method [17] described in Section 3.2.1. The step size of the reduced capacity model, y is given by (3.11). The 27-state capacity model was reduced by successively decreasing the number of capacity states (NoS) from 27 to 5.

4.4 Impact of Wind Penetration and Wind Farm Correlation

The IEEE Reliability Test System (IEEE-RTS)[36] was used in this study to investigate the effects of various factors on the reliability indices of a WIPS obtained using multi-state wind models. The system LOLE of the IEEE-RTS is 9.44 h/year. The system peak load is 2850 MW. The details of load data of the IEEE-RTS are provided in [36] and Appendix A from which the daily and hourly load models can be obtained. A Computer program called SIPSREL [41] was

used to calculate the LOLE values in this study. The LOLE of the IEEE-RTS decreases by adding wind generation to the system. The LOLE values obtained for the various correlations between the two wind farms, and at different wind penetration levels are summarized in Table 4.1.

Table 4.1: LOLE in h/yr for the RTS with varying wind correlation and penetration

Correlation	**Penetration**			
	5%	**10%**	**15%**	**20%**
0.00	8.1065	6.9114	5.9108	5.0427
0.25	8.1121	6.9442	5.9772	5.1453
0.50	8.1186	6.9803	6.049	5.2543
0.75	8.1231	7.0133	6.1161	5.3572
1.00	8.1263	7.0440	6.1798	5.4549

The impact of wind correlation on the WIPS reliability is shown in Figure 4.7 by applying a 27-state wind capacity model to the IEEE-RTS with 20% wind penetration. The total wind capacity in this case is 850 MW from two wind farms with equal installed capacities connected to the system.

It can be seen in Figure 4.7 that the system LOLE increases as the correlation coefficient between the two wind farms increases. Correlation between wind farms is therefore an important consideration in developing an appropriate wind model for reliability studies.

The multiple-state wind capacity model was simplified by gradually reducing the number of states from 27 to 5. The LOLE for the same system was evaluated for the different wind correlation values described in the previous study. The WIPS LOLE for different numbers of states in the wind capacity model are shown in Figure 4.8. It can be observed from Figure 4.8 that the LOLE results obtained using a reduced number of states in the wind model can have significant error. The error rapidly increases as the NoS is reduced below 10 in this study. The results obtained from the 27-state model are considered to be the most accurate in this study.

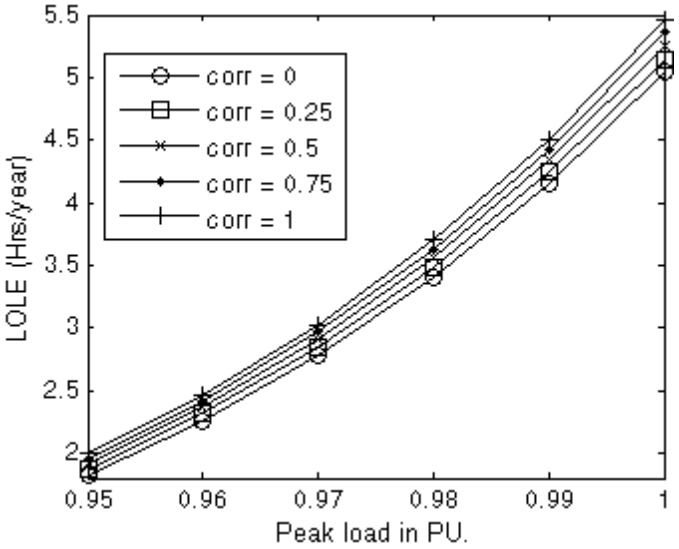

Figure 4.7: Variation in LOLE with peak load for different correlations.

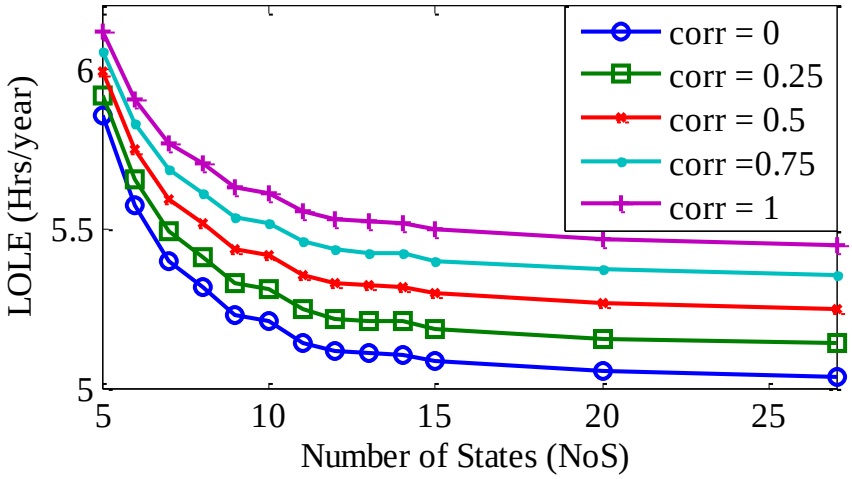

Figure 4.8: Variation in LOLE results with the NoS in the wind model for different wind correlations.

The impact of wind penetration on the LOLE accuracy obtained using different number of states in the wind model was also studied considering 5%, 10%, 15% and 20% wind penetration in the IEEE-RTS. The correlation between the wind farms was taken to be 0.5 in this case. The WIPS LOLE for the varying number of states in the wind capacity model at the different wind penetration levels are shown in Figure 4.9.

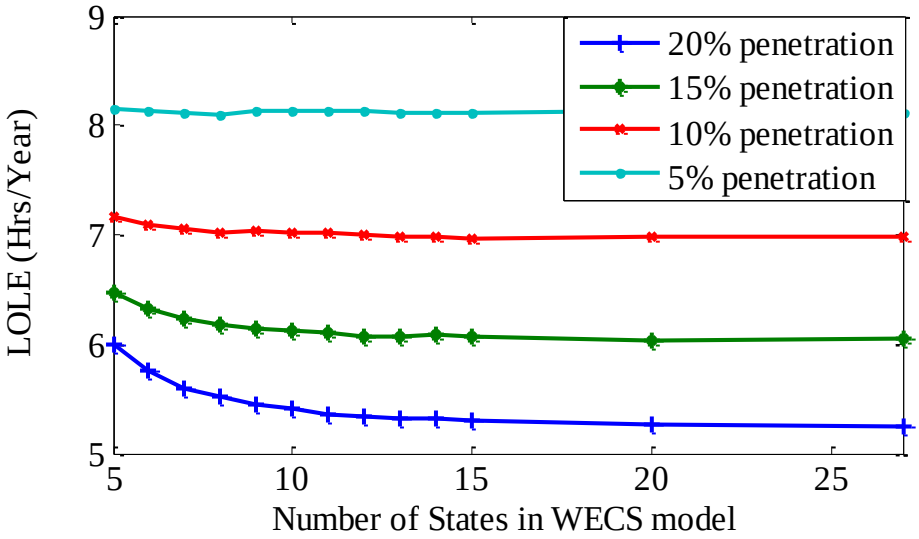

Figure 4.9: Variation in LOLE results with the NoS in the wind model at different wind penetrations.

It can be seen from Figure 4.9 that the error in LOLE increases as the NoS is reduced. The increase in the error is less significant at low wind penetration, and very significant at high penetration. It can be inferred from Figure 4.9 that the determination of an appropriate NoS in the wind capacity model also depends upon the wind penetration level in a power system.

4.5 Appropriate Wind Capacity Model Considering Wind Correlation and Penetration

Table 4.1 presents the reliability evaluation results considering different wind penetrations in the IEEE-RTS for different correlations between the two wind farms connected to the system. The results were obtained using a 27-state wind capacity model. Similar studies were carried out using wind capacity models with a reduced number of states. Reducing the number of states in the wind model simplifies the evaluation process at the cost of accuracy in the results. The errors in the WIPS LOLE obtained using reduced wind models at different wind penetrations and wind farm correlations were calculated using the Table 4.1 results obtained from the 27-state model as the reference. The results are shown in Figure 4.10.

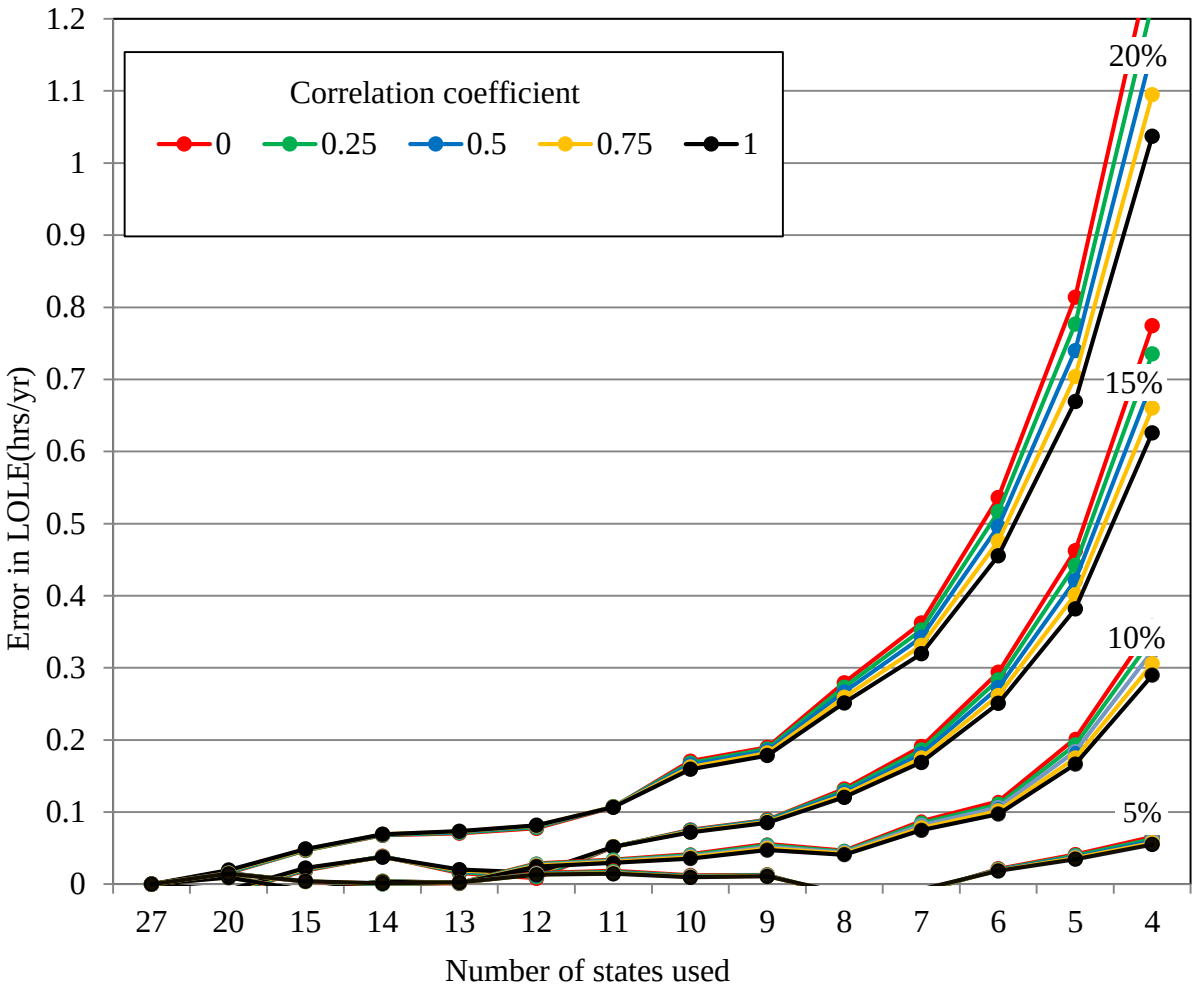

Figure 4.10: Error produced by using reduced number of states in the Wind Capacity model.

It can be seen in Figure 4.10 that the error in LOLE results generally increases as the number of states in the wind capacity model is reduced. The error is insignificant up to a certain NoS reduction, and then increases sharply as the NoS are further reduced. The error resulting from a reduced NoS is very sensitive to the wind penetration level. The errors increase rapidly with wind penetration as the number of states are reduced for model simplification. This is an important observation since the wind penetration in many WIPS around the world is expected to substantially increase within the next decade. Figure 4.10 also shows the impact of wind correlation on the LOLE errors obtained using a reduced wind capacity model. At low wind

penetration, the wind farm correlation does not really affect the LOLE errors as the NoS is reduced to simplify the wind model. The effect of correlation on the errors produced by NoS reduction is however significant at high wind penetration. The error increases as the correlation coefficient between the wind farms decreases. The effect of correlation on the LOLE errors can be significant if relatively low NoS are used in the wind model at the wind penetration levels anticipated in the foreseeable future.

Highly accurate results are usually not sought in a practical world if the methodologies to obtain the results are very difficult to apply. An easy to use method that provides results with reasonable accuracy is more suitable for real life application. A wind capacity model with the minimum number of states that produces reasonable accuracy should therefore be used in WIPS reliability evaluation. An evaluation model that can provide system LOLE results within an error of 0.1 h/year would be considered an appropriate model in practice. The minimum NoS to simplify a wind capacity model can be determined from Figure 4.10. Table 4.2 shows the appropriate wind capacity model at three different wind penetration levels.

Table 4.2: NoS for wind capacity model.

Penetration Level	**Minimum NoS**
up to 10%	7 states
up to 15%	9 states
up to 20%	11 states

The wind capacity models recommended in Table 4.2 were applied to the IEEE-RTS considering wind penetrations of 10%, 15% and 20% from two wind farms with zero wind correlation. It is shown in Figure 4.10 that the error is highest when correlations between sites are zero. The LOLE of the IEEE-RTS without considering wind penetration is 9.44 h/year, which is relatively high compared to the NERC recommended criterion of 0.1 day/year. This

criterion is equivalent to about 1 h/year [15]. The peak load of IEEE-RTS was reduced to 90% to get LOLE values close to 1 h/year. The WIPS LOLE at the three wind penetration levels were calculated for a range of system loads between 90% and 100% of the IEEE-RTS peak of 2850 MW. The errors in the system LOLE were calculated by comparing these values with results obtained using the 27-state model, and are shown in Figure 4.11.

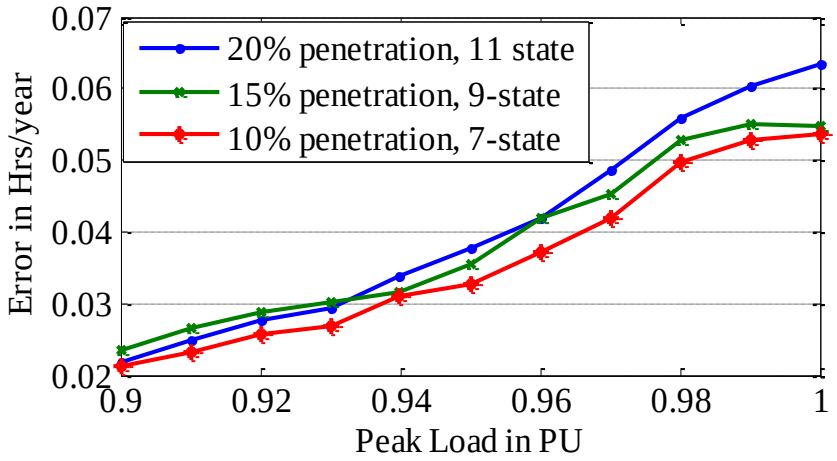

Figure 4.11: LOLE errors at different peak loads obtained using the recommended wind capacity models.

It can be seen from Figure 4.11 that the recommended wind capacity models provide results with acceptable accuracy at the different wind penetration levels. The error level is less than 0.03 h/year at a typical peak load level, which is 0.9 p.u. in the case of IEEE-RTS. This suggests that the wind models chosen are conservative for practical cases and may be used with confidence to obtain reasonable accuracy.

4.6 Conclusion

This chapter presents studies on modeling wind behavior with reasonable accuracy while incorporating the correlation between wind farms in evaluating the reliability of wind integrated power systems. The impacts of wind farm correlation on the system risk index were analyzed,

and a suitable wind model incorporating correlations between wind speeds of multiple wind farms is proposed. The appropriate model was deduced by integrating multiple correlated wind farms using the IEEE-RTS and analyzing the error produced by the various models. The impacts on the results of wind speed correlations between the sites, wind penetration levels, system peak loads and the number of states in the wind model were analyzed in the studies presented. The effect of correlation was found to be insignificant at relatively low wind penetration, whereas, at high penetration, it was an important consideration in determining the minimum number of states used to simplify the wind capacity model. It was found that the error in the system results increases as the wind speed correlation coefficient between the wind farms was decreased. This chapter provides recommendations to simplify wind models for the reliability evaluation of power systems connected to large multiple wind farms. Based on the study results, a wind capacity model consisting of 7, 9 and 11 states is recommended for power systems with wind penetration of up to 10%, 15% and 20% respectively. The paper also illustrates that the recommended wind models are conservative for practical cases and may be used with confidence to provide reasonable accuracy.

5 A SIMPLIFIED WIND MODEL FOR GEOGRAPHICALY DISTRIBUTED WIND SITES LACKING TIME-SYNCHRONIZED WIND DATA

5.1 Introduction

Many power utilities are considering generation expansion using multiple wind farms at different geographic locations in order to meet the wind penetration targets specified in their renewable portfolio commitments. A renewable portfolio standard is an obligatory requirement for power utilities to ensure that a certain percentage of the total generating capacity is obtained from renewable energy sources within a pre-specified point in time. Wind capacity model building is an important part of assessing the impact of the geographically diverse wind farms on the system reliability. Geographically distributed wind farms generally have cross correlation coefficients between their wind speeds that range from 0 and 1, which means the wind speeds in the wind farms are neither totally dependent nor totally independent of each other.

A technique based on conditional and mutually exclusive events is proposed in [9] to develop a combined capacity model of correlated wind sites. Another technique based on Markov models is proposed in [10], which can be extended to obtain combined capacity models. All of these analytical techniques require time-synchronized data for all the wind sites. Sufficient time-synchronized wind data is generally not available when system planners are considering prospective wind farm sites during the capacity expansion planning phases.

A Monte Carlo Simulation method using an autoregressive moving average (ARMA) model to simulate a series of wind data for the second wind site using random numbers correlated based

on the first wind site is presented in [31] and in Chapter 4. Non time-synchronized wind speed data of correlated wind sites, if available, can be used to develop an ARMA model of each wind farm separately. Correlated random numbers based on the estimated correlation in wind speed between the wind farms can then be used to generate synthetic wind speed series of individual wind sites. The individual wind speed series obtained have a correlation between them which is close to the estimated correlation used to generate the correlated random numbers. The synthetic wind speed series obtained are time-synchronized and can be used to develop the combined wind capacity model of the wind farms using the analytic techniques discussed in the earlier paragraph. Application of MCS methods however, require customized system specific software for implementation, and therefore, are not readily applied in practice as discussed in Chapter 1. Although this method does not require time-synchronized wind data, it requires sufficient data at each site to create the ARMA models. Many prospective sites have very limited or no wind data available at all. Adequacy evaluation considering such potential wind sites therefore cannot be carried out using many techniques.

A simple analytical method is proposed in this chapter to develop the combined capacity model of correlated wind sites when time-synchronized wind data is not available. The developed wind models are compared to conventional wind models that require time-synchronized wind data. The comparisons are done using adequacy studies on the IEEE-RTS [36] to examine the effectiveness of the proposed method. The proposed method is initially illustrated for two wind farm sites, and extended for more than two sites later in the chapter. A wide range of accuracy and sensitivity analysis are also presented to investigate the effectiveness of the proposed algorithm.

5.2 Wind Capacity Model using Time-synchronized Data

This section describes the basic analytical method to incorporate the cross correlations between multiple wind farms in adequacy assessment of a wind integrated power system when time-synchronized wind data is available for all the wind sites. The output power of each wind farm can be aggregated for each time interval to develop a combined wind power time series (WPTS) of all the wind farms using (4.6) and is designated as the PPM in the previous chapter.

The combined WPTS obtained is grouped into a suitable number of class intervals using Sturges' rule [38] , and a probability distribution of the combined power output of all the wind farms created. This constitutes the wind capacity model, which is then convolved with the capacity model of the conventional generating units to obtain the system generation model. The system generation model is combined with the system load model to obtain the adequacy indices [16].

The development of a wind capacity model from wind power data however, requires synchronized wind power output data for the different wind farms collected over a large number of years. This is only possible if the wind farms already exist and have been operating for a number of years. This method therefore cannot be used for the purpose of planning or policy making.

The PPM can, however, be used for potential wind sites if sufficient time-synchronized wind speed data is available for the sites. In this case, the wind speeds are converted to wind power data using the appropriate power curve, and the PPM can be applied to obtain the wind capacity model. Wind speed data may be collected for some years at the prospective sites or may be obtained from nearby weather stations. Preexisting wind speed data is generally available at an anemometer height of 10 m [42] for weather stations. Typical hub height of a wind turbine however ranges from 60 m to 80 m. The available wind speed should therefore be scaled to the

hub height before calculating the wind power output. A logarithmic velocity profile which assumes the atmosphere to be adiabatic is used in [43], and shown in (5.1).

$$\overline{u}_x(h_h) = \frac{u_*}{\kappa} ln\frac{h_h}{z_0} \quad (5.1)$$

where, $u_* = \frac{\kappa}{ln\frac{h_r}{z_0}} \times \overline{u}_x(h_r)$

h_h = hub height
h_r = reference height (10 m in this case)
z_0 = surface roughness length
$\kappa \sim 0.4$ (von Karman constant)

z_0 is related to the height of the roughness elements present on the ground surface. The surface roughness length is assumed to be 0.03 m for airport sites in [44].

The PPM is illustrated using two wind farms located at Swift Current and Regina. Both sites are located in Saskatchewan, Canada and the distance between them is approximately 230 km. Time-synchronized wind speed data collected over 19 years at the 10m height were obtained for these sites from Environment Canada [45]. The cross correlation coefficient between the wind speeds of these sites was evaluated from the data to be 0.48. The collected wind speed data was then scaled to a hub height of 70 m to obtain the individual wind speed time series for the Swift Current and Regina sites.

A typical 2 MW WTG with cut-in, rated and cut-out wind speeds of 15 km/hr, 50 km/hr and 90 km/hr respectively is considered in this study. The forced outage rate (FOR) of the WTG is not considered as the unavailability of power from a WTG is mainly dictated by the wind characteristics, and the FOR has a relatively small impact [32]. The rated capacities of the Swift Current and Regina wind farms are assumed to be 300 MW and 100 MW respectively.

The WPTS of each farm was obtained by converting the wind speeds into power using the power curve shown in Figure 3.2. Using the PPM, a combined WPTS for the two wind farms

was created which preserves the time chronology and the cross-correlation between the wind power outputs of the two farms. The 19 years of hourly data were grouped into 19 class intervals using Sturges' rule [38], and a probability distribution of the total power output from the two farms obtained. It is suggested in Chapter 4 that a nine state capacity model can be used to adequately model wind power for wind penetrations up to 15%. The 19 state probability distribution was therefore reduced to 9 states using the apportioning method [17] to reasonably simplify the evaluation. The wind capacity model obtained is shown in Figure 5.1.

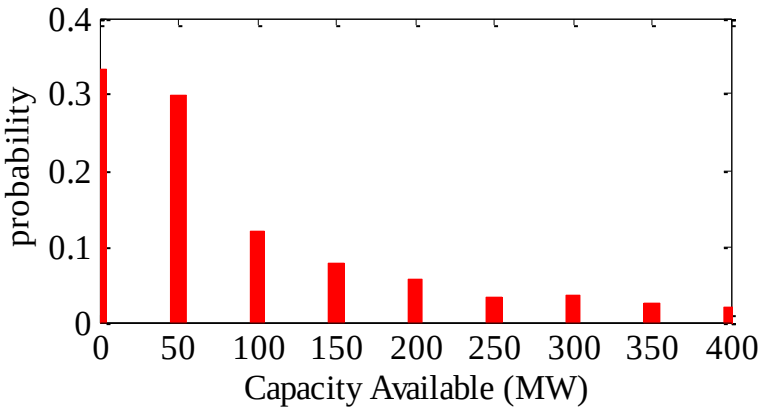

Figure 5.1: Combined capacity model for the Swift Current (300 MW) and Regina (100 MW) sites obtained from the PPM

The wind capacity model shown in Figure 5.1 was convolved with the capacity model of the remaining conventional generating units to obtain the overall system generation model. The overall generation model was convolved with the system load model to obtain the required adequacy index. The adequacy index used in this study is the Loss of Load Expectation (LOLE) [16].

5.3 The Proposed Algorithm

Time-synchronized wind data for wind sites of interest are usually not available, especially during planning and policy making. In many practical cases, wind data collected over different

time spans are available. The PPM cannot be applied in such cases. This section describes a simple analytical method to develop a combined wind capacity model for two wind farm sites for which time-synchronized wind data are not available.

A typical scenario is considered in this section assuming that hourly wind speed data for Swift Current is available from 1996 to 2005 and for Regina is available from 1986 to 1995. Ten years of hourly data is available for each site but they are not time-synchronized. The evaluation of the cross correlation in wind speed between the wind farms and the use of the PPM to obtain the combined capacity model of the wind farms is also not possible in this case. The proposed method and its application are illustrated in this section. The method consists of estimating the correlation coefficient, developing individual capacity models for each wind farm, combining the individual capacity models using a novel technique, convolving the capacity model with the rest of the system generation model and evaluating the adequacy indices. These steps are described in the following sub-sections.

5.3.1 Estimation of the correlation coefficient

If the cross correlation between the wind speeds at these sites for a period of one year is calculated taking all the combinations of the years for which the data is available, then a 10×10 correlation matrix can be obtained for this case when ten years of data is available for each site. The cross correlation in the wind speed of Swift Current and Regina by considering 1 year data for all the combination of years from 1996 to 2005 is shown in Table 5.1.

It can be seen from Table 5.1 that all the correlation values for different years are close to zero and do not represent the actual correlation. The average of all the correlations in the correlation matrix in Table 5.1 is 0.0573 which is far from the actual value of 0.48. If the cross correlation is calculated from the average hourly wind speeds obtained from 10 years of data of each of the

two sites for a period of one year, a correlation of 0.367 is obtained. This is closer to the actual value than in the earlier case but still has a significant error.

Table 5.1: Cross correlation between the wind speeds for Swift Current and Regina for one year of wind speed data

		Regina									
	Year	**1986**	**1987**	**1988**	**1989**	**1990**	**1991**	**1992**	**1993**	**1994**	**1995**
	1996	0.044	0.036	0.053	0.038	0.071	0.007	0.056	0.042	0.014	0.089
	1997	0.008	0.064	0.104	0.062	0.093	0.063	0.078	0.033	-0.017	0.067
	1998	0.035	0.088	0.042	-0.009	0.084	0.053	-0.033	0.067	0.078	0.053
	1999	0.065	0.109	0.057	0.030	0.091	0.064	0.076	0.075	-0.008	0.092
Swift	**2000**	0.051	0.031	0.082	0.016	0.081	0.098	0.077	0.028	0.055	0.065
Current	**2001**	0.095	0.113	0.067	0.004	0.102	0.136	0.037	0.056	0.061	0.035
	2002	0.089	0.097	0.054	0.140	0.075	0.068	0.061	0.052	0.048	0.052
	2003	0.093	-0.016	0.015	0.024	0.065	0.057	0.008	0.020	-0.003	0.137
	2004	0.047	0.097	-0.005	0.117	0.075	0.033	0.075	0.045	0.083	0.103
	2005	0.035	0.054	0.036	0.087	0.070	0.022	0.068	0.047	0.056	0.046

Studies have shown [27, 28, 46] that the cross correlation between the wind speeds tend to decrease as the distance between the sites increase. The relationship between correlation and distance can be graphically characterized for any geographic region of interest. Distance and correlation values for available combinations of pair of wind sites can be used to estimate the correlation between other pairs of wind sites in the region. Hourly wind speed measurements for 12 Saskatchewan wind sites which were available from Environment Canada [45] were considered in this study. The locations and names of the wind sites considered are shown in Figure 5.2. Hourly wind speeds collected at an anemometer height of 10 m between the year 1987 and 2005 were considered for all the sites.

The distance and the correlation between all the combinations of pairs of available wind sites were evaluated and are shown in Figure 5.3. A curve to fit the points is also shown in Figure 5.3.

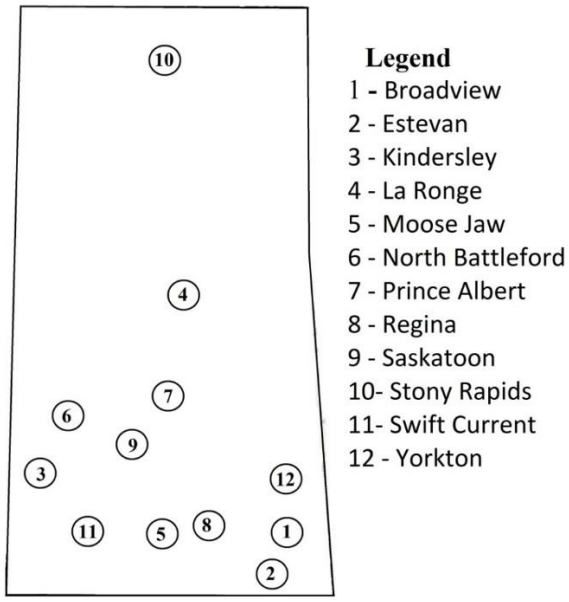

Figure 5.2: Saskatchewan map showing wind sites considered

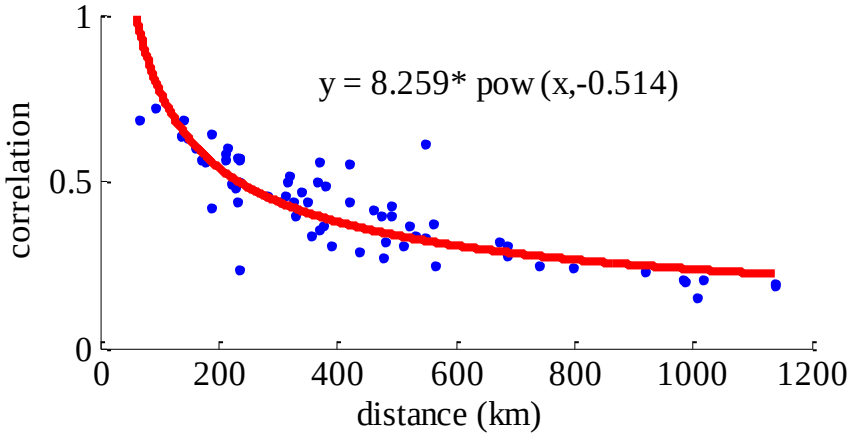

Figure 5.3: Distance vs wind speed correlation for 12 Saskatchewan sites

The correlation between the wind speeds for any pair of Saskatchewan sites can be estimated using the curve shown in Figure 5.3. The distance between Swift Current and Regina is approximately 230 km which when applied to the curve, corresponds to a correlation of 0.50. This is comparable to the actual correlation value of 0.48 obtained in Section 5.2.

5.3.2 Development of individual capacity models for each wind site

Individual wind capacity models for each wind farm are developed separately in the proposed method. Hourly WPTS were developed by applying the power curve to the available hourly wind speed time series for Swift Current and Regina sites separately. The wind power curve parameters and the capacity ratings of the two wind farms in Swift Current and Regina are given in the previous section of this chapter. Each WPTS is then used to develop a probability distribution of available capacity for the respective site. The number of class intervals for 10 years of hourly data was calculated to be 18 based on Sturges' Rule [38]. The 18 state probability distributions were reduced to 9 states [33] using the apportioning method. The capacity models for all the wind sites must be represented by an equal number of capacity states in the proposed method. The 9-state individual wind capacity models for the two sites are shown in Table 5.2. The capacity available is expressed in percent of the installed wind farm capacity in the table. It should be noted that the installed capacity of the Swift Current and Regina wind farms are assumed to be 300 MW and 100 MW respectively.

Table 5.2: Individual wind capacity models

Swift Current		**Regina**	
Capacity In (%)	**Probability**	**Capacity In (%)**	**Probability**
0.0	0.322	0.0	0.396
12.5	0.308	12.5	0.298
25.0	0.092	25.0	0.078
37.5	0.074	37.5	0.061
50.0	0.060	50.0	0.054
62.5	0.030	62.5	0.027
75.0	0.035	75.0	0.024
87.5	0.025	87.5	0.019
100.0	0.054	100.0	0.044

5.3.3 Combination of the individual wind capacity models

A combined wind capacity model is developed from the individual wind capacity models in the proposed method by assuming one of the wind capacity models to be the reference model and the other as the non-reference model in this section. The wind capacity probability distributions of the reference and the non-reference models are $p(WP_{ref})$ and $p(WP_{non\_ref})$ respectively. The installed wind capacity at the sites corresponding to the reference and the non-reference models are $P^{ref} = max(WP_{ref})$ and $P^{non\_ref} = max(WP_{non\_ref})$ respectively. The distribution $p(WP_{non\_ref})$ of the non-reference model is split into two parts, $p(WP_{\rho 0})$ and $p(WP_{\rho 1})$ as shown in (5.2), based on the correlation coefficient ρ between the two wind sites.

$$p(WP_{non\_ref}) = p(WP_{\rho 1}) + p(WP_{\rho 0}) \tag{5.2}$$

where the wind speeds in the $p(WP_{\rho 1})$ and $p(WP_{\rho 0})$ distributions have unity and zero correlation coefficient, or are dependent and independent respectively with the wind speeds in the $p(WP_{ref})$ distribution of the reference model. The two split distributions $p(WP_{\rho 1})$ and $p(WP_{\rho 0})$ are identical to $p(WP_{ref})$ and $p(WP_{non\_ref})$ respectively, when capacity values are expressed in percent as shown in Table 5.2. The maximum wind capacity values for the split models $p(WP_{\rho 1})$ and $p(WP_{\rho 0})$are calculated using (5.3) and (5.4) respectively.

$$P_{\rho 1}^{non\_ref} = max(WP_{\rho 1}) = \rho . P^{non\_ref} \tag{5.3}$$

$$P_{\rho 0}^{non\_ref} = max(WP_{\rho 0}) = (1 - \rho) . P^{non\_ref} \tag{5.4}$$

The split dependent model $p(WP_{\rho 1})$ is then convolved with the wind capacity model $p(WP_{ref})$ of the reference site in the proposed method. The resulting intermediate wind capacity model $p(WP_{ref+\rho 1})$ is identical to the two identical distributions being convolved, and the

available capacity values in $p(WP_{ref+\rho 1})$ are expressed in percent of the maximum wind capacity value given by (5.5).

$$max\left(WP_{ref+\rho 1}\right) = P^{ref} + P_{\rho 1}^{non\_ref} \tag{5.5}$$

The intermediate wind capacity model $p\left(WP_{ref+\rho 1}\right)$ is finally convolved with the independent wind capacity model $p\left(WP_{\rho 0}\right)$ to obtain the combined wind capacity model $\left(WP_{split}\right)$ of the two partially correlated sites$\left(\mathrm{WP_{split}}\right)$. The convolution theorem is directly applicable in this case as shown in (5.6) since the two probability distributions are independent of each other.

$$p\left(WP_{split}\right) = p\left(WP_{ref+\rho 1}\right) * p\left(WP_{\rho 0}\right) \tag{5.6}$$

The individual capacity models for the Swift Current and Regina sites shown in Table 5.2 are considered to illustrate the application of proposed method designated as the Split Method in this thesis. Swift Current is assumed to be the reference site with the wind capacity probability distribution $p(WP_{ref})$ and Regina is assumed to be the non-reference site with its wind capacity probability distribution $p(WP_{non\_ref})$. The two wind capacity models are shown in Table 5.2. The wind capacity model of Regina, the non-reference site, is split into two parts $p\left(WP_{\rho 1}\right)$ and $p\left(WP_{\rho 0}\right)$ based on the estimated correlation of 0.50 between the two sites using (5.2)-(5.4). The split models for the Regina site are shown in Table 5.3. The maximum wind capacity values were calculated using (5.3) and (5.4), and are 50 MW for both the models in Table 5.3.

The intermediate wind capacity model $p(WP_{ref+\rho 1})$ is subsequently obtained as described. The maximum wind capacity value calculated using (5.5) is 350 MW. The intermediate model $p(WP_{ref+\rho 1})$ is shown in Table 5.4, where the wind capacity values are expressed in MW.

Table 5.3: Split models for the Regina site

$p(WP_{\rho 1})$ (Dependent part)		$p(WP_{\rho 0})$ (Independent part)	
Capacity In (%)	**Probability**	**Capacity In (%)**	**Probability**
0.0	0.322	0.0	0.396
12.5	0.308	12.5	0.298
25.0	0.092	25.0	0.078
37.5	0.074	37.5	0.061
50.0	0.060	50.0	0.054
62.5	0.030	62.5	0.027
75.0	0.035	75.0	0.024
87.5	0.025	87.5	0.019
100.0	0.054	100.0	0.044

Table 5.4: Intermediate wind capacity model $p(WP_{ref+\rho 1})$

Capacity In (MW)	**Probability**
0.00	0.322
43.75	0.308
87.50	0.092
131.25	0.074
175.00	0.060
218.75	0.030
262.50	0.035
306.25	0.025
350.00	0.054

The intermediate wind capacity model $p(WP_{ref+\rho 1})$ is finally convolved with $p(WP_{\rho 0})$ using the recursive algorithm [16] for combining independent capacity models. The resulting wind capacity model was reduced to 9 states for consistency and comparison. The wind capacity model thus obtained by combining the individual capacity models for Swift Current and Regina sites $p(WP_{split})$ are shown in Figure 5.4. The combined wind capacity model previously obtained from the PPM is also shown in Figure 5.4 for comparison.

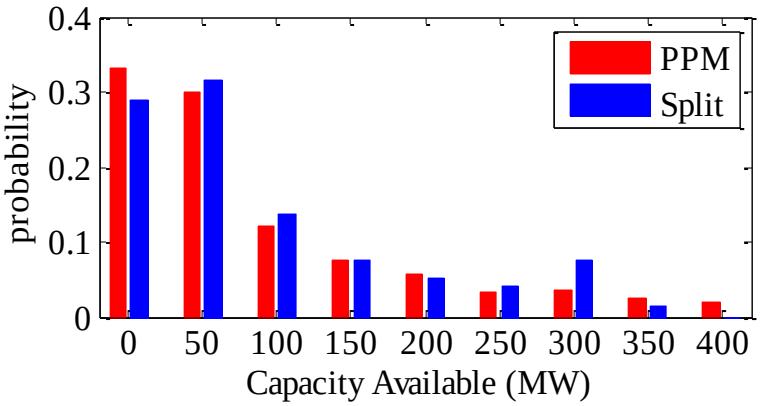

Figure 5.4: Combined wind capacity models obtained from the two methods

5.3.4 Evaluation of the System LOLE and Comparison with the PPM

The IEEE-RTS [36] was used in this study to evaluate and compare the LOLE index obtained from the PPM and the proposed split method. It was assumed that the IEEE-RTS is connected to a 300 MW wind farm at a site with Swift Current data and a 100 MW wind farm at another site with Regina data. The addition of the total 400 MW wind capacity results in a 10.5% wind penetration in the IEEE-RTS. The hourly load model for the IEEE-RTS [36] was used for this study. The system LOLE values evaluated for a range of peak loads using the two different combined capacity models obtained by the PPM and Split methods are shown in Figure 5.5. SIPSREL [41] was used to evaluate the LOLE.

It can be seen from Figure 5.5 that the system LOLE values obtained from the Split method are very close to the LOLE values obtained from the PPM for a range of peak loads. This suggests that satisfactory results can be obtained using the proposed Split method.

Further study was conducted to analyze the effectiveness of the proposed algorithm at different levels of correlation between the wind farms. The IEEE-RTS was again considered to be connected to two wind farms with 300 MW and 100 MW installed capacities. The wind

profiles for these wind sites were represented in this study by wind speed data obtained from twelve wind site pairs chosen with correlations ranging from 0.2 to 0.72 between their wind speeds. The LOLE was calculated for the IEEE-RTS for each pair of wind sites using the PPM. The combined capacity model of each pair of sites was obtained from the time-synchronized hourly wind speeds for 19 years between 1987 and 2005. Individual capacity models for each site were subsequently developed with the same data. The correlation between the wind speeds for all the pairs of sites were estimated using the correlation estimation curve in Figure 5.3. The combined capacity model of each pair of wind farms was developed using the Split method. The LOLE values for the IEEE-RTS connected to the wind farm pairs were then calculated using the Split method. The LOLE values evaluated using the PPM and the Split method are shown in Table 5.5.

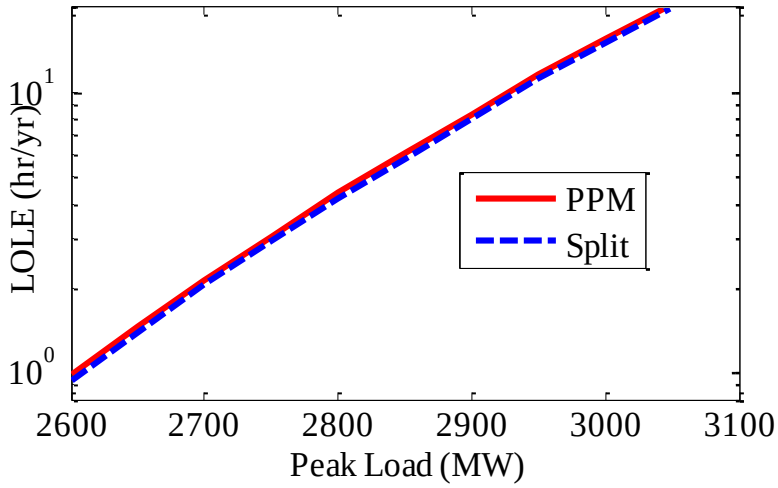

Figure 5.5: LOLE obtained from the two methods

It can be seen from Table 5.5 that the LOLE values obtained using the two methods for the wind farm pairs with varying correlation coefficients are very close. The results show that the proposed algorithm provides a satisfactory estimate of the actual combined capacity model. The PPM cannot be applied when time-synchronized data is not available. The Split method proposed in this paper should prove useful in such scenarios for wind power planning and policy making.

Table 5.5: LOLE comparison for selected combinations of Saskatchewan sites.

Reference Site (300 MW)	Non reference site (100 MW)	Distance (km)	Correlation		LOLE (hr/yr)	
			Actual	Estimated	PPM	Split
Broadview	Yorkton	92	0.72	0.81	6.77	6.68
Broadview	Estevan	141	0.68	0.65	6.61	6.58
North Battleford	Saskatoon	135	0.64	0.66	7.22	7.19
La Ronge	Prince Albert	215	0.60	0.52	7.79	7.78
Regina	Saskatoon	233	0.57	0.50	6.48	6.33
Broadview	Prince Albert	380	0.49	0.39	6.88	6.72
Estevan	Prince Albert	492	0.43	0.34	6.84	6.69
Prince Albert	Swift Current	355	0.34	0.40	7.23	7.30
Estevan	La Ronge	685	0.31	0.29	6.85	6.72
Saskatoon	Stony Rapids	797	0.24	0.27	7.51	7.37
Regina	Stony Rapids	982	0.20	0.24	6.74	6.58
Stony Rapids	Swift Current	1006	0.15	0.24	7.75	7.74

5.3.5 Discussions on the Proposed Algorithm

The wind capacity probability distribution $p(WP_{\rho 1})$ of the dependent part of the non-reference site has an identical probability distribution to that of the reference site in the proposed method. The choice of the reference site is an important part of the proposed method as this will affect the accuracy of the results. A study was therefore conducted to investigate the impact of the reference site selection on the accuracy of the proposed approach.

The ratio of the wind farm capacities connected to the IEEE-RTS is 3 (300MW:100MW) in the above studies. A sensitivity study was carried out considering a range of capacity ratios for four different wind farm pairs having correlation levels ranging from 0.15 to 0.72. The total 400 MW wind capacity was divided between the reference site and the non -reference site in a given ratio. All the other wind turbine parameters and data were assumed to be the same as in the earlier sections. The system LOLE for each capacity ratio was evaluated using the PPM and the Split method. The percent error in LOLE calculated for the Split method is shown in Figure 5.6. The first wind farm site in each case in the legend in Figure 5.6 is the reference site.

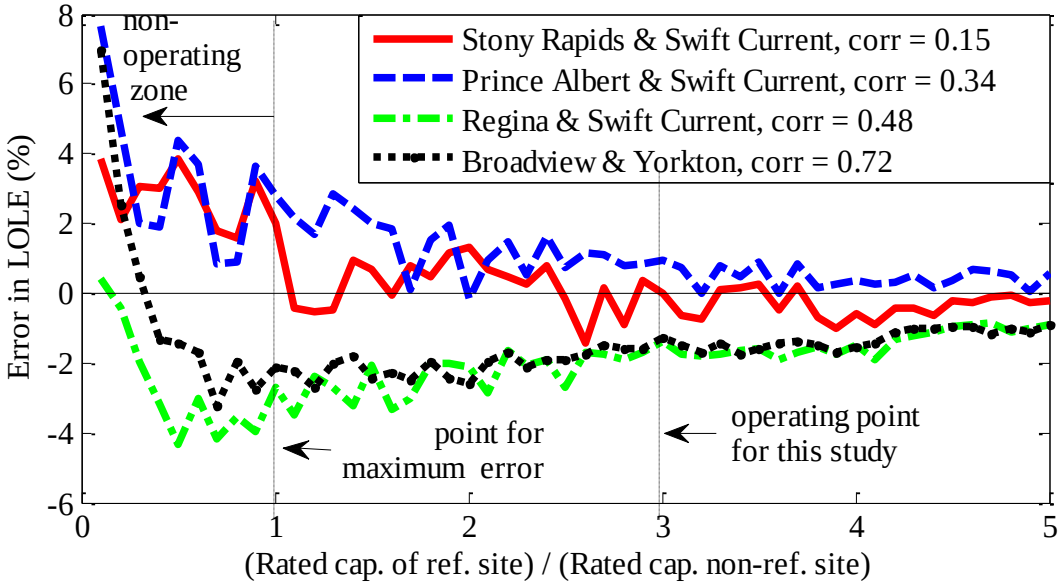

Figure 5.6: Error produced for a range of wind farm capacity ratios

It can be seen from Figure 5.6 that the error in the LOLE tends to decrease as the ratio of the size of the reference wind farm to the size of the non-reference wind farm increases. It can therefore be inferred that the largest wind farm should always be considered as the reference site in the proposed method. The region in Figure 5.6 where the reference to non-reference site capacity ratio is less than 1 does not exist when the largest wind farm is chosen as the reference site. The maximum error occurs when both wind farms are of equal capacities.

5.4 The Approximate Split Method

The proposed Split method presented in Section 5.3 should prove useful in an adequacy assessment when time-synchronized wind data for wind sites are not available, but adequate wind data is available to obtain accurate individual wind capacity models of the wind farms. However, in many wind power planning and policy formulation situations extremely limited data are available for prospective wind sites. In such cases, wind capacity models cannot be developed as described in Section 5.3. This chapter also proposes an approximate Split method

that can be applied to incorporate the wind farm correlations in adequacy evaluation when wind data are not available for the prospective wind sites.

The proposed approximate method requires the mean and the standard deviation of the wind speeds at the sites of interest. These parameters can either be calculated by taking wind speed measurements at the sites for a limited time (generally one or two years) or estimated with the help of some form of wind atlas similar to [47] . A particular case is considered in this section where wind data is not available for the Swift Current and Regina sites, and 26.38 and 24.7 km/hr are the estimated mean, and 12.64 and 13.93 km/hr are the estimated standard deviations of the wind speeds at the two sites respectively. The mean and the standard deviation data for each wind site are at a hub height of 70 m.

A six state wind speed model resembling a normal distribution is proposed in [22] for wind sites when adequate data is not available. As a six state wind speed model is not sufficient for the case considered in this section [33], a 9-state wind speed model was developed for each site with the normal distribution approximation [22]. The power curve in Figure 3.2 was applied to the approximate wind speed model to obtain the individual capacity models for Swift Current and Regina, and are shown in Figure 5.7.

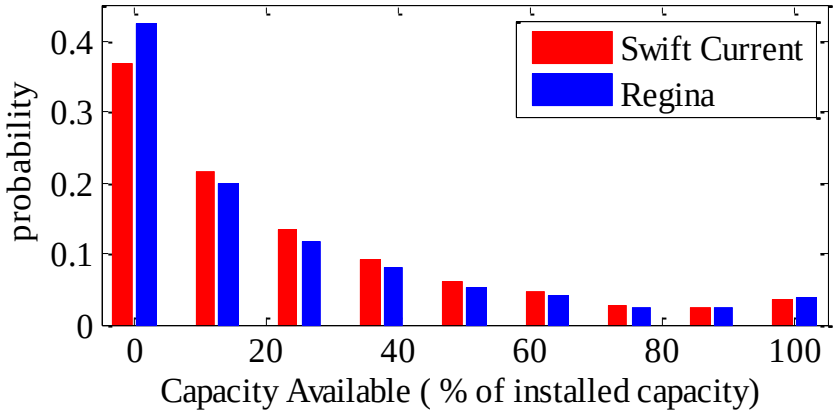

Figure 5.7 Individual wind capacity models obtained assuming normal wind speed distribution

The individual capacity models obtained for the 300 MW Swift Current site and the 100 MW Regina site were combined using the Split method to obtain the combined wind capacity model. The combined wind capacity models obtained from the PPM and Split methods illustrated and presented in Section 5.3, and the approximate Split method presented in this section are shown in Figure 5.8 for comparison.

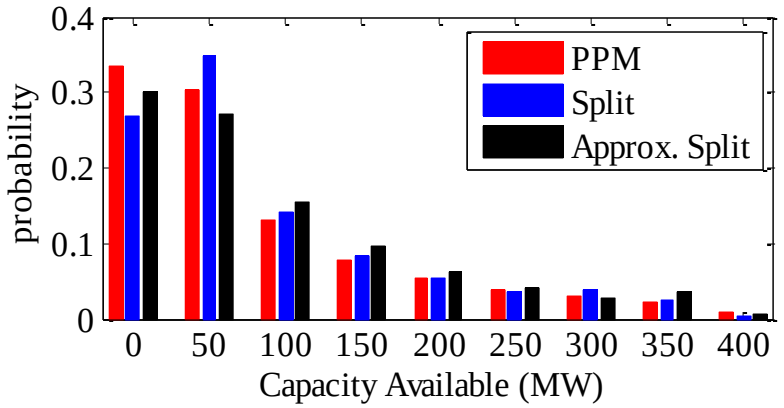

Figure 5.8: Combined wind capacity models from PPM, Split and approx. Split methods

The combined wind capacity model for the two wind sites obtained from the approximate Split method was then convolved with the conventional capacity model of the IEEE-RTS, and the system LOLE was evaluated for a range of peak loads. The results are shown in Figure 5.9. The results from the PPM are also shown for comparison.

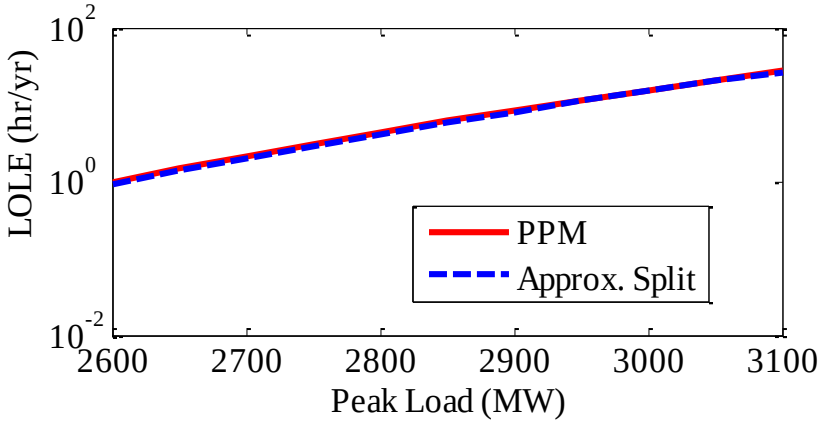

Figure 5.9: System LOLE obtained from the approximate method and the PPM

Figure 5.9 shows that the system LOLE values obtained from the approximate Split method are very close to the LOLE values obtained from the PPM for a range of peak loads. This illustrates that satisfactory results can be obtained from the application of the proposed approximate Split method in situations where sufficient wind data are not available for potential wind sites during system planning or policy making.

5.5 Extension of the split method

A simple and practical analytical technique designated as the Split Method is proposed in Section 5.3 for developing wind models incorporating the correlation between two wind farms for adequacy evaluation of wind integrated power systems. In many practical cases, more than two correlated wind sites which lack time-synchronized wind data are present. The PPM can be used to develop wind models for power systems with more than two wind sites only if time-synchronized wind data exists for all the sites. As the number of wind sites increases, it is less likely that wind data for exactly the same time span for all the sites are available. The split method presented in the previous section for two correlated wind sites, is extended in this section to more than two sites.

Three correlated Saskatchewan wind sites, Swift Current, Regina and North Battleford are considered in this chapter to illustrate the new technique. Wind speed data [45] collected for the three sites between the year 1987 and 2005 are considered in the study. The data available are time-synchronized, and therefore, the PPM can be used to develop the combined wind model of the three wind farms. The distance between the wind farm sites, the actual correlations between the wind speeds calculated using the time-synchronized data, and the rated capacities considered

are shown in Figure 5.10. The total installed wind capacity of the three wind farms is considered to be 400 MW, which is consistent with earlier studies.

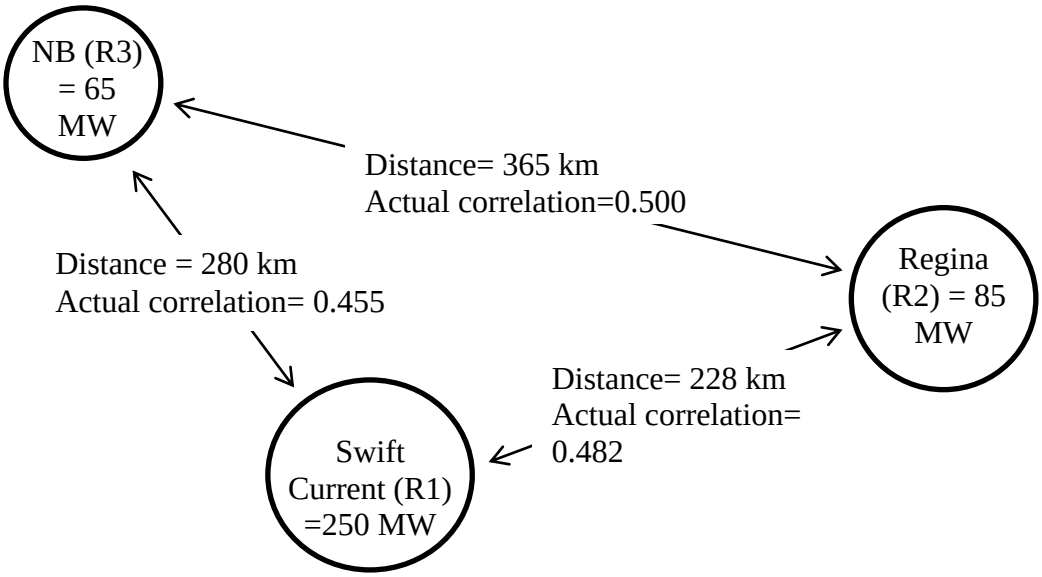

Figure 5.10 : Three Saskatchewan wind sites considered in the study

The wind speed of each site was first scaled to the appropriate hub height and then converted to corresponding output power of the wind farm by applying the wind power curve shown in Figure 3.2. A hub height of 70 m was used in the study. An individual wind capacity model for each site was then developed as described earlier in the proposed Split method. The individual probability distributions of available capacity for the Swift Current, Regina and North Battleford sites were developed by grouping the hourly wind power series into 19 class intervals [38]. The probability distributions were then reduced to 9 states using the apportioning method. The 9-state individual wind capacity models for the three sites are shown in Table 5.6.

The PPM was used to compare the results of the proposed Split method extended for more than two wind sites. Time-synchronized wind data for the three sites were used in this study so that the results from the proposed method would be compared with the PPM values. The

combined 9-state wind capacity model for the three sites obtained using the PPM is shown in Table 5.7.

Table 5.6: Individual capacity models for the three Saskatchewan wind sites

Swift Current		Regina		North Battleford	
Capacity In (MW)	**Probability**	**Capacity In (MW)**	**Probability**	**Capacity In (MW)**	**Probability**
0.00	0.340	0.000	0.393	0.000	0.509
31.25	0.311	10.625	0.291	8.125	0.291
62.50	0.089	21.250	0.076	16.250	0.062
93.75	0.073	31.875	0.061	24.375	0.047
125.00	0.063	42.500	0.054	32.500	0.035
156.25	0.029	53.125	0.027	40.625	0.015
187.50	0.030	63.750	0.028	48.750	0.015
218.75	0.021	74.375	0.022	56.875	0.008
250.00	0.046	85.000	0.049	65.000	0.019

Table 5.7: Combined wind capacity model for the three wind farms using the PPM

Capacity In (MW)	Probability
0	0.3349
50	0.3043
100	0.1322
150	0.0774
200	0.0540
250	0.0371
300	0.0293
350	0.0217
400	0.0092

5.5.1 Combined model from individual models

The individual wind capacity models are combined one at a time in the proposed method. The wind farms are sorted in decreasing order based on the rated capacity, and are designated as Reference 1 (R1), Reference 2 (R2), Reference 3 (R3), etc., respectively. The wind capacity models of the wind sites are represented by $p(WP_{R1})$, $p(WP_{R2})$, $p(WP_{R3})$, etc, in the same order. The cross correlations between the wind sites, $\rho_{12}, \rho_{13}, \rho_{23}$, etc. are then estimated based on the distances between them using a curve similar to that shown in Figure 5.3. The wind

capacity models of the largest wind site, $p(WP_{R1})$ and the second largest wind site, $p(WP_{R2})$, are first combined using the split method described in section 5.3 considering R1 as the reference site and R2 as the non-reference site as shown in (5.7). $\boxed{\dot{S}_{\rho_{12}}}$ in (5.7) denotes the combination of two wind capacity models using the split method with the correlation between the two models being ρ_{12}. The reference wind capacity model is always placed first in the relevant equations presented in this thesis.

$$p(WP_{R1R2}) = p(WP_{R1}) \ \boxed{\dot{S}_{\rho_{12}}} \ p(WP_{R2}) \tag{5.7}$$

The combined wind model of R1 and R2 $p(WP_{R1R2})$ is then combined with the wind model $p(WP_{R3})$ of site R3 as shown in (5.8).

$$p(WP_{R1R2R3}) = p(WP_{R1R2}) \ \boxed{\dot{S}_{\rho_{12-3}}} \ p(WP_{R3}) \tag{5.8}$$

The value of correlation coefficient ρ_{12-3} used in (5.8) is the weighted average of the correlations of R3 and the first two sites represented by $p(WP_{R1R2})$ based on the rated capacities of the wind farms as shown in (5.9). This process is repeated to incorporate additional wind farms.

$$\rho_{12-3} = Weighted\ Average(\rho_{13}, \rho_{23}) =$$

$$[\rho_{13} \times \max(WP_{R1}) + \rho_{23} \times \max(WP_{R2})]/[\max(WP_{R1}) + \max(WP_{R2})] \tag{5.9}$$

The proposed technique is illustrated using an example of three wind sites shown earlier in Figure 5.10 and tabulated in Table 5.8. The actual correlation in the wind speeds between the wind farm sites shown in Figure 5.10 are used in this study.

Table 5.8: Illustration example of three sites

Site Name	Rated Capacity(MW)	Designation
Swift Current	250	R1
Regina	85	R2
North Battleford	65	R2

The wind capacity model of Swift Current site, $p(WP_{R1})$ is combined with the wind capacity model of Regina, $p(WP_{R2})$ as shown in (5.7) using the correlation between the sites ρ_{12} = 0.482. The resulting combined capacity model is shown in Table 5.9.

Table 5.9: Combined capacity model of Swift Current and Regina, $p(WP_{R1R2})$

Capacity In (MW)	Probability
0.000	0.2812
41.875	0.3381
83.750	0.1293
125.625	0.0807
167.500	0.0562
209.375	0.0352
251.250	0.0288
293.125	0.0417
335.000	0.0088

The weighted average correlation between the capacity model of R3, $p(WP_{R3})$ and the two sites represented by $p(WP_{R1R2})$ calculated using (5.9) is ρ_{12-3} = 0.466. The equivalent wind model of R1 and R2, $p(WP_{R1R2})$ is then combined with the wind model of R3, $p(WP_{R3})$ using (5.8). The resulting wind capacity model, $p(WP_{R1R2R3})$ is the combined wind capacity model of all the three wind sites and is shown in Figure 5.11. The combined wind capacity model obtained from the PPM earlier is also shown in Figure 5.11 for comparison.

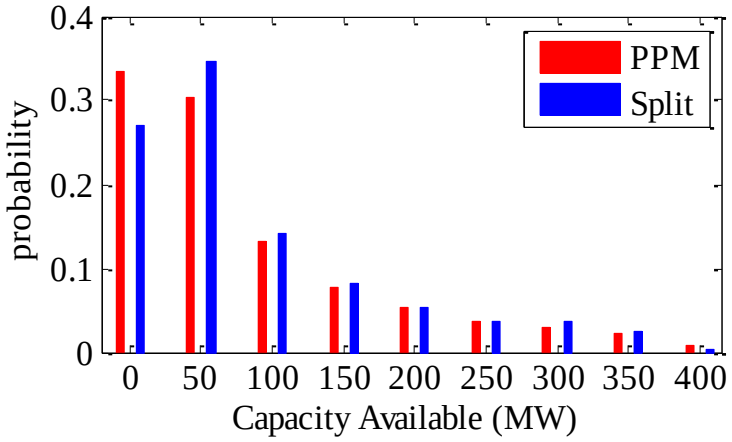

Figure 5.11: Capacity models obtained from two methods for three sites

5.5.2 Evaluation of the System LOLE and comparison with the PPM

The wind capacity model obtained using the proposed method for the three sites shown in Figure 5.11 is convolved with the generation model of the IEEE-RTS [36]. The resulting generation model is finally convolved with the hourly load model of the IEEE-RTS [36] to obtain the LOLE of the wind integrated power system. The total installed generation capacity of the IEEE-RTS is 3405 MW resulting in a 10.5 % wind penetration when 400 MW of wind generation is added to it. The hourly load model of the IEEE-RTS used in the study has a peak load of 2850 MW. The LOLE values, however, were calculated for a range of peak loads, and are shown in Figure 5.12.

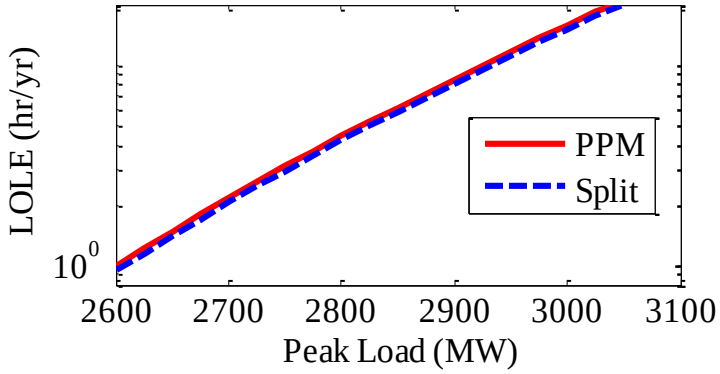

Figure 5.12: LOLE obtained from the two methods

Further study was also carried out to investigate the effectiveness of the proposed method for different combinations of wind regimes and correlations. Seven combinations of wind sites as shown in Table 5.10 were considered for the study. The rated capacities of the first, second and third sites were assumed to be 250 MW, 85 MW and 65 MW respectively. The hourly wind speed data collected at 10 m anemometer height [45] between the years 1987 and 2005 were used in the study. The wind speed data were first scaled to 70 m hub height using (5.1). The combined wind capacity models for seven different combinations of three wind farms were then developed using both the PPM and the proposed Split method. Seven different case studies were

done by convolving the combined wind capacity models with the generation model of the IEEE-RTS. The wind capacity was 400 MW in each case. The resulting generation model was convolved with the hourly load model of the IEEE-RTS with a peak load of 2850 MW to obtain the LOLE of the wind integrated power system. The results are shown in Table 5.10.

Table 5.10: LOLE comparison for selected combinations of Saskatchewan sites

Wind farm site names			**Correlation**				**LOLE (hr/yr)**	
R1 (250 MW)	**R2 (85 MW)**	**R3 (65 MW)**	**S1-S2**	**S1-S3**	**S2-S3**	ρ_{12-3}	**PPM**	**Split**
Estevan	Moose Jaw	Saskatoon	0.57	0.44	0.57	0.47	6.473	6.293
Swift Current	Prince Albert	Regina	0.34	0.48	0.52	0.49	6.279	6.022
Yorkton	Swift Current	Saskatoon	0.31	0.44	0.49	0.46	6.850	6.719
Saskatoon	North Battleford	Kindersley	0.64	0.55	0.61	0.57	7.135	7.016
La Ronge	Regina	Estevan	0.37	0.31	0.64	0.39	7.125	7.126
Prince Albert	Yorkton	Broadview	0.50	0.49	0.72	0.55	7.397	7.402
Kindersley	Swift Current	Moose Jaw	0.56	0.44	0.60	0.48	6.485	6.430

It can be seen in Table 5.10 that the difference between the results obtained from the two methods is not significant, and that the proposed method can be considered to be reasonable in situations where time-synchronized data is not available. It can however be seen that the error increases as the number of sites considered increases due to increased number of approximations involved.

5.5.3 Sensitivity studies

5.5.3.1 Impact of the size of the wind farms

It is concluded in Section 5.3.5 that the largest wind farm should be chosen as the reference site when developing a combined wind capacity model for two correlated wind farms using the

proposed Split method. Studies were also carried out to investigate the effect of the sizes of the wind farms when three wind sites are considered. The total wind capacity of 400 MW was added to the IEEE-RTS similar to the previous study. Swift Current, Regina and North Battleford were considered to be the first (R1), the second (R2) and the third (R3) reference sites respectively. Seven different cases with different capacity ratios of the rated capacity of North Battleford site (R3) with respect to the Regina site (R2) were examined by varying the ratio of the rated capacity of Regina site (R2) to the rated capacity of the Swift Current site (R1). The system LOLE obtained were compared with the results obtained using the PPM. The errors in LOLE for the seven case studies are shown in Figure 5.13. Each curve in the figure was obtained for a constant ratio of the rated capacity of the third reference site (R3) to the rated capacity of the second reference site (R2).

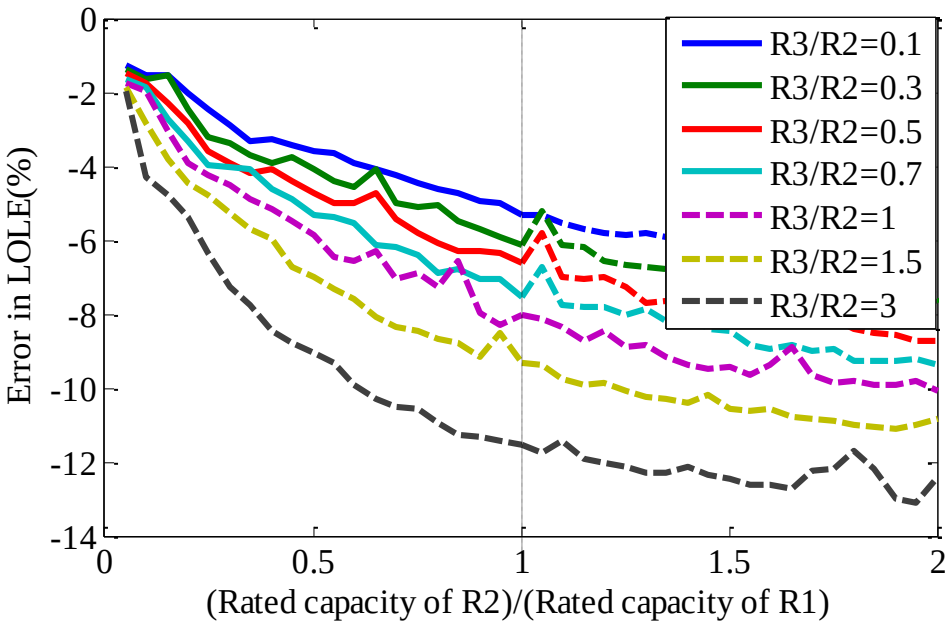

Figure 5.13: Variation of the ratio of the rated capacity of R1 with respect to the rated capacity of R2 for 10.5% wind penetration

It can be seen in Figure 5.13 that the error in the results tend to increase as the capacity ratio of R2 with respect to R1 increases for a constant capacity ratio of the rated capacity of R3 with respect to R2 for a given wind penetration in the power system. It can also be seen that, as the ratio of rated capacity of R3 with respect to R2 increases, the error significantly increases. It can be seen that the error is significant in the dotted portions of the plot which correspond to wind farm combinations where either R3 capacity exceeds R2 capacity, or R2 capacity exceeds R1 capacity. The dotted region in Figure 5.13 will not be encountered if the reference sites are chosen in decreasing order based on the rated wind farm capacities, i.e. R1>R2>R3. In this case, the errors are relatively small for practical purposes, and lie in the region shown by the solid plots in Figure 5.13.

Case studies were also carried out to investigate the impact of the variation of the ratio of the rated capacity of R3 with respect to the rated capacity of R1. The errors in the LOLE are similarly plotted and shown in Figure 5.14.

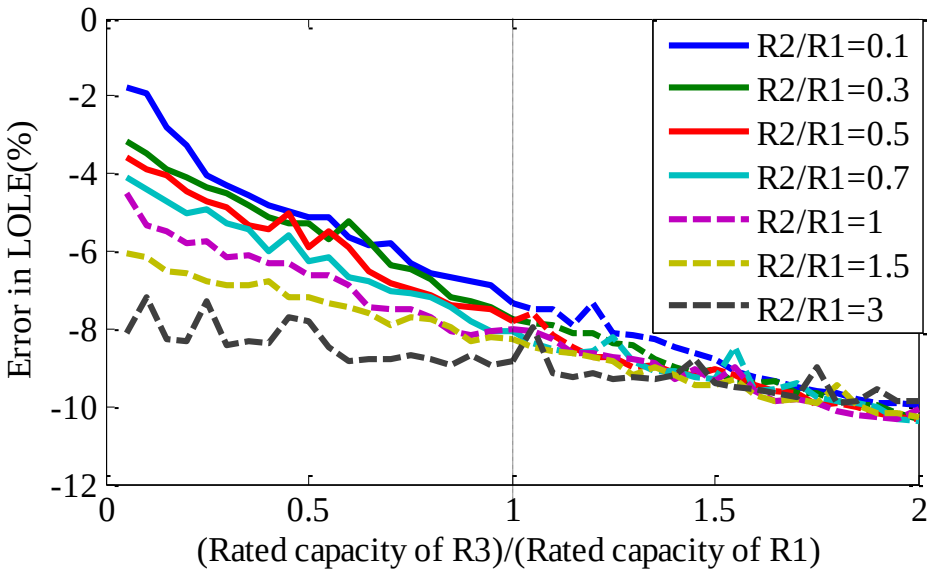

Figure 5.14: Variation of the ratio of the rated capacity of R3 with respect to R1 for 10.5% wind penetration

It can be seen in Figure 5.14 that the error tends to increase as the ratio of the capacity of R3 to the capacity of R1 increases. The error also increases as the ratio of the rated capacity of R2 with respect to the rated capacity of R1 increases. These are the same observations obtained from Figure 5.13. Similar to Figure 5.13, the errors are represented by solid portions of the curves when the wind sites are referenced in the decreasing order of their rated capacities, and the errors in this region is relatively small.

5.5.3.2 Impact of the mean wind speed of the wind farms

It is concluded from Section 5.5.3.1 that the maximum error is encountered when all three wind farms have equal rated capacities. Three wind sites, each having a rated capacity of 133.33 MW with the wind regimes for Swift Current, Regina and North Battleford respectively were used in this study. The total wind capacity connected to the IEEE-RTS[36] therefore is 400 MW which results in a 10.5% wind penetration similar to previous studies. The wind farms along with their respective mean wind speeds are shown in Table 5.11. The wind farms are sorted in the decreasing order based on the mean wind speed, and are designated as Site A, Site B and Site C respectively.

Table 5.11: Wind farm sites and their mean wind speeds

Site ID	Site Name	Mean wind speed (Km/hr)
A	Swift current	19.41
B	Regina	18.46
C	North Battleford	13.96

Since the order of the reference sites cannot be determined for equal sized wind farms based on the conclusion drawn in Section 5.5.3.1, all possible permutations are considered in this study and are listed in Table 5.12. Six LOLE values were obtained for each permutation using the Split method and are compared with those obtained using the PPM in Table 5.12. It should be noted

that each wind farm site has a rated capacity of 133.33 MW and only the order of choosing the reference site (R1, R2 and R3) for the Split method have been varied in Table 5.12.

Table 5.12: Permutations for the order of reference site

	R1	R2	R3	LOLE(hr/yr)		
				PPM	Split	Error (%)
permutation	C	B	A	6.3374	6.3295	-0.1246568
	C	A	B		6.2841	-0.8410389
	B	C	A		5.9647	-5.8809606
	B	A	C		5.9084	-6.7693376
	A	B	C		5.8079	-8.3551614
	A	C	B		5.8557	-7.6009089

It can be seen in Table 5.12 that the lowest error value is obtained for the permutation C-B-A and the highest error value is obtained for the permutation A-B-C. The result suggests that the order of the reference site should be chosen based on the increasing mean wind speed while using the Split method in order to minimize the possible error. The impact of the mean wind speed was further investigated using the combinations of all the wind sites shown in Table 5.10. The wind farm sites, in each case, are arranged in a descending order based on the mean wind speed of the wind farm site as shown in Table 5.13. Each wind farm is assumed to have a rated capacity of 133.33 MW and the actual correlation in the wind speeds between the wind farms shown in Table 5.10 are used for the evaluations using the Split method.

The IEEE-RTS system LOLE values were evaluated using the Split method and the PPM for all the possible permutations of the order of the reference site for each case. The relative error that arises by using the Split method with respect to the PPM is shown in Figure 5.15.

The results in Figure 5.15 show that the errors tend to be minimum for the permutation C-B-A in most of the cases, i.e. when the reference site is chosen based on increasing mean wind speed. Similarly, the errors tend to be relatively high for the permutation A-B-C in most of the cases,

i.e. when the reference site is chosen based on decreasing mean wind speed. Other permutations yield intermediate amount of error. It can therefore be concluded that the one with the lowest mean wind speed should be considered as the reference wind farm site when the wind farms are of equal size.

Table 5.13: Combination of wind sites used for the study

	Site A		Site B		Site C	
Case	**Name**	**Mean wind speed (km/hr)**	**Name**	**Mean wind speed (km/hr)**	**Name**	**Mean wind speed (km/hr)**
I	Swift current	19.41	Regina	18.46	North Battleford	13.96
II	Estevan	17.82	Moose Jaw	17.73	Saskatoon	15.50
III	Swift Current	19.41	Regina	18.46	Prince Albert	11.92
IV	Swift Current	19.41	Saskatoon	15.50	Yorkton	14.80
V	Kindersley	16.36	Saskatoon	15.50	North Battleford	13.96
VI	Regina	18.46	Estevan	17.82	La Ronge	11.88
VII	Broadview	17.20	Yorkton	14.80	Prince Albert	11.92
VIII	Swift Current	19.41	Moose Jaw	17.73	Kindersley	16.36

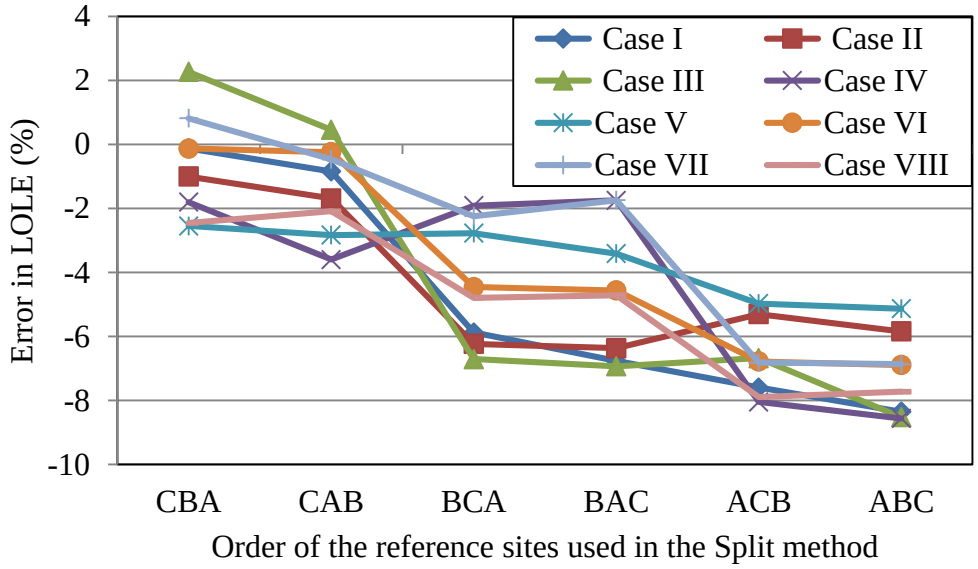

Figure 5.15: Variation in the order of reference sites used in Split method for different cases

5.5.3.3 Impact of the correlation coefficient value used

The cross correlation value ρ_{12-3} used in the Split method to combine the wind capacity model of the third reference site, $p(WP_{R3})$ with the combined capacity model of the first and the second reference sites, $p(WP_{R1R2})$ is considered to be the weighted average cross correlation in wind speed of the third reference site with the first and the second reference sites in (5.9). Studies were conducted to investigate the impact of the correlation value, ρ_{12-3} on the error produced in the results obtained using the Split method. Three wind farms with rated capacities of 200 MW, 133.33 MW and 66.67 MW were considered in this study. Selected combinations of wind farm sites as shown in Table 5.14 were considered. The actual correlation in wind speeds between the wind farms obtained from time-synchronized hourly wind speed data for 19 years have been used in this study and are also shown in Table 5.14.

Table 5.14: Wind farm combinations considered for the study

Case	**I**	**II**	**III**	**IV**	**V**	**VI**	**VII**	**VIII**
R1	North Battleford	Saskatoon	Prince Albert	Yorkton	North Battleford	La Ronge	Prince Albert	Stony Rapids
R2	Regina	Moose Jaw	Regina	Saskatoon	Saskatoon	Estevan	Yorkton	Yorkton
R3	Swift Current	Estevan	Swift Current	Swift Current	Kindersley	Regina	Broadview	Swift Current
$\boldsymbol{\rho_{12}}$	0.50	0.57	0.52	0.44	0.64	0.31	0.50	0.228
LOLE (hrs/yr) (from PPM)	6.5594	6.6559	6.7909	6.8905	7.1232	6.9596	7.3065	7.5092
weighted $\boldsymbol{average(\rho_{13}, \rho_{23})}$	0.47	0.49	0.40	0.38	0.59	0.48	0.58	0.22

The error in the LOLE was evaluated by varying the correlation value ρ_{12-3} from 0 to 1 with a step size of 0.01 for each case. The actual correlation, ρ_{12} between the wind speeds of first and second reference sites which are shown in Table 5.14 were used for all the evaluations. The results of the evaluation are shown in Figure 5.16.

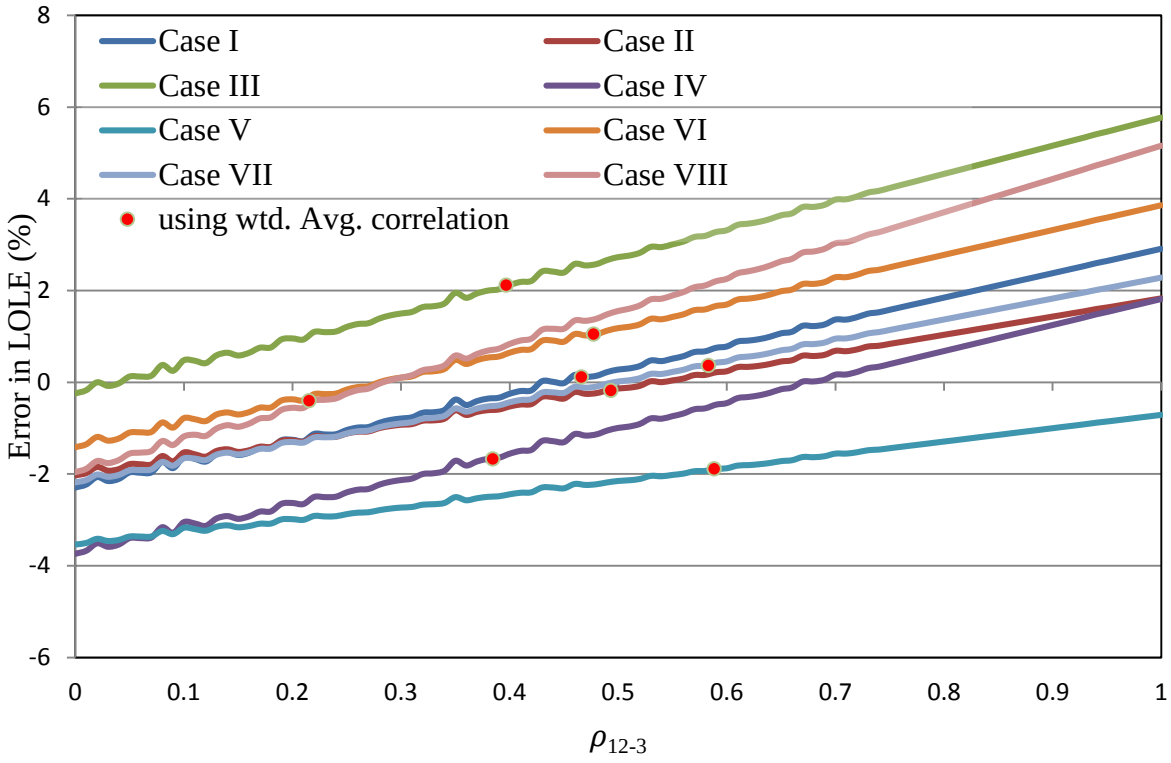

Figure 5.16: Error in LOLE obtained due to the variation in ρ_{12-3}

It can be seen in Figure 5.16 that the error changes from negative values to positive values as ρ_{12-3} increases from 0 to 1. The errors that occur for $\rho_{12-3} = Weighted\ Average(\rho_{13}, \rho_{23})$, which are shown by dots in the diagram, are reasonably close to the zero. Figure 5.16 suggests that satisfactory results can be achieved using the weighted average correlation for ρ_{12-3} as shown in (5.9).

5.5.4 Evaluation of the system LOLE for more than three wind farms and comparison with the PPM

The system LOLE of the IEEE-RTS connected to more than three wind farms is evaluated in this section and compared to the system LOLE obtained from the PPM. Four wind farm sites, Swift Current, Broadview, Kindersley and Moose Jaw with rated capacities of 149.4 MW, 26.4

MW, 11.2 MW and 11 MW respectively were considered. The order of the reference sites was chosen based on the rated capacities of the respective wind farms as concluded in Section 5.5.3.1 and is shown in Table 5.15. The rated capacities chosen in this section are based on the rated capacities of four existing Saskatchewan wind farms. The total installed wind capacity is 198 MW which results in a 5.5% wind penetration when added to the IEEE-RTS.

Table 5.15: Wind farm sites considered in the study with respective rated capacities

Reference order	Wind Farm	Rated Capacity (MW)
R1	Swift Current	149.4
R2	Broadview	26.4
R3	Kindersley	11.2
R4	Moose Jaw	11

The weighted average value of the correlation given by (5.9) was used to combine the wind capacity model of the third and the fourth reference wind farm sites while using the Split method. The results of the evaluations for a range of peak loads are shown in Figure 5.17.

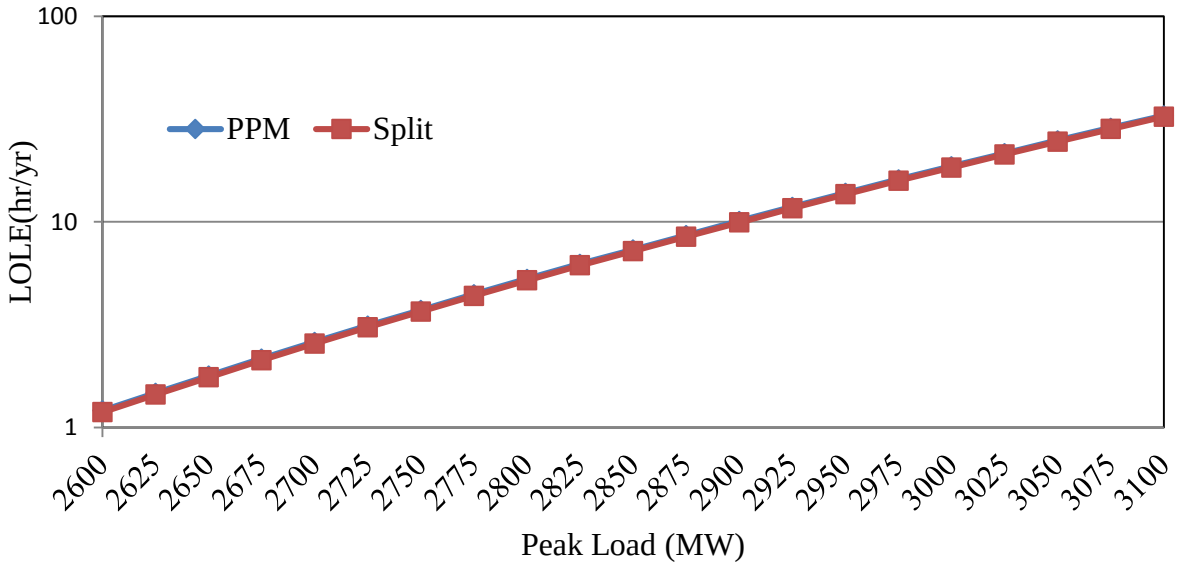

Figure 5.17: LOLE value for the IEEE-RTS connected to four wind farms at 5.5 % wind penetration

A study was carried out to incorporate up to ten wind farm sites for which time-synchronized wind speed data were collected between the years 1987 and 2005 [45]. The sites considered with the respective reference order are shown in Table 5.16.

Table 5.16: Wind farm sites considered for the study

Reference order	Wind farm	Mean wind speed(km/hr) @10 m height
R1	Prince Albert	11.9187
R2	North Battleford	13.9603
R3	Yorkton	14.7976
R4	Saskatoon	15.4953
R5	Kindersley	16.3562
R6	Broadview	17.1967
R7	Moose Jaw	17.7342
R8	Estevan	17.8208
R9	Regina	18.4617
R10	Swift Current	19.4094

The system LOLE of the IEEE-RTS for a peak load of 2850 MW was evaluated considering different numbers of wind farms using both the PPM and the Split method. The study was conducted considering two wind farms at a time, three wind farms at a time, etc., up to ten wind farms at a time. The total wind capacity is 400 MW, which is distributed equally between all the considered wind farm sites in each case. The results obtained are shown in Figure 5.18 and indicates that the proposed method yields reasonably accurate results.

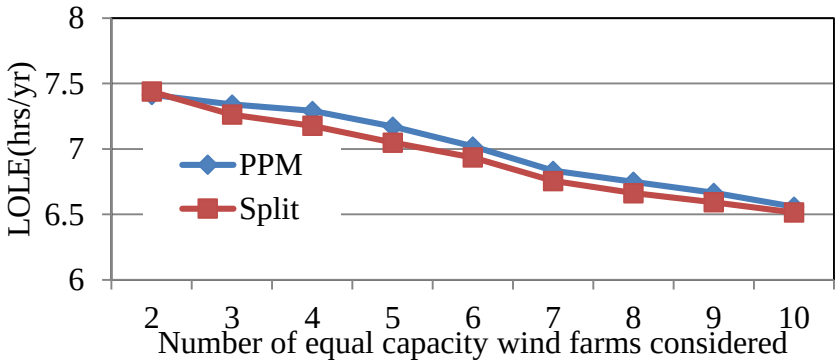

Figure 5.18: System LOLE for the IEEE-RTS connected to multiple wind farms of equal capacity with the total wind capacity of 400 MW.

5.6 Conclusion

The reliability contribution of wind power to a wind-integrated power system is greatly affected by the correlation in the wind speeds of the wind farms connected to the system. The correlation between the wind farms can be incorporated in an adequacy evaluation using existing techniques if sufficient time-synchronized wind data is available at the wind sites. Unfortunately, such data is not usually available when considering or determining new wind power installations during capacity planning or during formulation of an appropriate wind power policy for a jurisdiction. This chapter presents a simple approach to develop a combined wind model for correlated wind farm sites, which can then be convolved with the system generation model to obtain the system adequacy indices. The validity of the proposed algorithm was investigated for a range of wind regimes and wind speed cross correlations. This chapter also presents an approximate technique to incorporate the wind speed correlation between wind sites with minimal wind data. The presented method can be used in such cases using only the mean and the standard deviation in wind speeds estimated in a wind map. The results indicate that the combined wind power model obtained using the proposed method is a reasonable approximation of the actual wind model in a practical situation where the required wind data is not available. The method is extended to be applicable for more than two sites. Various sensitivity studies are presented in order to minimize the error that could arise when applying the proposed method.

6 SUMMARY AND CONCLUSIONS

Wind power installations are expected to continue to grow substantially in the next few decades to meet renewable energy targets put in place to address increasing public concerns about the environmental impacts of conventional electric energy sources. Substantial increases in intermittent generation and the uncertain nature of wind power creates significant difficulty in maintaining the system reliability. It becomes increasingly important to develop suitable reliability models to incorporate the important factors associated with wind generation that influence the overall system performance. The lack of proper and adequate data is a major setback in obtaining appropriate wind generation models for reliability evaluation. This problem is often encountered during wind policy making or system capacity planning considering geographic locations for new wind farm installations. This thesis addresses some of the problems currently being encountered in this field. The thesis presents an analytical method to incorporate the cross correlation between the system load and wind speed on a seasonal as well as on a diurnal basis, and to evaluate the adequacy indices. Time-synchronized wind data is generally required to consider the impact of cross correlation in wind speeds between multiple wind farms in reliability assessments of wind integrated power systems. The availability of time-synchronized data for multiple wind farm locations is extremely rare in practice. A novel technique is proposed in this thesis to develop a wind capacity model for two correlated wind farms when sufficient time-synchronized wind data is not available. The proposed technique is

extended to incorporate more than two sites in the development of an aggregate wind model for the system.

Chapter 1 presents an introduction of the thesis and provides some relevant basic reliability concepts regarding power systems including wind resources. The research problem statement and an outline of the thesis are presented. Chapter 2 introduces basic numerical concepts and illustrates the incorporation of wind power in the adequacy evaluation of a wind integrated power system. Generation and load models including wind generation models are introduced and illustrated with the help of a simple example. The process of calculating risk indices from the developed models are illustrated with an example. The concepts of peak load carrying capability of a power system, load forecast uncertainty, and period analysis in reliability evaluation are introduced. The capacity credit and capacity factor of a wind farm are also described in this chapter.

Chapter 3 presents an analytical technique to incorporate the seasonal and diurnal load following capability of wind speed in the adequacy evaluation of a wind integrated power system. The basic analytical technique normally performed on an annual basis is illustrated using data from the IEEE-RTS and the Saskatchewan power system. The studies are then extended to incorporate seasonal correlation between the wind speed and the load characteristics. The annual period is divided into four seasons designated as winter, shoulder 1, summer and shoulder 2 for seasonal evaluations. The results from the seasonal analysis are compared with the results obtained from the annual analysis for both the IEEE-RTS and the Saskatchewan power system. The differences in the results show the impact of seasonal correlation between the system load and the wind variation. The reliability in both the considered power systems improved when seasonal correlation was incorporated as the seasonal correlation in load and wind in

Saskatchewan is positive. In general, when the seasonal correlation is considered, reliability indices improve if there is a positive correlation between the wind and the load, and deteriorate if there is a negative correlation between the wind and the load. Reliability indices are unaffected when seasonal correlation is considered if there is zero correlation between the wind and the load.

The evaluation was then further extended to incorporate the diurnal load following capability of wind. The period of a day is sub divided into peak and off peak hours for each season. The sub-division was incorporated based on the existing practice of various utilities which consider the peak five hours in the peak load season for assigning capacity credit to a wind farm. The results obtained for the Swift Current wind characteristics and the Saskatchewan load characteristics do not show significant changes in the risk indices due to the very low diurnal correlation between wind and load. The reliability indices obtained considering diurnal correlation between wind and load can improve or deteriorate depending upon positive or negative correlation between them. The results are highly reliant on the wind regime and the load characteristics. The proposed technique can be used to incorporate the diurnal correlation between wind speed and load in order to ensure that the evaluated reliability indices accurately represent the system reliability.

Chapter 4 proposes a simple wind capacity model which incorporates the cross correlation between the wind speeds of multiple wind farm sites and wind penetration levels. This technique requires a large amount of time-synchronized wind data. A technique to generate artificial wind data series of two farms with desired correlation coefficients using the Cholesky decomposition method is presented. Two wind farm sites represented by Swift Current wind characteristics were used to investigate the impact of the wind model on the accuracy of the reliability index at

different penetration levels. The wind capacity model is represented by a discrete number of capacity states in an analytical method. Reducing the capacity states reduces the computation burden at the cost of accuracy in the results. Wind capacity models with seven, nine and eleven states are recommended in this thesis for wind penetration up to 10, 15 and 20 percent respectively.

Chapter 5 presents a new technique, designated as the Split method, to create a combined wind capacity model for multiple correlated wind farms lacking time-synchronized wind data. The results obtained from the proposed Split method is compared with the results obtained from a reference method that utilizes adequate time-synchronized wind data. The closeness of the results suggest that the proposed method can be applied satisfactorily when time-synchronized wind data are not available. Wind data for various Saskatchewan weather stations obtained from Environment Canada were used for the study. An approximate Split method is proposed to develop the combined wind capacity model of correlated wind farms when very limited wind data are available. The only data required are the mean and the standard deviation of the wind speed, and can be obtained from a wind atlas. The wind characteristic of a wind farm is assumed to be normally distributed in this method.

The reliability of a wind integrated system with wind farms having wind speeds correlations close to zero is higher compared to that of a similar system with wind farms having correlation in wind speeds close to one. Geographically diverse wind farms have comparatively lower correlation in wind speeds resulting in higher reliability benefits in a wind integrated system. The number of wind farms connected to a power system similarly affects the system reliability. A higher number of wind farms results in less intermittent aggregate power output compared to a smaller number of wind farms. Multiple small wind farms, for a given total wind capacity,

therefore result in higher system reliability compared to one or two large wind farms. The Split method used to incorporate two correlated wind farms is therefore extended to incorporate multiple wind farm sites. Selected Saskatchewan wind farm sites are used for the illustration. Sensitivity analysis is used to study the impacts of wind farm sizes, mean wind speeds and correlation levels.

In conclusion, this thesis presents methods to incorporate the correlation between the wind speed and load as well as the correlation in wind speeds between wind farm sites during the evaluation of reliability indices using analytical techniques. The method proposed to incorporate diurnal load following capability of wind by considering the peak five hours of the peak season to differentiate the peak and off peak periods is expected to be very useful in extending the utilization of analytical techniques in HL I adequacy evaluations. The simplified wind models using 7, 9 and 11 capacity states, obtained taking wind speed correlations into account, provide system planners and researchers with a guideline for wind capacity model building in HL I adequacy evaluations. Some of the studies presented in this thesis have been published [33], [48] and some other studies have been submitted for publication. The proposed Split method created for developing combined wind capacity models when time-synchronized wind data is unavailable should prove extremely useful for system planners and policy makers involved in expanding the utilization of wind power in electric power systems.

LIST OF REFERENCES

[1] R. Billinton and R. N. Allan, *Reliability evaluation of power systems*, 2nd ed. New York: Plenum Press, 1996.

[2] R. Billinton, R. N. Allan, and L. Salvaderi, *Applied Reliability Assessment in Electric Power Systems*. New York: IEEE Press, 1991.

[3] R. N. Allan, R. Billinton, and S. H. Lee, "Bibliography of the Application of Probability Methods in Power System Reliability Evaluation 1977-1982," *Power Eng. Rev. IEEE*, vol. PER-4, no. 2, pp. 24–25, 1984.

[4] R. N. Allan, R. Billinton, A. M. Breipohl, and C. H. Grigg, "Bibliography on the application of probability methods in power system reliability evaluation: 1987-1991," *Power Syst. IEEE Trans.*, vol. 9, no. 1, pp. 41–49, 1994.

[5] R. Billinton, M. Fotuhi-Firuzabad, and L. Bertling, "Bibliography on the application of probability methods in power system reliability evaluation 1996-1999," *Power Syst. IEEE Trans.*, vol. 16, no. 4, pp. 595–602, 2001.

[6] R. N. Allan, R. Billinton, A. M. Breipohl, and C. H. Grigg, "Bibliography on the application of probability methods in power system reliability evaluation," *Power Syst. IEEE Trans.*, vol. 14, no. 1, pp. 51–57, 1999.

[7] R. Billinton, "Bibliography on the Application of Probability Methods In Power System Reliability Evaluation," *Power Appar. Syst. IEEE Trans.*, vol. PAS-91, no. 2, pp. 649–660, 1972.

[8] P. Giorsetto and K. F. Utsurogi, "Development of a new procedure for reliability modeling of wind turbine generators," *Power Appar. Syst. IEEE Trans.*, vol. PAS-102, no. 1, pp. 134–143, 1983.

[9] S. H. Karaki, B. A. Salim, and R. B. Chedid, "Probabilistic model of a two-site wind energy conversion system," *Energy Conversion, IEEE Trans.*, vol. 17, no. 4, pp. 530–536, 2002.

[10] F. C. Sayas and R. N. Allan, “Generation availability assessment of wind farms,” in *Generation, Transmission and Distribution, IEE Proceedings-*, 1996, vol. 143, pp. 507–518.

[11] W. Wangdee and R. Billinton, “Considering load-carrying capability and wind speed correlation of WECS in generation adequacy assessment,” *Energy Conversion, IEEE Trans.*, vol. 21, no. 3, pp. 734–741, 2006.

[12] Y. Gao and R. Billinton, “Adequacy assessment of generating systems containing wind power considering wind speed correlation,” *Renew. Power Gener. IET*, vol. 3, no. 2, pp. 217–226, 2009.

[13] R. Billinton, Y. Gao, D. Huang, and R. Karki, “Adequacy Assessment of Wind-Integrated Composite Generation and Transmission Systems,” in in *Innovations in power system reliabilityty*, Springer London, 2011, pp. 141–167.

[14] C. W. E. Association, “Economic Benefits of Wind Energy,” 2013. [Online]. Available: http://www.canwea.ca/images/uploads/File/NRCan_-_Fact_Sheets/canwea-factsheet-economic-web.pdf. [Accessed: 10-Nov-2013].

[15] R. Billinton and D. Huang, “Basic considerations in generating capacity adequacy evaluation,” in *Electrical and Computer Engineering, 2005. Canadian Conference on*, 2005, pp. 611–614.

[16] R. Billinton and R. N. Allan, “Generating capacity - basic prabability methods,” in *Reliability evaluation of power systems*, 2nd ed., New York: Plenum Press, 1996, pp. 18–82.

[17] Y. Li, “Bulk system reliability evaluation in a deregulated power industry,” University of Saskatchewan, Saskatoon, 2003.

[18] R. Billinton and G. Bai, “Generating Capacity Adequcy Associated With Wind Energy,” *IEEE Trans. Energy Convers.*, vol. 19, no. 3, pp. 641–646, 2004.

[19] R. Karki and P. Hu, “Wind power simulation model for reliability evaluation,” in *Electrical and Computer Engineering, 2005. Canadian Conference on*, 2005, pp. 541–544.

[20] Y. Gao, “Adequacy assessment of electric power systems incorporating wind and solar energy,” University of Saskatchewan, 2006.

[21] M.-R. Haghifam and M. Omidvar, “Wind Farm Modeling in Reliability Assessment of Power System,” in *9th International Conference on Probabilistic Methods Applied to Power Systems*, 2006, pp. 1–5.

[22] R. Karki, P. Hu, and R. Billinton, “A Simplified Wind Power Generation Model for Reliability Evaluation,” *IEEE Trans. Energy Convers.*, vol. 21, no. 2, pp. 533–540, Jun. 2006.

[23] M. S. Miranda and R. W. Dunn, “Spatially correlated wind speed modelling for generation adequacy studies in the UK,” in *Power Engineering Society General Meeting, 2007. IEEE*, 2007, pp. 1–6.

[24] F. Vallée, J. Lobry, and O. Deblecker, “Impact of the Wind Geographical Correlation Level for Reliability Studies,” *IEEE Trans. power Syst.*, vol. 22, no. 4, pp. 2232–2239, 2007.

[25] M. Milligan and K. Porter, “Wind capacity credit in the United States,” *2008 IEEE Power Energy Soc. Gen. Meet. - Convers. Deliv. Electr. Energy 21st Century*, pp. 1–5, Jul. 2008.

[26] J. Hetzer, D. C. Yu, and K. Bhattarai, “An Economic Dispatch Model Incorporating Wind Power,” *IEEE Trans. Energy Convers.*, vol. 23, no. 2, pp. 603–611, 2008.

[27] T. Adams and F. Cadieux, “Wind Power in Ontario: Quantifying the Benefits of Geographic Diversity,” in *2nd Climate Change Technology Conference. Engineering Institute of Canada: Ontario.*, 2009.

[28] S. Gloor, “A Report on the Correlation Between Wind Speed and Distance for 12 WA Wind Speed Datasets,” 2010.

[29] I. Abouzahr and R. Ramakumar, “An approach to assess the performance of utility-interactive wind electric conversion systems,” *Energy Conversion, IEEE Trans.*, vol. 6, no. 4, pp. 627–638, 1991.

[30] S. Mishra, “Wind power capacity credit evaluation using analytical methods,” University of Saskatchewan, 2010.

[31] Y. Gao, “Adequacy assesment of composite generation and transmission systems incorporating wind energy conversion systems.,” University of Saskatchewan, Saskatoon, 2010.

[32] R. Billinton and Y. Gao, “Multistate wind energy conversion system models for adequacy assessment of generating systems incorporating wind energy,” *Energy Conversion, IEEE Trans.*, vol. 23, no. 1, pp. 163–170, 2008.

[33] R. Karki, D. Dhungana, and R. Billinton, “An appropriate wind model for wind integrated power system reliability evaluation considering wind speed correlations,” *Appl. Sci.*, 2013.

[34] R. . Billinton, H. Chen, and R. . Ghajar, “Time-series models for reliability evaluation of power systems including wind energy,” *Microelectron. Reliab.*, vol. 36, no. 9, pp. 1253–1261, 1996.

[35] R. Karki, “Reliability and cost evaluation of small isolated power systems containing photovoltaic and wind energy,” University of Saskatchewan, 2000.

[36] A. P. M. Subcommittee, “IEEE Reliability Test System,” *Power Appar. Syst. IEEE Trans.*, vol. PAS-98, no. 6, pp. 2047–2054, 1979.

[37] R. Billinton, Y. Gao, and R. Karki, “Composite System Adequacy Assessment Incorporating Large-Scale Wind Energy Conversion Systems Considering Wind Speed Correlation,” *Power Syst. IEEE Trans.*, vol. 24, no. 3, pp. 1375–1382, 2009.

[38] H. A. Sturges, “The choice of a class interval,” *J. Am. Stat. Assoc.*, vol. 21, no. 153, pp. 65–66, 1926.

[39] R. Billinton and R. N. Allan, “Generation capacity - basic probability methods,” Second., New York: Plenum Press, 1994, pp. 18–82.

[40] G. H. Golub and C. F. Van Loan, *Matrix computations*, vol. 3. Johns Hopkins Univ Pr, 1996.

[41] R. Karki and R. Billinton, *SIPSIREL user’s Manual*. Saskatoon: Power System Research group, University of Saskatchewan, 1997.

[42] T. R. Oke, “Initial Guidance to Obtain Representative Meteorological Observations at Urban Sites,” Geneva, 2006.

[43] J. H. Seinfeld and S. N. Pandis, *Atmospheric Chemistry and Physics : From Air Pollution to Climate Change*, 2nd ed. Hoboken, New Jersey: WILEY, 2006.

[44] W. Katzenstein, “Wind power variability, its cost, and effect on power plant emissions,” Carnegie Mellon University, 2010.

[45] Environment Canada, “Canadian Weather Energy and Engineering Datasets (CWEEDS).” [Online]. Available: ftp://ftp.tor.ec.gc.ca/Pub/Engineering_Climate_Dataset/Canadian_Weather_Energy_Engineering_Dataset_CWEEDS_2005/ZIPPED FILES/ENGLISH/. [Accessed: 22-Feb-2013].

[46] G. Czisch and B. Ernst, “High wind power penetration by the systematic use of smoothing effects within huge catchment areas shown in a European example,” *Wind. 2001*, 2001.

[47] J. L. Walmsley and R. J. Morris, “Wind Energy Resource Maps For Canada,” Downsview, Ontario, 1992.

[48] R. Karki, D. Dhungana, S. Shimu, and R. Billinton, “Reliability evaluation incorporating the load following capability of wind generation,” in *Canadian Conference of Electrical and Computer Engineering*, 2013.

APPENDIX A – IEEE-RTS DATA

Table A.1: Generating units of the IEEE-RTS

Unit No.	Rated Capacity (MW)	Failure Probability
1	50	0.01
2	50	0.01
3	50	0.01
4	50	0.01
5	50	0.01
6	50	0.01
7	12	0.02
8	12	0.02
9	12	0.02
10	12	0.02
11	12	0.02
12	155	0.04
13	100	0.04
14	100	0.04
15	100	0.04
16	197	0.05
17	197	0.05
18	197	0.05
19	20	0.10
20	20	0.10
21	76	0.02
22	76	0.02
23	20	0.10
24	20	0.10
25	76	0.02
26	76	0.02
27	155	0.04
28	155	0.04
29	350	0.08
30	400	0.12
31	400	0.12
32	155	0.04

Table A.2: Weekly peak load as a percentage of annual peak load

Week	Peak Load (%)	Week	Peak Load (%)
1	86.2	27	75.5
2	90	28	81.6
3	87.8	29	80.1
4	83.4	30	88
5	88	31	72.2
6	84.1	32	77.6
7	83.2	33	80
8	80.6	34	72.9
9	74	35	72.6
10	73.7	36	70.5
11	71.5	37	78
12	72.7	38	69.5
13	70.4	39	72.4
14	75	40	72.4
15	72.1	41	74.3
16	80	42	74.4
17	75.4	43	80
18	83.7	44	88.1
19	87	45	88.5
20	88	46	90.9
21	85.6	47	94
22	81.1	48	89
23	90	49	94.2
24	88.7	50	97
25	89.6	51	100
26	86.1	52	95.2

Table A.3: Daily peak load as a percentage of weekly peak load

Day	Peak Load (%)
Monday	93
Tuesday	100
Wednesday	98
Thursday	96
Friday	94
Saturday	77
Sunday	75

Table A.4: Hourly peak load as a percentage of daily peak load

	Winter weeks 1-8 & 44-52		Summer weeks 18-30		Spring/Fall 9-17 & 31-43	
Hour	**Weekday**	**Weekend**	**Weekday**	**Weekend**	**Weekday**	**Weekend**
12-1 am	67	78	64	74	63	75
1-2	63	72	60	70	62	73
2-3	60	68	58	66	60	69
3-4	59	66	56	65	58	66
4-5	59	64	56	64	59	65
5-6	60	65	58	62	65	65
6-7	74	66	64	62	72	68
7-8	86	70	76	66	85	74
8-9	95	80	87	81	95	83
9-10	96	88	95	86	99	89
10-11	96	90	99	91	100	92
11-Noon	95	91	100	93	99	94
Noon-1 pm	95	90	99	93	93	91
1-2	95	88	100	92	92	90
2-3	93	87	100	91	90	90
3-4	94	87	97	91	88	86
4-5	99	91	96	92	90	85
5-6	100	100	96	94	92	88
6-7	100	99	93	95	96	92
7-8	96	97	92	95	98	100
8-9	91	94	92	100	96	97
9-10	83	92	93	93	90	95
10-11	73	87	87	88	80	90
11-12	63	81	72	80	70	85